

AN ABSTRACT OF THE THESIS OF

Kriangsak Khownum for the degree of Master of Science in Chemistry presented on August 11, 2003. Title: Direct Atom Transfer vs. Ring Expansion in Reaction of Rhenium Oxo Complexes with Cyclooctene Epoxides and Episulfides.

*Redacted for Privacy*

Abstract

Approved: \_\_\_\_\_

Kevin P. Gable

The rhenium (V) complex  $Tp'ReO_2$  ( $Tp'$  = hydrido-*tris*-(3,5-dimethylpyrazolyl)borate), generated *in situ* from  $PPh_3$  reduction of  $Tp'ReO_3$ , reacts with small ring heterocycles such as epoxides and episulfides. The strained *trans*-cyclooctene ring provides an unusual thermodynamic bias against direct atom transfer, but *trans*-cyclooctene oxide still produces substantial amounts of *trans*-cyclooctene. Episulfides also react under the same conditions. These are more reactive than epoxides and show a greater propensity for direct atom transfer; under catalytic conditions the eventual products are dithiolate complexes. The differences in reaction outcome point to important differences in selectivity for O- vs. S-atom transfer.

The rate constant for *trans*-cyclooctene production was obtained using a parallel reaction model since an epoxide coordinated to rhenium as

the intermediated undergoes direct O-atom transfer to give alkene and  $\text{Tp}'\text{ReO}_3$  and ring expansion to give the diolate. The ratio of diolate/alkene is 2:1. The observed rate constant for ring expansion is  $(1.24 \pm 0.03) \times 10^{-5} \text{ s}^{-1}$  and the rate constant for direct atom transfer is  $(6.02 \pm 0.02) \times 10^{-6} \text{ s}^{-1}$ . *cis*-Cyclooctene showed a higher preference to give alkene (24.5:1) than *trans*-cyclooctene. The observed rate constant for direct atom transfer is  $5.07 \times 10^{-5} \text{ s}^{-1}$  and the rate constant for ring expansion is  $2.07 \times 10^{-6} \text{ s}^{-1}$ .

Desulfidation of *trans*- and *cis*-cyclooctene showed the reaction proceeds faster than deoxygenation to give the thermally stable dithiodiolate species and alkene at 75 °C. *cis*-Cyclooctene episulfide gave a higher alkene/diolate ratio (10:1) than *trans*-episulfide (5:1).

However, monothiodiolate formation in a phosphine free system ( $\text{Tp}'\text{ReO}(\text{OH})(\text{EtOH})$  as a  $\text{Tp}'\text{ReO}_2$  source) was observed, in addition to dithiodiolate.  $\text{Tp}'\text{ReOS}$  or  $\text{Tp}'\text{O}_2$  were suggested to serve as S-atom transfer agents.  $\text{Tp}'\text{ReO}_3$  was also detected in the phosphine free system by formation of diolate from excess *trans*-cyclooctene

Combining the kinetic and thermodynamic data, the order of reactivity of substrates is: *cis*-cyclooctene episulfide > *trans*-cyclooctene episulfide > *cis*-cyclooctene oxide > *trans*-cyclooctene oxide.

DIRECT ATOM TRANSFER VS. RING EXPANSION IN REACTION OF  
RHENIUM OXO COMPLEXES WITH CYCLOOCTENE EPOXIDES AND  
EPISULFIDES

by  
Kriangsak Khownum

A THESIS  
submitted to  
Oregon State University

in partial fulfillment of  
the requirements for the  
degree of

Master of Science

Presented August 11, 2003  
Commencement June 2004

Master of Science thesis of Kriangsak Khownum presented on August 11, 2003.

APPROVED:

*Redacted for Privacy*

Major Professor, representing Chemistry \_\_\_\_\_

*Redacted for Privacy*

Head of Department of Chemistry \_\_\_\_\_

*Redacted for Privacy*

Dean of Graduate School \_\_\_\_\_

I understand that my thesis will become part of the permanent collection of Oregon State University libraries. My signature below authorizes release of my thesis to any reader upon request.

*Redacted for Privacy*

\_\_\_\_\_  
Kriangsak Khownum, Author

## ACKNOWLEDGEMENTS

I certify that this thesis, and the research to which it refers, are the product of my own works and that any ideas or quotations from the work of other people, published or otherwise, are fully acknowledged in accordance with the standard referencing practices of the discipline. I deeply acknowledge Prof. Kevin Gable for all his support, guidance and encouragement as my advisor to make this thesis possible. I would like to thank my committee members Prof. Max Deinzer, Prof. Douglas Keszler and Prof. John Wager for their support. I also would like to thank to Rodger Kohnert for his support on NMR works, Dr. Christine Pastorek for her support on GC-MS work, and also Jeff Morre for his support on MS work. I am indebted to Dr. Eric Brown, Pitak Chuwong, Punlop Kuntiyong, and Sorasaree Tonsiengsom for their support and friendship. I also would like to express my gratitude to the Development and Promotion of Science and Technology Talents Project, DPST, of the Royal Thai Government for financial support through DPST scholarship. I also owe much gratitude to the OSU Chemistry Department for financial support through teaching assistantships, my advisor for financial support through research assistantships, and also the National Science Foundation, NSF, for research grant. Finally, I would like to thank my friends and family for their friendship and support.

## TABLE OF CONTENTS

	<u>Page</u>
Chapter 1. Introduction and Literature Review.....	1
1.1 Metal-Mediated Oxygen-Atom Transfer .....	1
1.2 Electronic Structure of Metal Terminal Oxo Complexes.....	6
1.3 C-O and C-S Bond Cleavage Mediated by Cp*Rhenium Oxo Complexes .....	8
1.4 C-O and C-S Cleavage Mediated By Tp'Rhenium Oxo Complex.....	13
1.5 Binding of alkene to Tetrathioperrhenate Anion (ReS <sub>4</sub> <sup>-</sup> ) and Influence of Hydrogen Sulfide and Thiols.....	14
1.6 Direct Atom Transfer vs. Ring Expansion.....	15
1.7 Rhenium Terminal-Sulfido Complexes.. ..	18
1.8 Desulfidation Catalytic Cycle Mediated by Rhenium Oxo Complex.....	20
1.9 Conclusion of the Literature Review and Research Goals..	21
Chapter 2. Results and Discussion.....	23
2.1 Independent Kinetic Measurement.....	24
2.2 Parallel First-order Reactions.....	32
2.3 Kinetic Measurement of 1,2- <i>cis</i> -Cyclooctene Oxide.....	35
2.4 Sulfur Analog Study.....	36

## TABLE OF CONTENTS (Continued)

	<u>Page</u>
2.4.1 Independent Synthesis and Characterization of Hydrido- <i>tris</i> -(3,5-dimethyl-1-pyrazoyl)borato ( <i>trans</i> -cyclooctane-1,2-monothiodiolato)(oxo) rhenium(V)(1).....	37
2.4.2 Synthesis and Characterization of Hydrido- <i>tris</i> -(3,5-dimethyl-1-pyrazoyl)borato ( <i>trans</i> -cyclooctane-1,2-dithio diolato)(oxo) rhenium(V) (2).....	45
2.4.3 Synthesis and Characterization of Hydrido- <i>tris</i> -(3,5-dimethyl-1-pyrazoyl)borato ( <i>trans</i> -cyclooctane-1,2-dithio diolato)(oxo) rhenium(V) (3).....	52
2.4.4 Selectivity and Desulfidation Products of Cyclooctene Episulfide.....	62
2.4.5 Monothiodiolate vs. Dithiodiolate.....	65
2.4.6 Metal Oxo Donor and Acceptor.....	69
2.4.7 Epoxide vs. Episulfide Selectivity.....	73
Chapter 3. Experimental.....	75
3.1 General Methods.....	75
3.2 NMR measurement.....	76
3.3 Measurement of Kinetics.....	77
3.4 Synthetic Procedures.....	78
3.4.1 <i>trans</i> -Cyclooctene Oxide.....	78
3.4.2 <i>trans</i> -Cyclooctene Episulfide.....	79
3.4.3 <i>cis</i> -Cyclooctene Episulfide.....	80
3.4.4 <i>trans</i> -Mercaptocyclooctanol.....	81
3.4.5 Hydrido- <i>tris</i> -(3,5-dimethyl-1-pyrazoyl)borato ( <i>trans</i> -cyclooctane-1,2-diolato)(oxo)rhenium(V).....	82

## TABLE OF CONTENTS (Continued)

	<u>Page</u>
3.4.6 Hydrido- <i>tris</i> -(3,5-dimethyl-1-pyrazolyl)borato ( <i>cis</i> -cyclooctane-1,2-diolato)(oxo)rhenium(V).....	82
3.4.7 Hydrido- <i>tris</i> -(3,5-dimethyl-1-pyrazolyl)borato ( <i>trans</i> -cyclooctane-1,2-monothiodiolato) (oxo)rhenium(V).....	82
3.4.8 Hydrido- <i>tris</i> -(3,5-dimethyl-1-pyrazolyl) borato( <i>trans</i> -cyclooctane-1,2-dithiodiolato) (oxo)rhenium(V).....	83
3.4.9 Hydrido- <i>tris</i> -(3,5-dimethyl-1-pyrazolyl) borato( <i>cis</i> -cyclooctane-1,2-dithiodiolato) (oxo)rhenium(V).....	85
3.5 Procedure for Recrystallization of Hydrido- <i>tris</i> - (3,5-dimethyl-1-pyrazolyl) borato( <i>trans</i> -cyclooctane-1,2- dithiodiolato)(oxo)rhenium(V).....	86
Chapter 4. Conclusion and Future Work.....	88
Bibliography.....	89
Appendices.....	94
Appendix I. NMR Spectra in C <sub>6</sub> D <sub>6</sub> .....	95
Appendix II. Spectra of Yellow-Green Compound.....	108



## LIST OF FIGURES

<u>Figure</u>	<u>Page</u>
1.1 Epoxidation Catalytic Cycle.....	2
1.2 Sharpless Asymmetric Epoxidation .....	3
1.3 Jacobsen-Suzuki Asymmetric Epoxidation Catalyst.....	4
1.4 Episulfidation Catalyzed by Molybdenum Complex.....	5
1.5 Mo/Co/S Cluster and an Desulfurization Reaction.....	5
1.6 Catalytic O-atom Transfer Reaction Cycle.....	7
1.7 Resonance Forms of Metal Oxide.....	8
1.8 Alkene Extrusion.....	10
1.9 Catalytic Cycle of Cp*ReO <sub>3</sub> .....	10
1.10 Dimerization of Cp*ReO <sub>2</sub> .....	11
1.11 Multi Step Fragmentation of Cp*Rhenium Ethane Dithiolate.....	12
1.12 Cycloreversion of Tp'Rhenium Diolate.....	13
1.13 Qualitative Reaction Coordinate of ReS <sub>4</sub> <sup>-</sup> , Hydrogen Sulfide, and Ethylene.....	15
1.14 Michaelis-Menton Enzymatic Model.....	16
1.15 Deoxygenation Catalytic Cycle.....	17
1.16 Coordinated Tethered Epoxide Rhenium Complex.....	18
1.17 Reaction of Cp'Re( $\eta^2$ -S <sub>3</sub> )Cl <sub>2</sub> with PPh <sub>3</sub> .....	19
1.18 Catalytic Cycle of Desulfidation.....	20

## LIST OF FIGURES (Continued)

<u>Figure</u>	<u>Page</u>
1.19 Thermodynamically Favored <i>trans</i> -Cyclooctane Diolate.....	22
2.1 Catalytic Cycle of Deoxygenation.....	24
2.2 Direct Atom Transfer vs. Ring Expansion.....	25
2.3 Spectra of Pure <i>trans</i> -Cyclooctane Diolate and Reaction Mixture...	27
2.4 Selected Pseudo-First Order Plots.....	28
2.5 Ring Expansion Rate Constant, $k_{\text{exp}}$ .....	31
2.6 Epoxide Coordinated to Re as an Intermediate.....	32
2.7 Competition Reaction Model Plot.....	33
2.8 1,2- <i>trans</i> -Monothiodiolate Synthesis.....	38
2.9 Diastereomers of <b>1</b> .....	38
2.10 COSY and HSQC of <b>1</b> .....	39
2.11 NOESY of <b>1</b> .....	42
2.12 nOe of <b>1</b> .....	43
2.13 Proton and Carbon Assignments for <b>1</b> .....	44
2.14 COSY and HSQC Spectra of <b>2</b> .....	46
2.15 NOESY of <b>2</b> .....	49
2.16 nOe of <b>2</b> .....	50
2.17 Proton and Carbon Assignment for <b>2</b> .....	51

## LIST OF FIGURES (Continued)

<u>Figure</u>	<u>Page</u>
2.18 COSY and HSQC of Mixture <i>syn</i> - and <i>anti</i> -Isomer of <b>3</b> .....	53
2.19 Different Thermal Stability of <i>syn</i> - and <i>anti</i> -Isomers.....	57
2.20 Comparing the NOESY from 10:7 and 10:1 mixture.....	58
2.21 nOe of <b>3</b> .....	60
2.22 Proton and Carbon Assignment for <i>cis</i> -Cyclooctane Dithiodiolate..	61
2.23 Decrease in the Alkene/Dithiodiolae Ratio.....	63
2.24 Diolate Formation in Tp'ReO(OH)(OEt) System.....	70
2.25 Desulfidation Catalytic Cycle, Initial Step.....	71
2.26 Desulfidation Catalytic Cycle, Middle Step.....	72

## LIST OF TABLES

<u>Table</u>	<u>Page</u>
2.1 $k_{\text{obs}}$ and Half Life of Ring Expansion for <i>trans</i> -Cyclooctene Oxide.....	29
2.2 Summarized $k_{\text{direct}}$ and $k_{\text{exp}}$ .....	34
2.3 NMR Results from 2D COSY and HSQC Experiments for <b>1</b> .....	41
2.4 NMR Results from 2D COSY and HSQC Experiments for <b>2</b> .....	48
2.5 NMR Results from 2D COSY and HSQC Experiments for <b>3</b> .....	55
2.6 S=PPh <sub>3</sub> /O=PPh <sub>3</sub> Ratio.....	64
2.7 PPh <sub>3</sub> Free System.....	66

## LIST OF APPENDIX FIGURES

<u>Figure</u>	<u>Page</u>
A1.1 $^1\text{H}$ NMR and $^{13}\text{C}$ of 1,2- <i>trans</i> -Cyclooctanediolate.....	95
A1.2 $^1\text{H}$ NMR and $^{13}\text{C}$ of 1,2- <i>trans</i> -Cyclooctanedithiolate.....	97
A1.3 $^1\text{H}$ NMR of 1,2- <i>cis</i> -Cyclooctanediolate.....	99
A1.4 $^1\text{H}$ NMR and $^{13}\text{C}$ of 1,2- <i>cis</i> -Cyclooctanedithiolate.....	100
A1.5 $^1\text{H}$ NMR and $^{13}\text{C}$ of 1,2- <i>trans</i> -Cyclooctanemonothiolate.....	102
A1.6 $^1\text{H}$ NMR of <i>trans</i> -Cyclooctene Oxide.....	104
A1.7 $^1\text{H}$ NMR of <i>trans</i> -Cyclooctene Episulfide.....	105
A1.8 $^1\text{H}$ NMR of <i>cis</i> -Cyclooctene Oxide.....	106
A1.9 $^1\text{H}$ NMR of <i>trans</i> -Cyclooctene Episulfide.....	107
A2.1 IR.....	108
A2.2 $^1\text{H}$ NMR and $^{13}\text{C}$ .....	109
A2.3 COSY.....	111
A2.4 HSQC.....	112

*This is dedicated to my family, Khom and Nhoonom Khownum, my sister  
Nheungruthai Khownum and all of my dear friends.*

DIRECT ATOM TRANSFER VS. RING EXPANSION IN REACTION OF RHENIUM OXO  
COMPLEXES WITH CYCLOOCTENE EPOXIDES AND EPISULFIDES

**Chapter 1. Introduction and Literature Review**

**1.1 Metal Mediated Oxygen- and Sulfur- Atom Transfer**

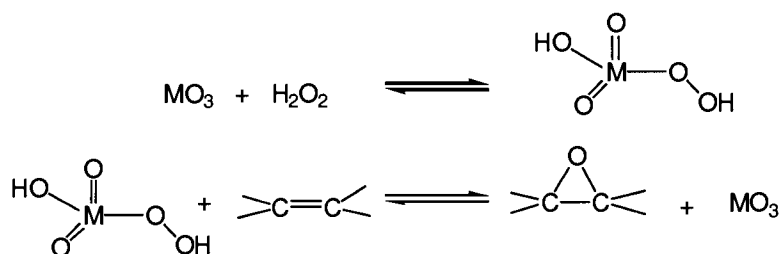
Transition metal catalysts are exquisitely exploited in many applications<sup>1</sup>. For example, products ranging from pharmaceuticals to pesticides are produced catalytically; our bodies are operated by catalysts, many of which are metalloenzymes<sup>2</sup>.

The chemistry of O- and S- atom transfers between a metal center and an organic substrate have recently received attention because of their importance in biological systems<sup>3</sup> and in catalytic reactions in the petroleum<sup>4</sup> and commodity chemical industries<sup>5</sup>. Transition metal complexes have been used in the stoichiometric and catalytic oxidation of organic compounds. An important industrial process based on PdCl<sub>2</sub> and alkene forming a Pd-alkene complex is the Wacker reaction<sup>6</sup>, a catalytic method for conversion of ethylene to acetaldehyde. Water is added to the Pd-activated alkene to give acetaldehyde and Pd. Pd is reoxidized to Pd<sup>2+</sup> by using the co-reagents CuCl<sub>2</sub> and O<sub>2</sub>.

Formation of C-O bonds can be achieved by using oxo metal complexes that can utilize a variety of oxygen sources for oxidation processes under mild conditions. High oxidation state oxo compounds, such as  $V_2O_5$ <sup>7</sup>,  $RuO_4$ <sup>8</sup>,  $MnO_2$ <sup>9</sup>, and  $OsO_4$ <sup>10</sup> have been used as catalysts for the conversion of olefins to epoxides. This can lead to forming two stereogenic carbons in one step, and the epoxide product can be converted to a variety of other useful compounds.

Vanadium(V)oxide and other acidic metal oxides (Cr, Mo, Nb, Ta, Th, V, W, Zr) catalyze the reactions of hydrogen peroxide via forming oxo or peroxometal complexes (Figure 1.1)<sup>11</sup>.

Figure 1.1: Epoxidation Catalytic Cycle



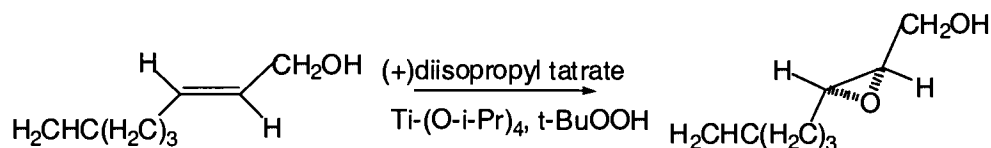
Transition metal complexes can exert the following four possible effects<sup>12</sup>: (1) Activation of reacting species by coordination, which offers alternative pathways with lower Gibbs free energies of activation. Examples are forming oxo or peroxy metal complexes to avoid spin forbidden reactions of dioxygen, (2) structural selectivity effect due to steric and (or)



electronic factors; (3) providing a pathway for inner-sphere or outer-sphere electron transport in the case of 2-centered redox catalysis, as in the catalysis by  $\text{PdCl}_2\text{-CuCl}_2$  in oxidation of ethylene to acetaldehyde; and (4) providing a pathway for coupled electron and energy transport. This last effect is important in electro-catalysis and photo-catalysis, as well as in ATP catalysis of some biological redox reactions.

In particular, the Sharpless asymmetric epoxidation<sup>13</sup> provides enantioselective product control through the use of either (+) or (-) tartrate ester. (Figure 1.2)

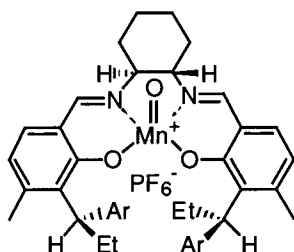
Figure 1.2: Sharpless Asymmetric Epoxidation



The enantioselective oxidation process is believed to involve a titanium complex in which the chirality of the tartrate ester controls the orientation of allylic alcohol. During the transition state, the oxygen atom from peroxide is transferred to the double bond. This reaction can be done with catalytic amounts of titanium isopropoxide and the tartrate ester. In addition, by using molecular sieves to remove water, both the rate and enantioselectivity of the reaction are enhanced.

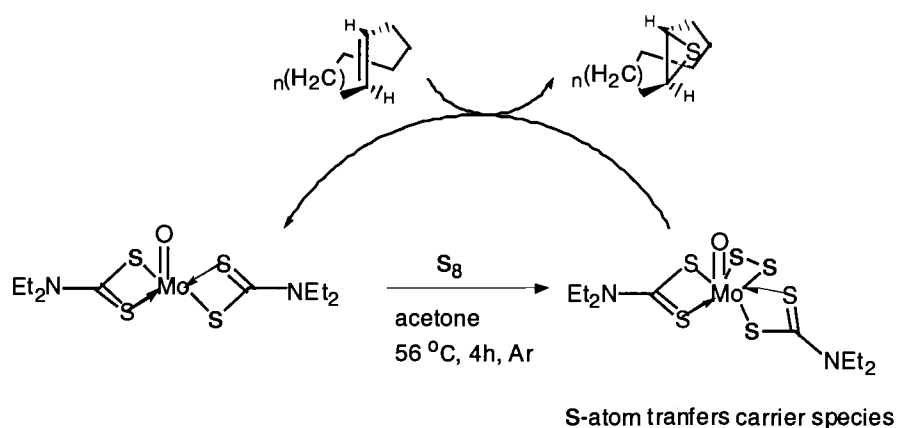
In 1990, Jacobsen reported unfunctionalized alkenes could be epoxidized with high enantioselectivities using chiral manganese(III) salen<sup>14</sup> (Figure 1.3) in combination with a stoichiometric amount of a simple oxidant such as aqueous hypochlorite, iodosylarenes and amine *N*-oxides. For example, asymmetric epoxidation of *cis*- $\beta$ -methylstyrene by commercial bleach (NaOCl) afforded (*R,S*)-*cis*- $\beta$ -methylstyrene oxide in 87% yield and 82% ee.

Figure 1.3: Jacobsen-Suzuki asymmetric epoxidation catalyst



For S-atom transfer, to date little is known about how the catalytic S-atom transfer compares to O-atom transfer. Adam<sup>15</sup> and co-workers developed a molybdenum oxo complex that efficiently catalyzes the sulfur atom transfer to alkenes to make their episulfides. Stereoselective reaction of trans-cyclooctene were obtained in high yield from catalytic episulfidation by elemental sulfur catalyzed by Mo(O)(S<sub>2</sub>)(S<sub>2</sub>CNEt<sub>2</sub>)<sub>2</sub> as shown in Figure 1.4.

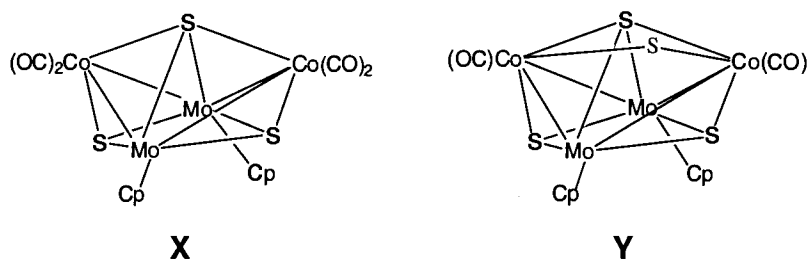
Figure 1.4: Episulfidation Catalyzed by Molybdenum Complex



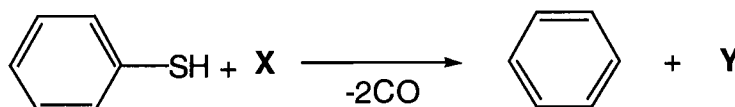
In contrast to forming C-S bonds, molybdenum<sup>16</sup> is used in hydrodesulfurization (HDS) catalysts for treating heavy crude oil in the petroleum industry. The catalyst typically consists of small clusters of molybdenum disulfide with low concentrations of cobalt or nickel additives to promote chemical reaction.

Figure 1.5: Mo/Co/S Cluster and an Desulfurization Reaction

a) Mo/Co/S cluster



## b) Desulfurization of ArSH by Mo/Co/S Cluster



Clusters **X** and **Y** are used as models for the “CoMoS” phase in for study of HDS catalysts. The nature of these complexes is still under investigation and has been the subject of interest for nearly 30 years.

### 1.2 Electronic Structure of Metal Terminal Oxo Complexes

Many catalytic O-atom transfer reactions can be described<sup>18</sup> by Figure 1.6. Metal oxidation and substrate reduction will be enhanced by a strongly reducing metal center, a strong M-O bond, and an oxygen atom donor with a relatively weak X-O bond. The oxygen atom donor (**SO**), such as O<sub>2</sub>, H<sub>2</sub>O<sub>2</sub>, PhIO, *m*-ClC<sub>6</sub>H<sub>4</sub>CO<sub>3</sub>H, *t*-BuOOH, Me<sub>2</sub>SO, epoxides or amine *N*-oxides, donates an oxygen atom to the transition metal complex, **M**, forming either an oxo- or peroxometal complex, **MO**. The oxo- or peroxometal complex can either transfer the newly acquired oxygen atom back to **S** or it can transfer the oxygen atom to the oxygen atom acceptor **R**. The most common oxygen atom acceptors are olefins, sulfides, tertiary

phosphines and phosphates whose basicities or nucleophilicities usually increase with the number of alkyl groups.

Figure 1.6: Catalytic O-atom Transfer Reaction Cycle

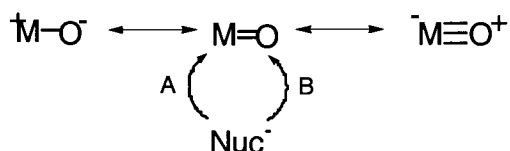


Oxometal groups<sup>18</sup> which have been structurally defined by X-ray diffraction are MO, linear MO<sub>2</sub>, bent MO<sub>2</sub> and pyramidal MO<sub>3</sub>. In general, metal oxo bonds have length of 1.6-1.8 Å and stretching frequency in the range 850-1100 cm<sup>-1</sup>, both properties establishing their multiple-bond character. Metal-oxo bonds are usually designated as M=O, with recognition that bond order may vary depending on the d<sup>n</sup> configuration.

The reactivity of an oxometal can be described by resonance forms which show that each canonical form will describe different reactivity for the metal and oxygen. Typically for metal oxides the LUMO is localized on the metal, which is subject to attack and coordination by nucleophiles<sup>19</sup>. However, polarization of the oxo group can lead oxygen to be subjected to attack by nucleophiles as well. This can be ascribed to lowering of the

energy of the LUMO orbital,  $\pi^*$ . The LUMO can attain more oxygen character, or the metal can make the oxygen electrophilic<sup>20</sup>.

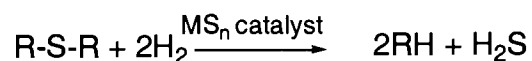
Figure 1.7: Resonance Forms of Metal Oxide



### 1.3 C-O and C-S Cleavage Mediated By Cp\*Rhenium Oxo Complex

Metal oxo complexes mediate cleavage of C-O bonds with concomitant formation of one or more new M=O bonds. This can be used in converting biomass to alkenes with high complexity. Biomass is the most abundant source of carbon but most parts are composed of carbohydrates which are often too oxygen-rich to be of any direct value without extensive modification. In addition, selective removal of oxygen can retain stereocenters while reducing structural complexity<sup>21</sup>.

The chemistry of C-S bond cleavage can be exploited in hydrodesulfurization in large scale industrial processes to remove sulfur from petroleum via hydrogenolysis.

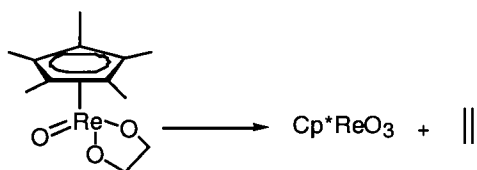


Desulfurization in this process is catalyzed by metal sulfides, typically  $\text{MoS}_x/\text{CoS}_y$ , but sulfides of rhenium, ruthenium, and other metals are even more active<sup>23</sup>. Both organometallic and inorganic systems have been studied as homogeneous models for HDS. For instance, the complex species  $\text{Cp}^*_2\text{TiS}^{24}$ ,  $\text{Cp}_2\text{MoS}_4^{25}$ , and  $(\text{PR}_3)_6\text{Rh}_2\text{S}_2^{2+}$  (26) have been known to activate  $\text{H}_2$  in this process.

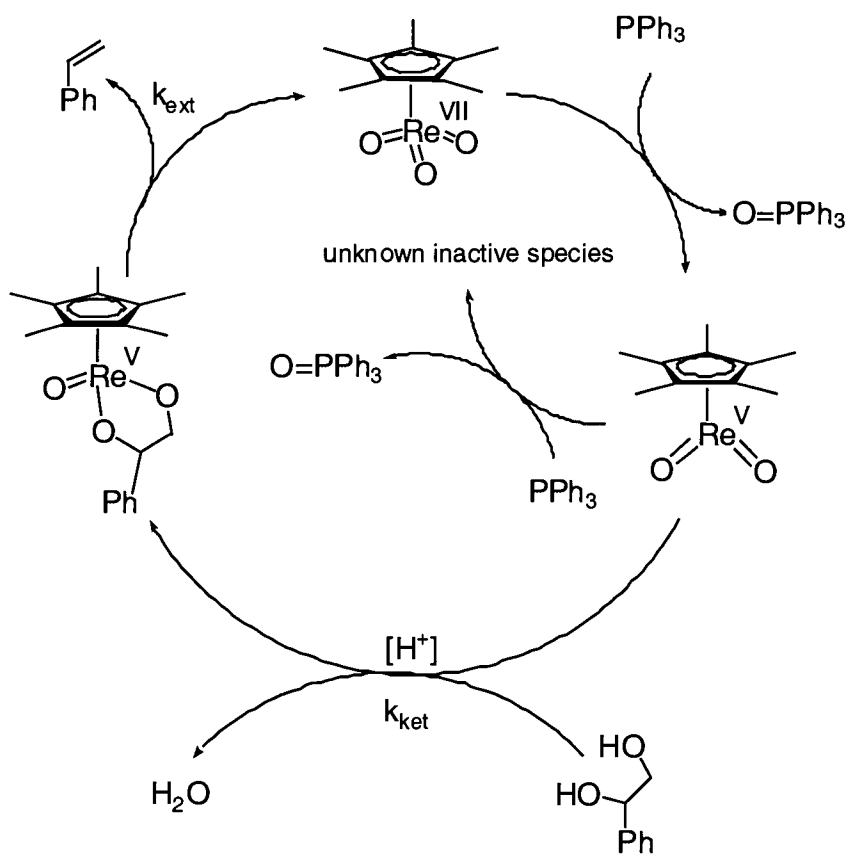
In principle, molybdenum sulfides are the major HDS catalysts; the reactivity of thiomolybdenates such as  $\text{MoS}_4^{2-}$  have been of particular interest to understand the catalytic cycle. Unfortunately, thiomolybdenates display little or no affinity for alkenes, dihydrogen, or the organosulfur species found in petroleum<sup>27</sup>. In contrast,  $\text{ReS}_4^-$ , which is isoelectronic and isostructural with  $\text{MoS}_4^{2-}$ , reacts with alkenes and alkynes to produce the tetrahedral  $d^2$  adducts  $\text{ReS}_2(\text{S}_2\text{alkene})^-$  (28). Recent interest in rhenium oxo chemistry highlights the structural diversity of  $\text{LReO}_n$  systems and the practical possibility for adjusting overall thermodynamics through structural modifications of the organorhenium compound.

The exploration of catalytic rhenium mediated O-atom transfer from diols and polyols to alkenes and allylic alcohols was recognized after the report of alkene extrusion from rhenium(VII)diolate complexes by Herrmann in 1987<sup>29</sup> (Figure 1.8). The diolate complex was observed to cyclorevert to  $\text{Cp}^*\text{ReO}_3$  ( $\text{Cp}^*$  = pentamethylcyclopentadienyl) and ethylene in refluxing toluene.

Figure 1.8: Alkene Extrusion



In particular, catalytic deoxygenation or conversion of vicinal diols or polyols to alkene had been studied by Cook and Andrews in 1996 (Figure 1.9)<sup>30</sup>.

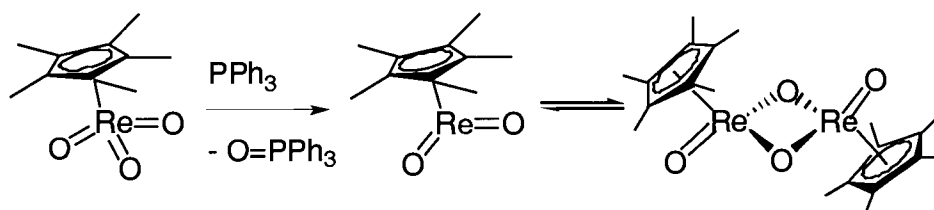
Fig 1.9: Catalytic Cycle of  $\text{Cp}^*\text{ReO}_3$ 



The catalytic cycle involves *in situ* reduction of  $\text{Cp}^*\text{ReO}_3$  with triphenylphosphine. When the rhenium diolate complex cycloreverts it gives alkene and  $\text{Cp}^*\text{ReO}_3$  which is reduced and returned to the deoxygenation catalytic cycle. However, the catalytic cycle is deactivated by forming an unknown species. The result is low turnover numbers ranging from 1 to 60.

The stoichiometric reduction of  $\text{Cp}^*\text{ReO}_3$  with oxophilic  $\text{PPh}_3$  results in the formation of the bridging oxo dimer  $(\text{Cp}^*\text{ReO})_2(\mu\text{-O})_2$  (Figure 1.10)<sup>31</sup>. Fragmentation of the dimer to the reactive monomer,  $\text{Cp}^*\text{ReO}_2$ , was observable by both NMR and UV-vis spectroscopy<sup>32</sup>.

Figure 1.10: Dimerization of  $\text{Cp}^*\text{ReO}_2$

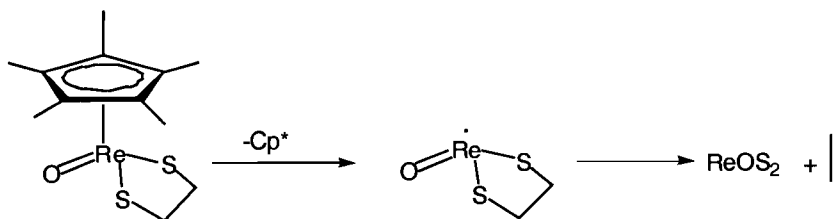


A deoxygenation process for epoxides was developed using catalytic amounts of  $\text{Cp}^*\text{ReO}_3$ <sup>33</sup>. The catalytic cycle is similar to the deoxygenation process for diols. Again, low turnover numbers were observed for each of the epoxides; this was attributed to formation of a tetranuclear cluster that was unreactive to epoxides; This originated from conproportionation of

reduced and oxidized intermediates. The crystal structure of the cluster was elucidated by X-ray crystallography and exhibited a unique IR peak at  $736\text{ cm}^{-1}$ . Increasing the concentration of triphenylphosphine led to improved conversion from  $<5\%$  to  $50\%$  by reducing any amount of  $\text{Cp}^*\text{ReO}_3$  and preventing  $\text{Cp}^*\text{ReO}_3$  from conproportionating with  $\text{Cp}^*\text{ReO}_2$ .

For a sulfur analog study, cycloreversion of  $\text{Cp}^*$ rhenium(V)ethane dithiodiolate was reported by Herrmann<sup>34</sup>. The dithiodiolate analogs were more stable than diolate; however, on heating to  $200\text{ }^\circ\text{C}$  over 30 minutes a quantitative production of ethylene was observed (though none of the rhenium species was characterized). There are two possibilities to generate ethylene: (1) in the cycloreversion process or (2) from multi step fragmentation(Figure 1.11).

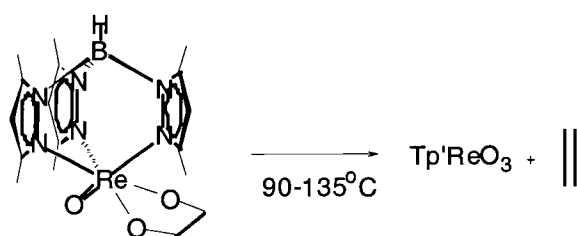
Figure 1.11: Multi Step Fragmentation of  $\text{Cp}^*$ Rhenium Ethanedithiodiolate



#### 1.4 C-O and C-S Cleavage Mediated By Tp'Rhenium Oxo Complex

The sterically bulkier Tp' ligand (Tp'=hydrido-tris-(3,4-dimethyl pyrazoyl)borate) was developed and known as a "cyclopentadienyl equivalent" because it is anionic, 6 electron donor<sup>35</sup>. Because of its steric bulk, it was predicted to suppress formation of the dimeric bridged oxo compound  $[(LReO)_2(\mu-O)_2]$ , but it should have similar chemistry such as cycloreversion. In 1999, Gable and co workers<sup>36</sup> reported that Tp'rhenium(V) diolates also cyclorevert stereoselectively to form  $Tp'ReO_3$  and alkenes (Figure 1.12).

Figure 1.12: Cycloreversion of Tp'Rhenium Diolate



In contrast to diolate chemistry, Gable and Chuawong<sup>37</sup> reported the high thermal stability of Tp'Re(V) ethanedithiolate which is unlike the corresponding Tp'Re(V)ethanediolate. This dithiolate was heated at 120 °C in benzene or toluene for at least one week. No alkene or new rhenium

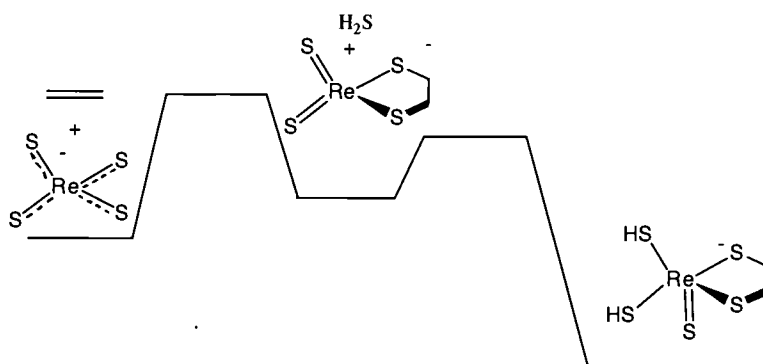
compound was observed. The barrier for cycloreversion was ascribed to thermodynamic stability of Tp'Re(V)ethanedithiodiolate by comparison of calculated reaction energies based on DFT calculations performed at the B3LYP/LACVP\*\* level. The analysis reveals that substitution of each sulfur raises the  $\Delta E_{\text{rxn}}$  for alkene extrusion by about 10 kcal/mol.

### **1.5 Binding of alkene to Tetrathioperrhenate Anion (ReS<sub>4</sub><sup>-</sup>) and Influence of Hydrodensulfide and Thiols**

Tetrathioperrhenate anion, ReS<sub>4</sub><sup>-</sup>, is isoelectronic<sup>38</sup> with OsO<sub>4</sub> or MoS<sub>4</sub><sup>2-</sup> and it react with alkenes. Rauchfuss reported in 1999 that ReS<sub>4</sub><sup>-</sup> reversibly binds with alkenes<sup>39</sup>. Thermodynamic parameters of binding for norbornene was obtained by evaluating K<sub>eq</sub> over the range of 5-50 °C,  $\Delta H^\circ = -12.67 \text{ kcal}\cdot\text{mol}^{-1}$  and  $\Delta S^\circ = -23.44 \text{ cal}\cdot\text{mol}^{-1}\text{K}^{-1}$ . The binding of ReS<sub>4</sub><sup>-</sup> to norbornene appeared to be a favorable process due to high equilibrium constant observed at 23 °C in acetonitile.

The influence of hydrogen sulfide and thiols on the binding of alkenes to ReS<sub>4</sub><sup>-</sup> was also measured. The Re(S)(S<sub>2</sub>)(alkene)(SH)<sub>2</sub><sup>-</sup> derivatives were the product . The qualitative reaction coordinate in which ethylene was used as alkene is shown in Figure 1.13.

Figure 1.13: Qualitative Reaction Coordinate of  $\text{ReS}_4^-$ , Hydrogen Sulfide, and Ethylene



The first step was reported to be favored with high equilibrium constant. The second step is even more favorable which can explain by the spectator sulfido effect<sup>40</sup>, " Addition of RSH across a  $\text{Re}=\text{S}$  bond provides the very highly stabilized  $\text{X}_4\text{Re}=\text{S}$  species".

### 1.6 Direct Atom Transfer vs. Ring Expansion

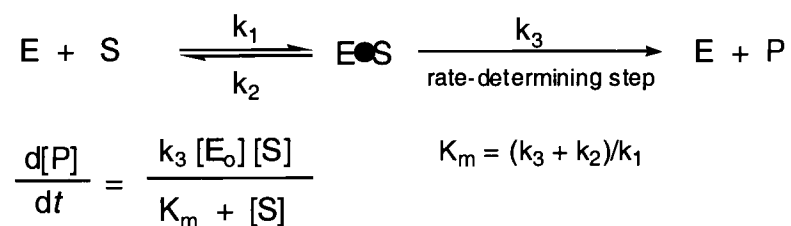
In 1999, Gable and Brown reported epoxides can be subjected to catalytic O-atom transfer<sup>41</sup> by a reduced rhenium species,  $\text{Tp}'\text{ReO}_2$ , generating *in situ* by reduction of  $\text{Tp}'\text{ReO}_3$  using triphenylphosphine or triethylphosphite at 75-105 °C. *cis*-Epoxides react faster than *trans*-epoxides, and terminal alkene epoxides proceed faster than internal alkene epoxides suggesting the reaction is governed by steric issues. Alkyl substituents slow the reaction in comparison with aryl groups. The choice of

functional groups also can interfere with the reaction, as in the presence of a nitro group a conversion of epoxide to alkene was low.

A linear free energy relationship study<sup>41</sup> of a series of *para*-substituted styrene oxides, as substrates in a Hammett study, showed electron donors had a  $\rho = -1.28$ , while electron-withdrawing groups had a  $\rho = +0.52$  which results in an upward V-shaped Hammett plot. It indicates a change in mechanism or at least two competing pathways.

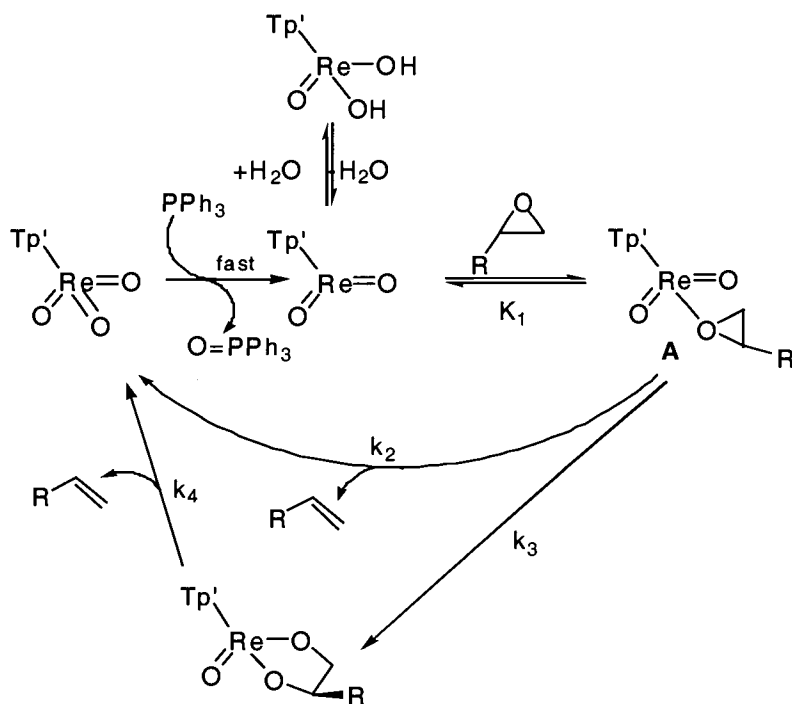
Saturation kinetics were reported<sup>42</sup> in deoxygenation of *cis*-stilbene oxide and styrene oxide with  $\text{Tp}'\text{ReO}_3/\text{PPh}_3$ . From an observed rate versus concentration plot at a constant concentration of  $\text{Tp}'\text{ReO}_3$ , the reaction rate increased with increasing epoxide concentration until a maximum rate was reached. This kinetic behavior was attributed to an enzymology model which is described by the Michaelis-Menten equation (Figure 1.14).

Figure. 1.14: Michaelis-Menten Enzymatic Model



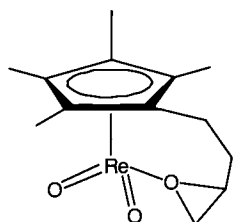
Since metastable diolates were obtained which cyclorevert to  $\text{Tp}'\text{ReO}_3$  and alkene with retention of stereochemistry, a ring expansion needs to part of mechanism. In the meantime, an initial "burst" for *cis*-stilbene formation was also observed. The alkene/diolate ratio was 4.4 after six minutes at  $75^\circ\text{C}$ ; even though cycloreversion of diolate is slow,  $k = 4.62 \times 10^{-7} \text{ M/s}$ . This rate constant was too slow to explain the observed rate of alkene production under catalytic conditions. Thus another pathway must be direct O-atom transfer. Deoxygenation was proposed<sup>43</sup> as shown in Figure 1.15.

Figure 1.15: Deoxygenation Catalytic Cycle



A coordinated tethered epoxide rhenium complex, 3,4-epoxy-1-butyltetramethylcyclopentadienyltrioxorhenium(VII)<sup>44</sup>, was synthesized by the Gable group in 2003. This compound confirms the existence of **A** during the reaction.

Figure 1.16: Coordinated Tethered Epoxide Rhenium Complex



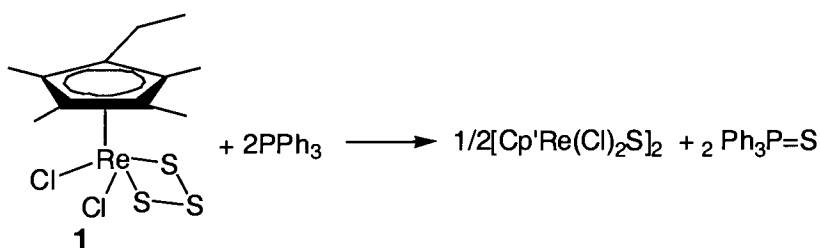
### 1.7 Rhenium Terminal-Sulfido Complexes

The rhenium terminal sulfido group is of particular interest because of the potential for comparing reactivity and electronic structures with a range of multiply bonded terminal ligands from group 14 through 16. Rakowski-Dubois<sup>45</sup> and coworkers reported the synthesis and reactivity of  $\text{Cp}'\text{Re}=\text{S}$  ( $\text{Cp}' = 1\text{-ethyl-tetramethylcyclopentadienyl}$ ) derivatives including reactivity of each species in 2003. Rapid abstraction of two sulfur atoms with only half of the rhenium starting material consumed to give  $\eta^2$ -disulfide ligand  $\text{Cp}'\text{ReCl}_2(\text{S}_2)$  from  $\text{Cp}'\text{Re}(\eta^2\text{-S}_3)\text{Cl}_2$  and 1 equivalent of triphenylphosphine. A sulfur-free complex,  $\text{Cp}'\text{ReCl}_2$ , was obtained when



more than 2 equivalent of phosphine reagent were used. The dimer  $[\text{Cp}'\text{ReCl}_2\text{S}]_2$  was obtained with 1.8 equiv of  $\text{PPh}_3$  as shown in Figure 1.17.

Figure 1.17 Reaction of  $\text{Cp}'\text{Re}(\eta^2\text{-S}_3)\text{Cl}_2$  with  $\text{PPh}_3$

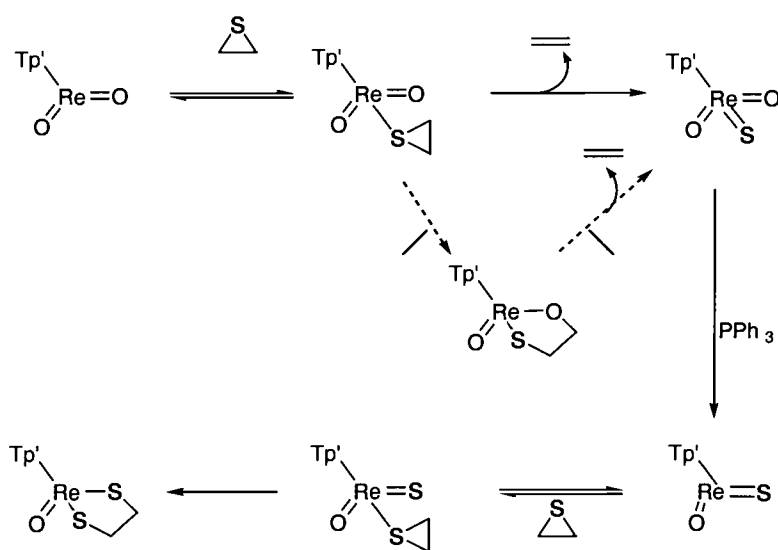


In a similar manner, a terminal sulfido ligand complex,  $\text{Cp}'\text{Re}(\text{S})(\text{S}_2)$  **2**, was obtained 30 % yield by reacting **1** with bis(trimethylsilyl)sulfide. In addition,  $\text{Cp}'\text{Re}(\text{S}_3)(\text{S}_2)$ , **3** was formed in this reaction. The reaction of **3** with 2 equivalent of  $\text{PPh}_3$  gave **2** and  $\text{Ph}_3\text{P}=\text{S}$  in a rapid reaction. Complex **2** was used to compare the relative reactivities and electrochemical behavior with the oxo analogue,  $\text{Cp}'\text{Re}(\text{O})(\text{SC}_2\text{H}_4\text{S})$ , **4**. Both compounds are stable in air, when **2** was reacted with 5-6 equivalent of water in toluene- $d_8$  at  $60^\circ\text{C}$  for 24 h, 40% of **2** was converted to **4**. The cyclic voltammograms of these oxo and sulfido species showed the sulfido complex is both easier to reduce and easier to oxidized than the oxo analog. This results are consistent with Parkin's report<sup>46</sup> that the  $\text{M}=\text{S}$  group is more reactive than  $\text{M}=\text{O}$  due to the weaker  $\pi$ -donor ability of  $\text{S}^{2-}$ .

### 1.8 Desulfidation Catalytic Cycle Mediated by Rhenium Oxo Complex

Desulfidation of an episulfide mediated by a Tp'rhenium oxo complex is analogous to deoxygenation of epoxide. Chuawong reported a 30% yield of Tp'Re(V)ethanedithiodiolate was obtained as a product from reaction of ethylene episulfide with Tp'ReO<sub>3</sub>/PPh<sub>3</sub> at room temperature<sup>47</sup>. Since mono- and dithiodiolate complexes were shown to be thermally stable (no cycloreversion to alkene) for more than a week at 120°C, then the direct S-atom transfer from the episulfide must occur at some point to get to the observed dithiodiolate. The proposed mechanism<sup>47</sup> is shown in Figure 1.18.

Figure 1.18: Catalytic Cycle of Desulfurization



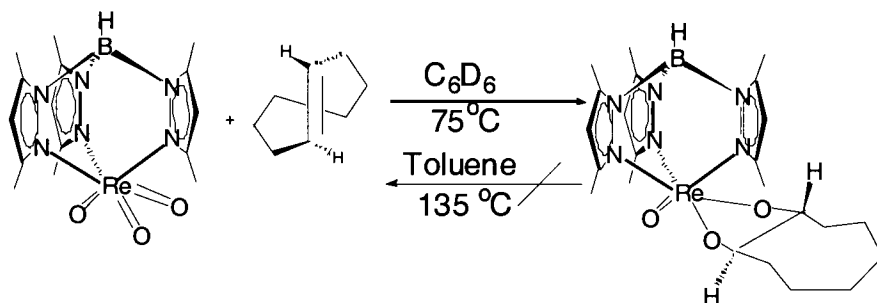
However, it seems unusual that the system switches from selective S-atom transfer (first step) to selective ring expansion (last step). This mechanism also requires selectivity in atom transfer to  $\text{PPh}_3$ .

### 1.9 Conclusion of the Literature Review and Research Goals

A number of O- and S- atom transfer catalysts were developed for industry and academic purposes.  $\text{Tp}^*\text{ReO}_3$  was developed to be used in the deoxygenation process for epoxides leading to retention of the stereochemistry in the alkene product. The catalytic cycle was reported by Gable and Brown showed that direct atom transfer and ring expansion are competing in this deoxygenation cycle mediated by  $\text{Tp}^*\text{ReO}_3$ ; however, there is some need to get more insight the proposed mechanism.

In this study we first attempted to determine whether a strained epoxide could allow measurement of rate constants for individual processes involved in deoxygenation mediated by rhenium oxo complexes. Early indications of Gable's work appeared to lend weight to our hypothesis that *trans*-cyclooctene, a strained alkene, thermodynamically favors formation of a *trans*-cyclooctane diolate<sup>48</sup> which is stable to a cycloreversion in toluene at 135 °C.

Figure 1.19: Thermodynamically Favored of *trans*-Cyclooctane Diolate



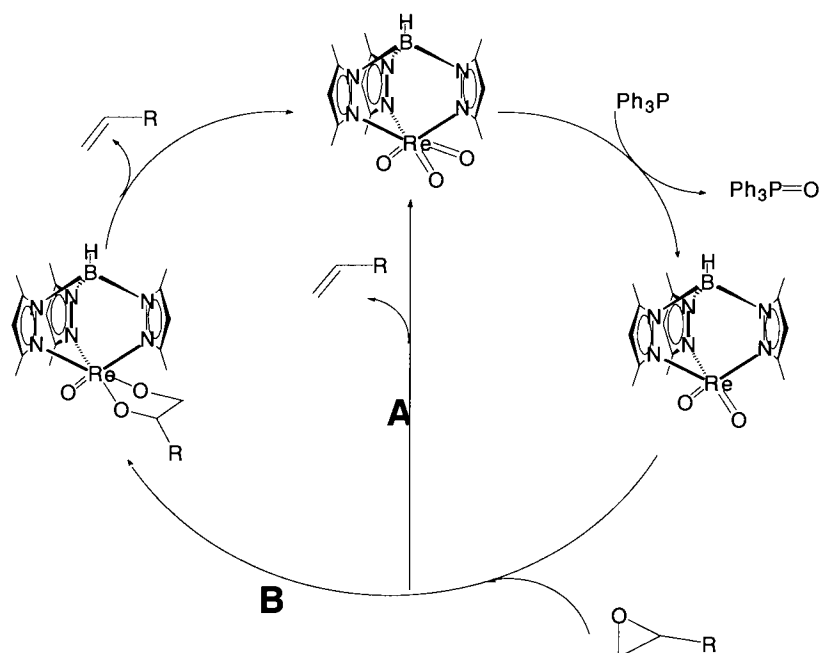
A second challenge was based on the first, to see the impact of sulfur for oxygen substitution on product, rate and selectivity. We expected to observe similar chemistry by using cyclooctene episulfide, as using ethylene episulfide. We expected that the *trans*-cyclooctene episulfide in particular could illustrate atom transfer versus ring expansion selectivity for the sulfur analogs.

## Chapter 2. Results and Discussion

Given the interest in developing deoxygenation catalysts, numerous reagents are known to deoxygenate epoxides<sup>49</sup>. One example, the low valent tungsten halide derived from  $WCl_6$ , is used to convert epoxides to olefins; in some cases chlorohydrins are formed as by-products and limited stereoselectivity for acyclic di- and tri-substitued epoxides is seen<sup>50</sup>. Stoichiometric amounts of tungsten are required. The development of a catalytically deoxygenating species would be attractive.

A deoxygenation process mediated by rhenium oxo complexes was developed by the Gable group. A catalytic cycle for deoxygenation was proposed in the system by which  $Tp'ReO_3/PPh_3$  ( $Tp'$ = hydrido-*tris*-(3,5-dimethyl pyrazoyl)borate) reacts with epoxides (Figure 2.1). O-atom transfer was observed to occur via two distinct processes: (1) a ring expansion mechanism to form a metastable diolate intermediate which cycloreverts to alkene and  $Tp'ReO_3$ , and (2) a direct atom transfer mechanism to form alkene and  $Tp'ReO_3$ .

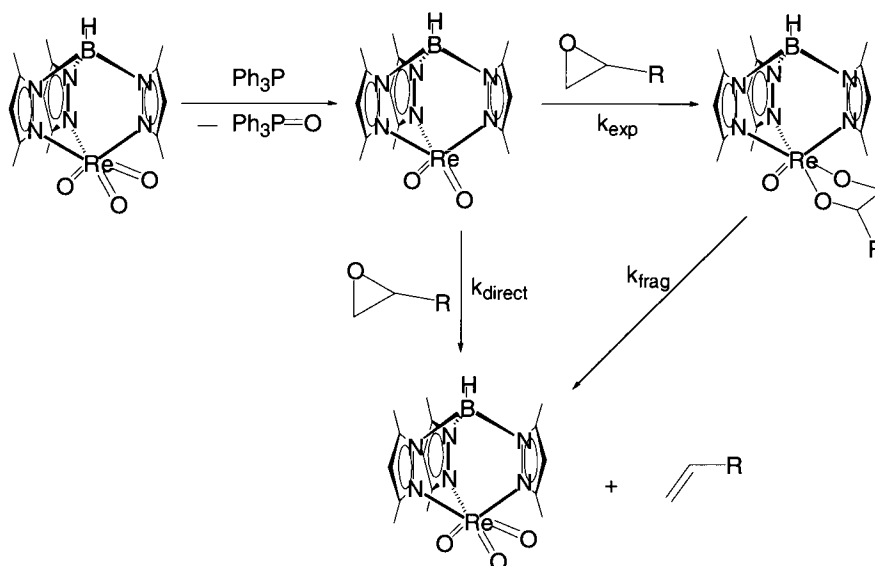
Figure 2.1: Catalytic Cycle of Deoxygenation



## 2.1 Independent Kinetic Measurement

To answer questions on the selectivity for each process, we need to know reaction rates of these processes (Figure 2.2).

Figure 2.2: Direct Atom Transfer VS Ring Expansion



If we can measure the rate of ring expansion directly, then we could infer from selectivity ratios the rate of direct atom transfer. It was previously known that  $\text{Tp}'\text{Re}(\text{O})(\textit{trans}\text{-cyclooctane-1,2-diolate})$  is thermodynamically favored and would not cyclorevert to give *trans*-cyclooctene (Figure 1.19).

Therefore, we set out to discover whether thermodynamically blocking the diolate-to-alkene reaction allows measurement of  $k_{\text{exp}}$ ,  $k_{\text{frag}}$ , and  $k_{\text{direct}}$ .

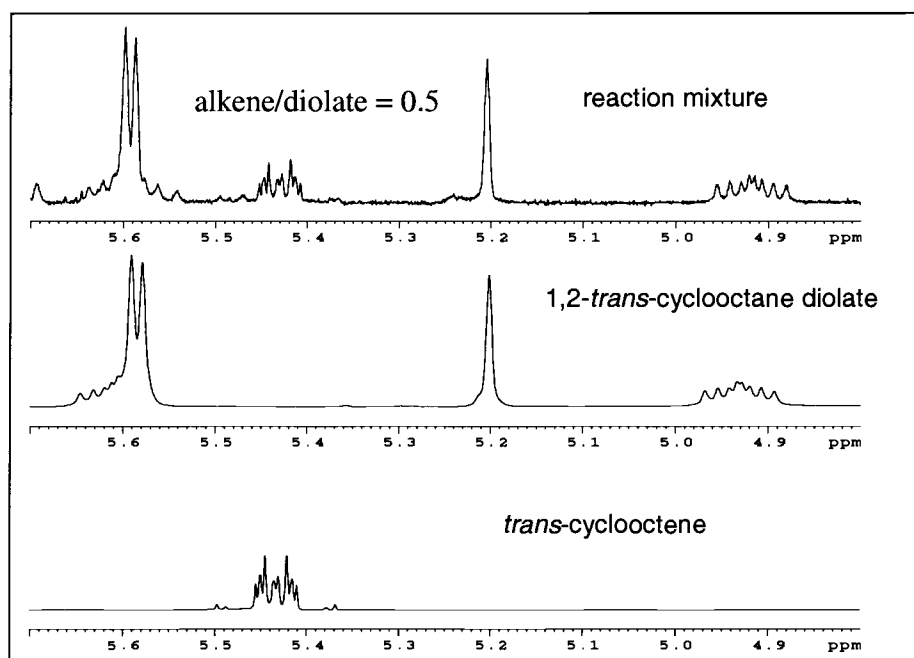
Reaction of insoluble solid  $\text{Tp}'\text{ReO}_3$  with  $\text{PPh}_3$  in  $\text{C}_6\text{D}_6$  at  $75^\circ\text{C}$  leads to formation of soluble  $\text{Tp}'\text{ReO}_2$ . This reacts with *trans*-cyclooctene oxide to form thermally stable *trans*-cyclooctane diolate with  $\text{C}_1$  symmetry. Stereoselective formation of *trans*-cyclooctene was also observed (alkene/diolate = 0.5) although 1,2-diolate is thermodynamically favored.

Tp'ReO<sub>3</sub> was previously shown to react with *trans*-cyclooctene to form the diolate<sup>48</sup>.

Deoxygenation of *trans*-cyclooctene oxide was followed in deuterated benzene at 75 °C by <sup>1</sup>H NMR under pseudo-first order kinetic conditions: epoxide:PPh<sub>3</sub>:Tp'ReO<sub>3</sub> = 5:3:1. Anisole or tetramethylsilane were used as internal integration standards. The sample tube was periodically removed and cooled to 25°C and the <sup>1</sup>H NMR spectrum was collected. The rate of ring expansion was estimated at different concentrations of Tp'ReO<sub>3</sub>.

The <sup>1</sup>H NMR spectrum of 1,2-diolate shows characteristic peaks of carbinolic protons on the cyclooctane ring at 4.97 ppm and 5.68 ppm in d<sub>6</sub>-benzene(Figure 2.3). *trans*-Cyclooctene has a distinct multiplet at 5.43 ppm.



Figure 2.3: Spectra of Pure *trans*-cyclooctane diolate and reaction mixture

Product diolate formation was observed after heating a sample for 6h at 75 °C. The pseudo-first order rate constants for *trans*-cyclooctene oxide deoxygenation at 75 °C were obtained at different epoxide concentrations: 0.0573 mM, 0.1146 mM, 0.1688 mM, 0.2256mM, and 0.6783 mM which ratio to 0.009 or 0.011 mM Tp'ReO<sub>3</sub> at 1:5, 1:10, 1:15, 1:20, and 1:60 in order. The psuedo-first order rate law is given by:

For reaction  $A \longrightarrow P$

Rate law  $-d[A]/dt = k_{\text{obs}}[A]$  ; Integrated rate law  $\ln[A]_t - \ln[A]_0 = -k_{\text{obs}}t$

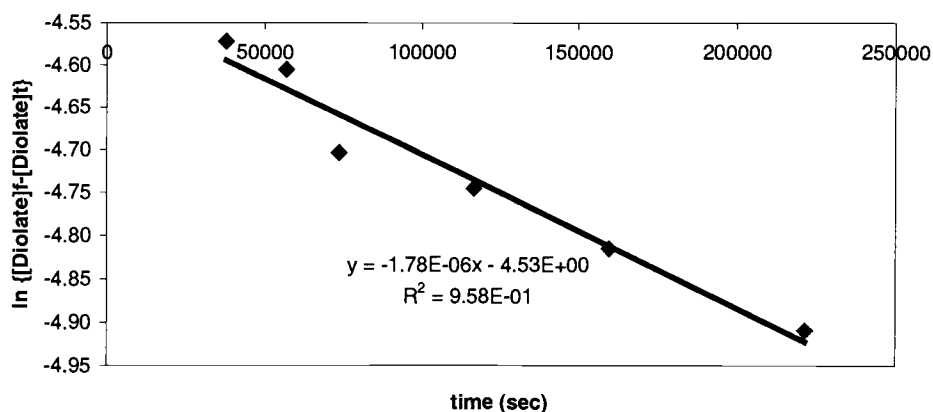
And  $k_{\text{obs}} = k[\text{epoxide}]$

The concentration of  $\text{Tp}'\text{ReO}_3$ ,  $[\text{A}]_t$ , is followed indirectly by measurement of the diolate signal at 4.97 ppm vs. anisole signal at 3.30 ppm. We assume  $[\text{Tp}'\text{ReO}_3] = [\text{Re}]_{\text{Total}} - [\text{Diolate}]$  and actually, the reactant we worry about is  $\text{Tp}'\text{ReO}_2$ ; if the reduction is fast,  $[\text{Tp}'\text{ReO}_2]_t = [\text{Re}]_{\text{Total}} - [\text{Diolate}]$ . The data did not show a good linear behavior as indicated by a low  $r^2$  value (Figure 2.4).

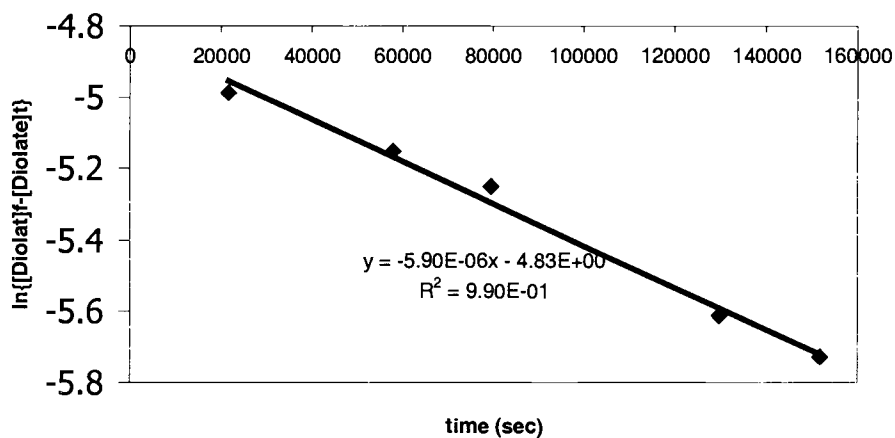
However, several attempts were performed to get a better pseudo-first order plot. The phase change that occurs as insoluble  $\text{Tp}'\text{ReO}_3$  is reduced by  $\text{PPh}_3$  to form  $\text{Tp}'\text{ReO}_2$  might affect the  $k_{\text{obs}}$ . By changing the amount of  $\text{Tp}'\text{ReO}_3$  from 3.0 mg to 2.4 mg, the disappearance of insoluble  $\text{Tp}'\text{ReO}_3$  was observed after 3 hours while a large amount of  $\text{Tp}'\text{ReO}_3$  still left after 6 hours passed for the larger scale.

Figure 2.4: Selected Pseudo-first Order Plots

a) 5:1 of trans-cyclooctene oxide :  $\text{Tp}'\text{ReO}_3$  ;  $\text{Tp}'\text{ReO}_3$  3.0 mg



b) 5:1 of *trans*-cyclooctene oxide:  $\text{Tp}'\text{ReO}_3$  ;  $\text{Tp}'\text{ReO}_3$  2.4 mg



Although the  $r^2$  value was better at low concentrations of epoxide, high concentrations led to low  $r^2$  values again. Selected  $k_{\text{obs}}$  values are shown in table 2.1.

Table 2.1:  $k_{\text{obs}}$  and half life of ring expansion for *trans*-cyclooctene oxide at different  $\text{Tp}'\text{ReO}_3$  amount

a)  $\text{Tp}'\text{ReO}_3 = 2.4$  mg

Epoxide: $\text{TpRe}_3$	[Epoxide] (M)	$r^2$	Half-Life $10^4(\text{sec}^{-1})$	$k_{\text{obs}} 10^{-6}(\text{sec}^{-1})$
5	0.0573	0.990	11.70	5.90
10	0.1146	0.983	7.80	8.89
15	0.1688	0.860	5.73	12.10

b)  $\text{Tp'ReO}_3 = 3.0 \text{ mg}$

Epoxide: $\text{TpRe}_3$	[Epoxide] (M)	$r^2$	Half-Life $10^4(\text{sec}^{-1})$	$k_{\text{obs}} 10^{-6}(\text{sec}^{-1})$
5	0.0573	0.958	38.94	1.78
20	0.2256	0.942	23.58	2.94
60	0.6783	0.979	16.08	4.31

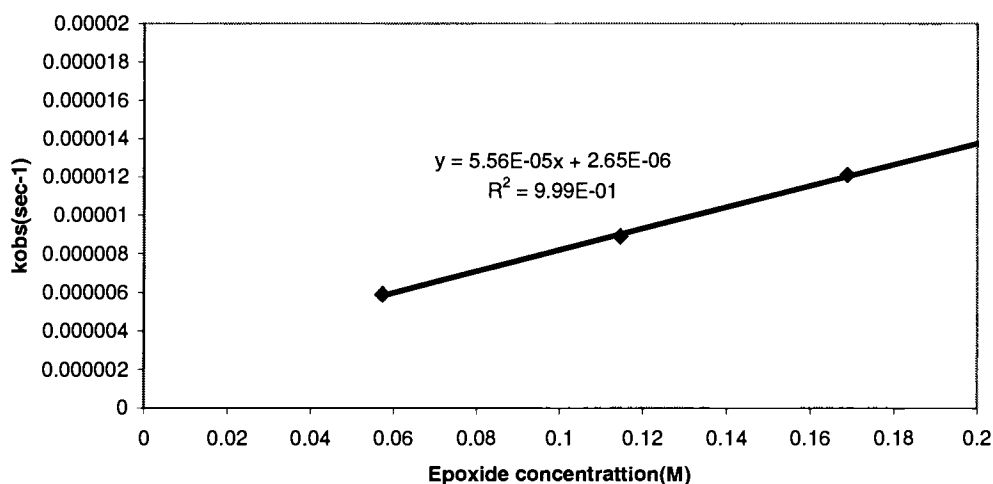
The ring expansion rate constant is given by:

$$\text{Rate of ring expansion} = k_{\text{exp}}[\text{epoxide}][\text{Tp'ReO}_3]$$

$$\text{where } k_{\text{obs}} = k_{\text{exp}}[\text{epoxide}]$$

Thus  $k_{\text{exp}}$  is a slope of linear plot between  $k_{\text{obs}}$  and concentration of epoxide. (Figure 2.5)

Figure 2.5: Ring expansion rate constant,  $k_{\text{exp}}$ ,  $\text{Tp}'\text{ReO}_3$  2.4 mg,  $\text{Tp}'\text{ReO}_3$  concentration = 9.0 mM



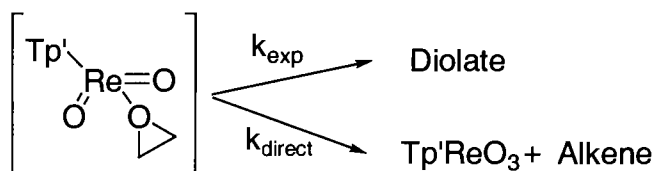
$k_{\text{exp}}$  is  $(5.56 \pm 3.97) \times 10^{-5} \text{ M}^{-1} \text{ s}^{-1}$ .

We observed a substantial amount of *trans*-cyclooctene in the reaction as confirmed by a characteristic peak of the vinylic proton of *trans*-cyclooctene at 5.43 ppm. The cyclooctene/diolate ratio in the products was 0.5:1. The GC-MS spectrum was conclusive in establishing *trans*-cyclooctene with a major peak at  $m/z = 110$ . Since *trans*-cyclooctane diolate is thermodynamically favored and would not cyclorevert to give alkene, *trans*-cyclooctene must form by direct O-atom transfer as noted previously. Alkene also underwent cyclocondensation with  $\text{Tp}'\text{ReO}_3$  to give diolate. Therefore diolate is not generated exclusively from ring expansion, and treatment of diolate formation as first order is not valid.

## 2.2 Parallel First-order Reactions

Formation of alkene competing with ring expansion for *trans*-cyclooctene oxide deoxygenation led us to new methodology to obtain  $k_{\text{exp}}$  and  $k_{\text{direct}}$ . As proposed by Gable<sup>43</sup>, an epoxide coordinated to rhenium is an intermediate to give either diolate or alkene (Figure 2.6).

Figure 2.6: Epoxide Coordinated to Re as an Intermediate



Direct O-atom transfer and ring expansion rate constants were recalculated on the basis that under pseudo first-order conditions the coordinated epoxide concentration over time was equal to  $\text{Tp}'\text{ReO}_2$  concentration. Provided equilibrium formation of epoxide complex is fast,  $k_{\text{exp}}/k_{\text{direct}}$  is equal to  $[\text{diolate}]/[\text{alkene}]$ . The amount of diolate and alkene at any time are given by:

$$[\text{diolate}] = k_{\text{exp}}[\text{Tp}'\text{ReO}_3]_0 / (k_{\text{exp}} + k_{\text{direct}}) \{1 - \exp[-(k_{\text{exp}} + k_{\text{direct}})t]\}$$

$$[\text{alkene}] = k_{\text{direct}}[\text{Tp}'\text{ReO}_3]_0 / (k_{\text{exp}} + k_{\text{direct}}) \{1 - \exp[-(k_{\text{exp}} + k_{\text{direct}})t]\}$$

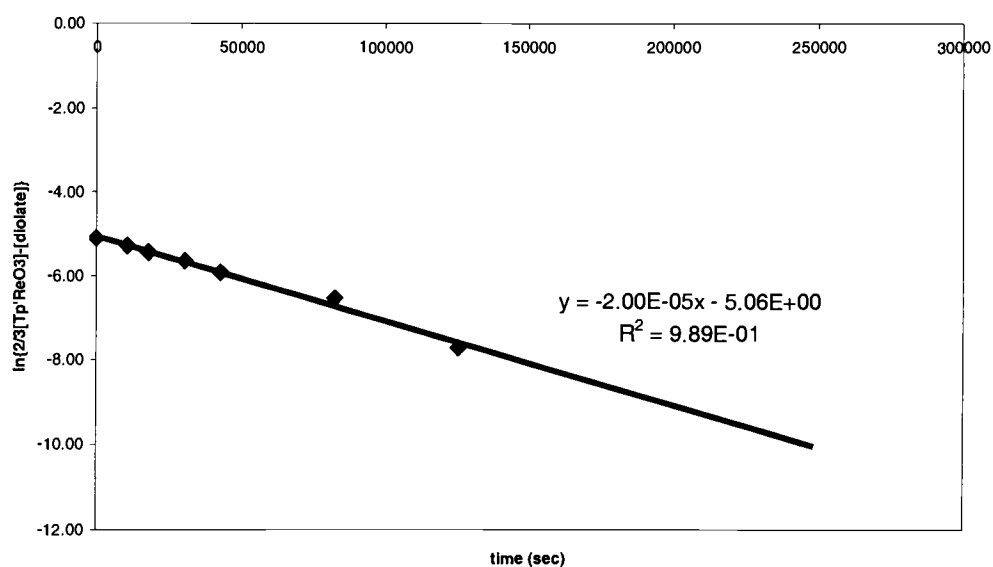
$$[\text{diolate}]/[\text{alkene}] = k_{\text{exp}}/k_{\text{direct}} = 2/1$$

$$\therefore [\text{diolate}] = 2/3[\text{Tp}'\text{ReO}_3]_0 \{1 - \exp[-3/2(k_{\text{exp}})t]\}$$

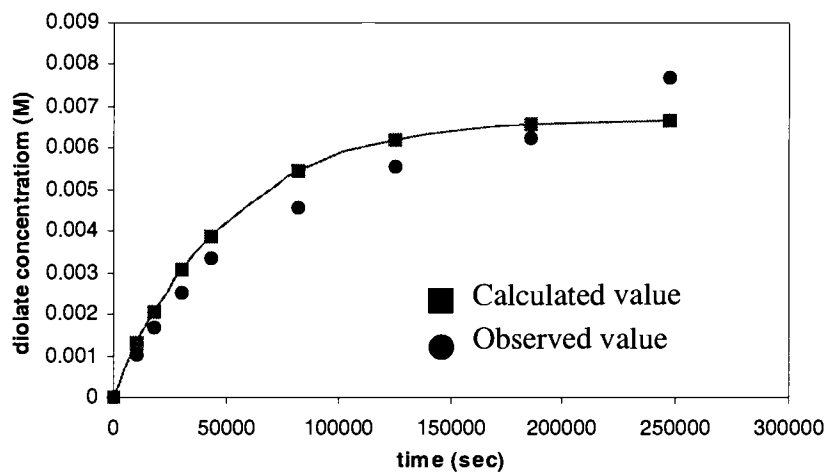
By plotting  $\ln\{(2/3)[\text{Tp}'\text{ReO}_3]_0 - [\text{diolate}]\}$  vs.  $t$ ,  $k_{\text{exp}}$  is equal to  $-2/3 \cdot \text{slope}$ .  
The  $k_{\text{exp}}$  then was used to simulate the diolate concentration over time comparing with the observed value (Figure 2.7).

Fig 2.7: Competition Reaction Model Plot

a) 60:1 epoxide:Tp'ReO<sub>3</sub>  $k_{\text{exp}} = (1.33 \pm 0.002) \times 10^{-5} \text{ sec}^{-1}$  and  $k_{\text{direct}} = (6.67 \pm 0.001) \times 10^{-6} \text{ sec}^{-1}$



b) Comparing calculated value with observed value, standard deviation = 0.0024



The  $k_{\text{direct}}$  and  $k_{\text{exp}}$  measurement at different concentration ratios of epoxide to diolate were calculated by the same methodology. All measurements gave the result in the same magnitude as shown in Table 2.2.

Table 2.2: Summarized  $k_{\text{direct}}$  and  $k_{\text{exp}}$

Epoxide: TpReO <sub>3</sub>	[Epoxide] (M)	$k_{\text{exp}}$ $10^{-5}(\text{sec}^{-1})$	$k_{\text{direct}}$ $10^{-6}(\text{sec}^{-1})$	$r^2$
5	0.0573	1.31	6.55	0.939
15	0.1688	1.09	5.45	0.941
20	0.2256	1.23	6.15	0.986
60	0.6783	1.33	6.65	0.989



From Table 2.2, the average of  $k_{\text{exp}}$  is  $(1.24 \pm 0.03) \times 10^{-5} \text{ sec}^{-1}$  and  $k_{\text{direct}}$  is  $(6.20 \pm 0.02) \times 10^{-6} \text{ sec}^{-1}$ .

### 2.3 Kinetic Measurement of 1,2-*cis*-Cyclooctene Oxide

*cis*-Cyclooctene oxide prefers to give more alkene, and also it was known that at temperatures above 105 °C 1,2-*cis*-cyclooctanediolate cycloreverts<sup>35</sup> to give an alkene and  $\text{Tp}'\text{ReO}_3$ , not like 1,2-*trans*-cyclooctane diolate. A control experiment was done to estimate the thermal stability range of diolate for this diolate at 75 °C.

1,2-*cis*-Cyclooctanediolate (3.0 mg) was dissolved in  $\text{C}_6\text{D}_6$  and anisole was used as an internal standard. The sample tube was periodically removed from a thermostatted water bath at 75 °C and cooled to 25°C and the  $^1\text{H}$  NMR spectrum was collected. No alkene formation was observed although the reaction was heated for 19 hours.

To estimate  $k_{\text{exp}}$  and  $k_{\text{direct}}$ , the same methodology as for *trans*-cyclooctene oxide was applied to a 45.16 mM mixture of *cis*-cyclooctene oxide of (5:1:3 epoxide: $\text{Tp}'\text{ReO}_3$ : $\text{PPh}_3$ ). *cis*-Cyclooctene, 0.33 mM, was observed initially after 3 hours at room temperature. After 5 minutes at 75 °C, 0.59 mM of *cis*-cyclooctene was formed and also there was no diolate.

After 24 hours 1.37 mM of alkene was observed, and the ratio of *cis*-cyclooctene/diolate was 24.5:1 at 75 °C. Thus,  $k_{\text{direct}}$  is  $5.07 \times 10^{-5} \text{ s}^{-1}$ ,  $r^2 = 0.993$ .  $k_{\text{exp}}$  must then be approximately  $2.07 \times 10^{-6} \text{ s}^{-1}$ .

Direct O-atom transfer dominates ring expansion for *cis*-cyclooctene oxide deoxygenation by observing alkene formation even at room temperature and slow rate of diolate formation.

## 2.4 Sulfur Analog Study

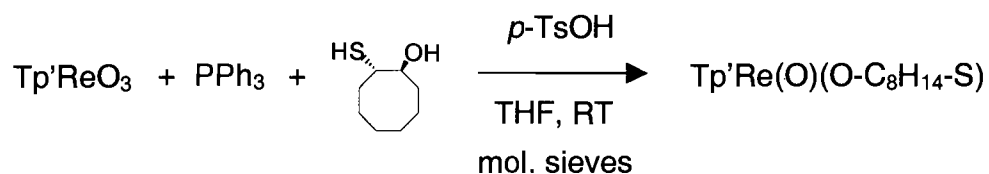
Metal sulfur chemistry has been investigated in catalysis of hydrodesulfurization systems (HDS), such as clusters of  $\text{MoS}_x/\text{CoS}_y$ . Sulfides of rhenium, ruthenium, and other metals are even more active<sup>23</sup>. Desulfurization of episulfides and dithiols mediated by rhenium oxo complex has been explored by the Gable group. A desulfidation catalytic cycle was proposed in 2001 but some issues on S-atom transfer selectivity and activity of each species involved in the reaction including some parts of proposed catalytic cycle needed more study.

As previously mentioned in section 1.4, the thermally stable compound 1,2-ethanedithiodiolate was claimed as a major product from ethylene sulfide reacting with  $\text{Tp}'\text{ReO}_3/\text{PPh}_3$ . At least one mole of episulfide needs to transfer its S-atom via direct atom transfer. By changing from ethylene episulfide to cyclooctene episulfide, the same chemistry behavior

should be observed. Strain in trans-cyclooctene episulfide would add another variable with which to probe the system.

#### **2.4.1 Independent Synthesis and Characterization of Hydrido-*tris*-(3,5-dimethyl-1-pyrazoyl)borato(*trans*-cyclooctane-1,2-monothio diolato)(oxo)rhenium(V) (1)**

*trans*-Cyclooctanemonothiodiolate, **1**, was synthesized according to a one pot procedure<sup>58</sup> as shown in Figure 2.8. Cyclocondensation of *trans*-mercaptocyclooctanol with Tp'ReO<sub>3</sub>/PPh<sub>3</sub> in dry THF under Ar gave a light blue-green compound. After filtration, solvent was removed in vacuo. The crude product was then purified by column chromatography. The light blue-green product was characterized by means of <sup>1</sup>H NMR, <sup>13</sup>C NMR, IR, and mass spectrometry. The integration ratio of 1:1:1 for vinylic protons and 3:3:3:3:3:3 for methyl protons from Tp' showed the C<sub>1</sub> symmetry of this complex. An infrared band at 949.64 cm<sup>-1</sup> belonged to the Re=O stretch, and the mass spectrometry using FAB ionization showed the M<sup>+</sup> ion (<sup>187</sup>Re) at 658.6 m/z .

Figure 2.8: 1,2-*trans*-Monothiodiolate Synthesis

COSY and HSQC spectra in Figure 2.10 allowed for the assignment of protons on Tp' and *trans*-cyclooctane ring. Table 2.3 shows the correlations used to make assignments. The *J* coupling constant between carbinol and thiocarbinol protons, 13.90 Hz, suggested the cyclooctane ring should be the *trans*-isomer. NOESY and nOe experiments on Tp'Re(O)*trans*-1,2-cyclooctane monothiodiolate were done in order to confirm the *trans*-stereochemistry and assign which of two possible diastereomers formed: these give definitive assignments for the two diolate signals at, 3.95 ppm and 4.89 ppm.

Figure 2.9: Diastereomers of 1

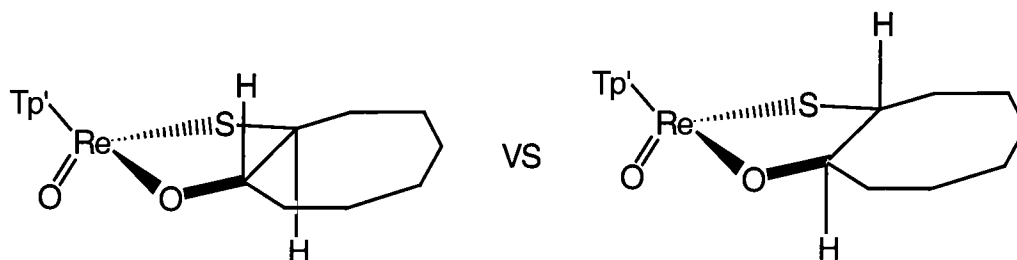
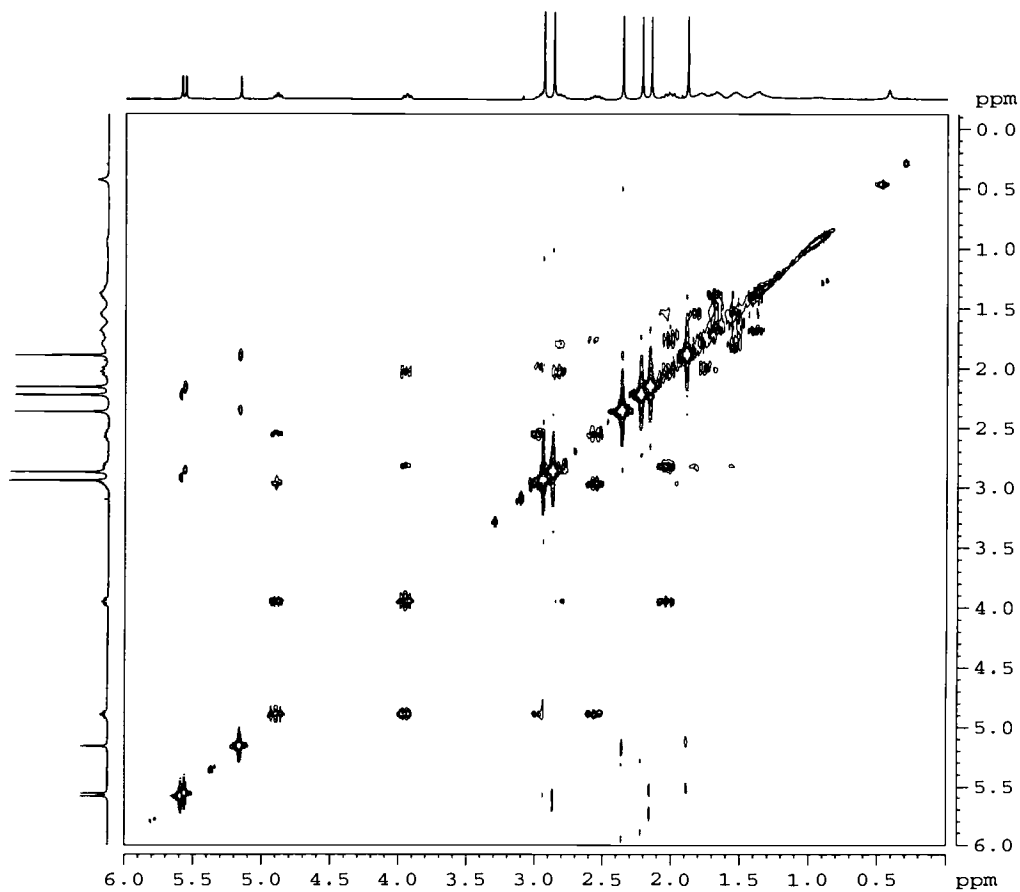


Figure 2.10: COSY and HSQC of 1

a) COSY



b) HSQC

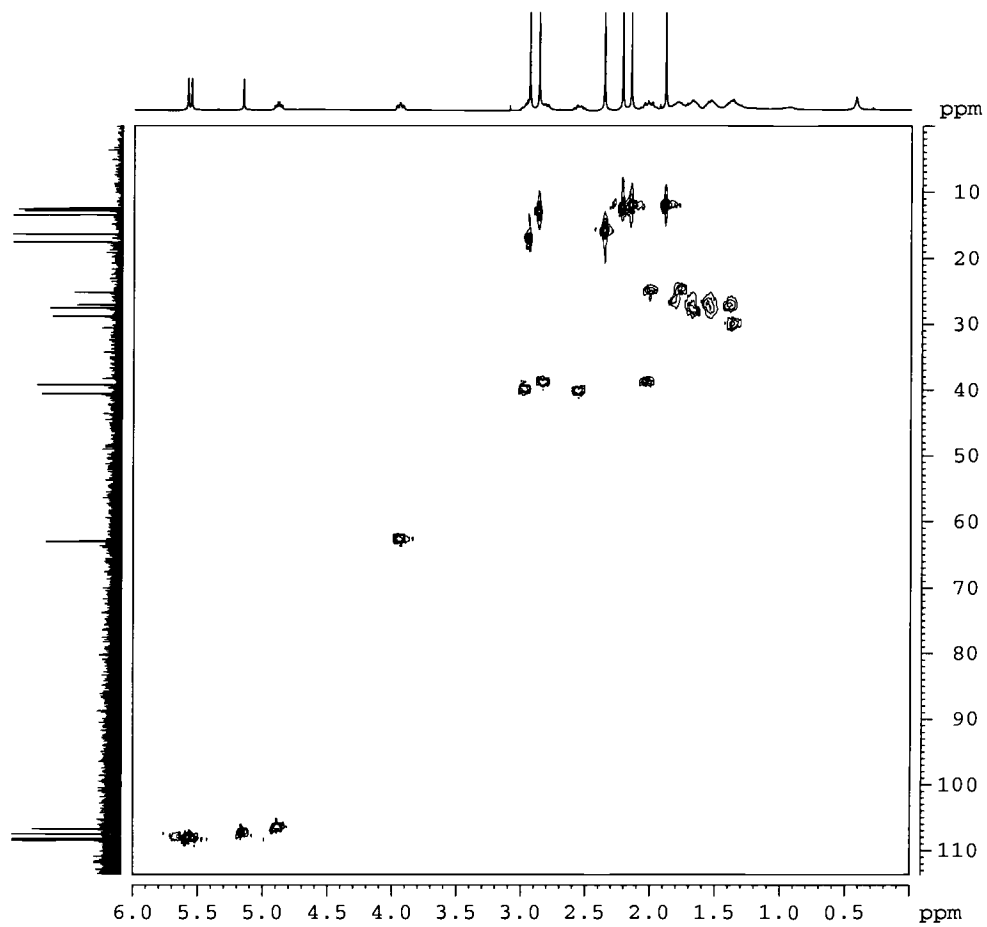
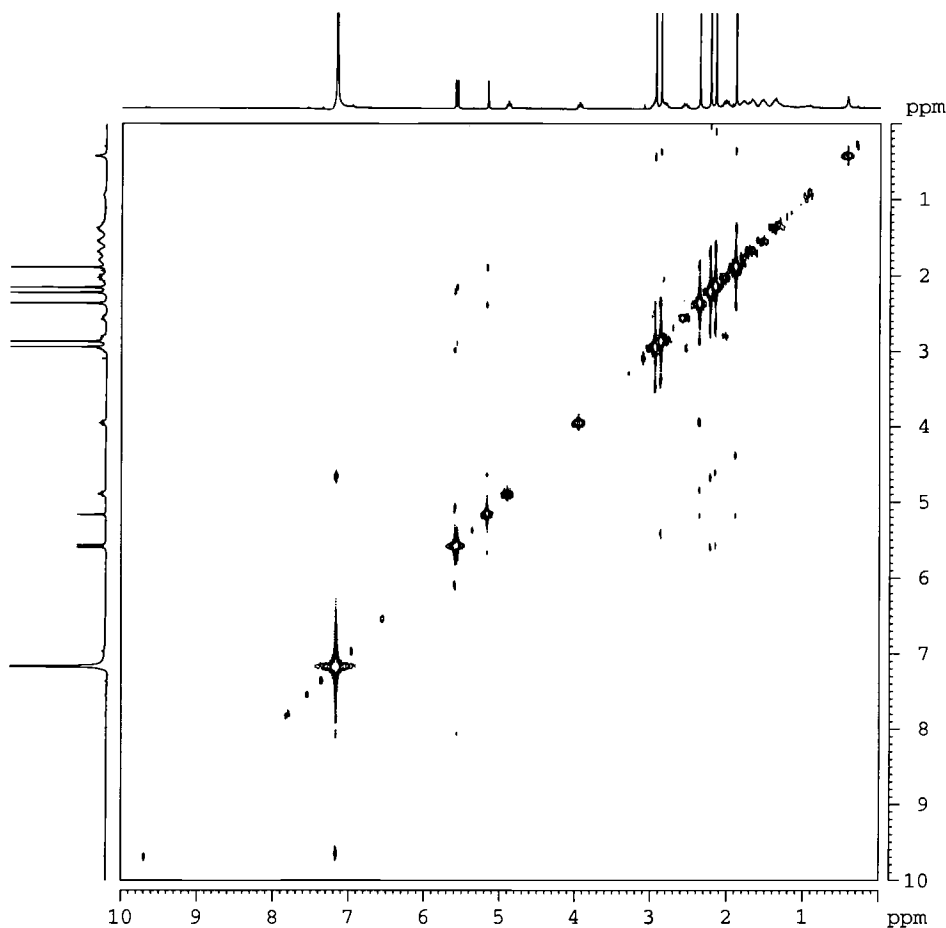


Table 2.3: NMR Results from 2D COSY and HSQC experiments of 1

<sup>1</sup> H NMR shifts, ppm	Coupled protons	Coupled carbons
<b>TP'</b>		
1.88(s, 3H)		12.13
2.15(s, 3H)		12.13
2.22(s, 3H)		12.13
2.35(s, 3H)		15.84
2.87(s, 3H)		12.52
2.94(s, 3H)		17.02
5.16(s, 1H)		107.17
5.56(s, 1H)		107.95
5.59(s, 1H)		108.29
<b>Cyclooctane ring</b>		
1.38(m, 1H)	*	26.70
1.53(m, 2H)	1.82, *	27.15
1.68(m, 2H)	*	27.56
1.77(m, 1H)	*	24.95
1.82(m, 1H)	1.53, *	26.70
1.99(m, 1H)	2.96, 2.56, 1.77	24.95
2.02(m, 1H)	2.83, 3.95, 1.82	38.90
2.55(m, 1H)	2.96, 4.89, 1.99	40.26
2.82(m, 1H)	3.95, 2.02, 1.82	38.90
2.96(m, 1H)	2.55, 4.89, 1.99	40.26
3.95(ddd, J= 4.85, 9.15, 13.90, 1H)	4.89, 2.83, 2.02	62.69
4.89(ddd, J= 4.76, 10.70, 13.90, 1H)	3.95, 2.96, 2.55	106.47
<b>* Not Clearly identified</b>		

Figure 2.11: NOESY of 1

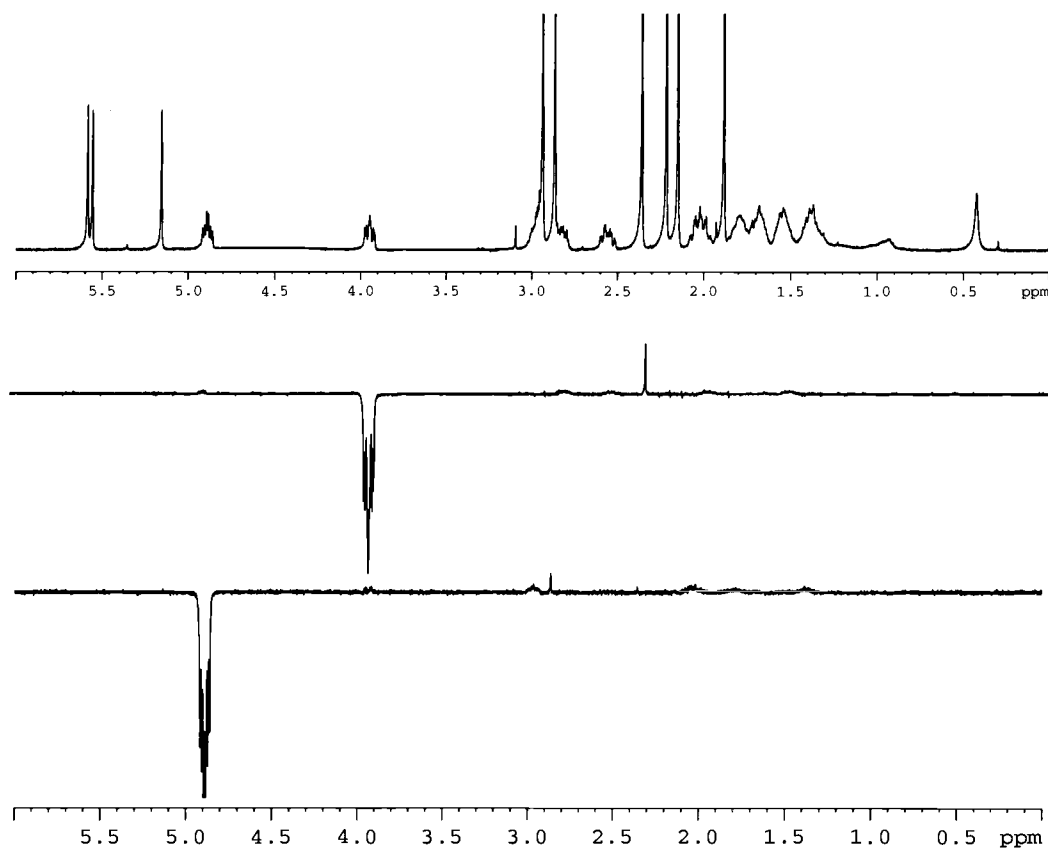


The cross peak in the NOESY spectrum between the thiocarbinolic signal at 3.95 ppm and the methyl signals at 2.36 ppm allowed assignment of this proton adjacent to S-atom as being in the *syn* position vs. the Tp' ligand while the the carbinolic proton adjacent to O-atom shows no nOe and thus must be in the *anti* position. Strong correlations among vinylic protons



and methyl groups confirmed the COSY experiment as shown in Figure 2.10.

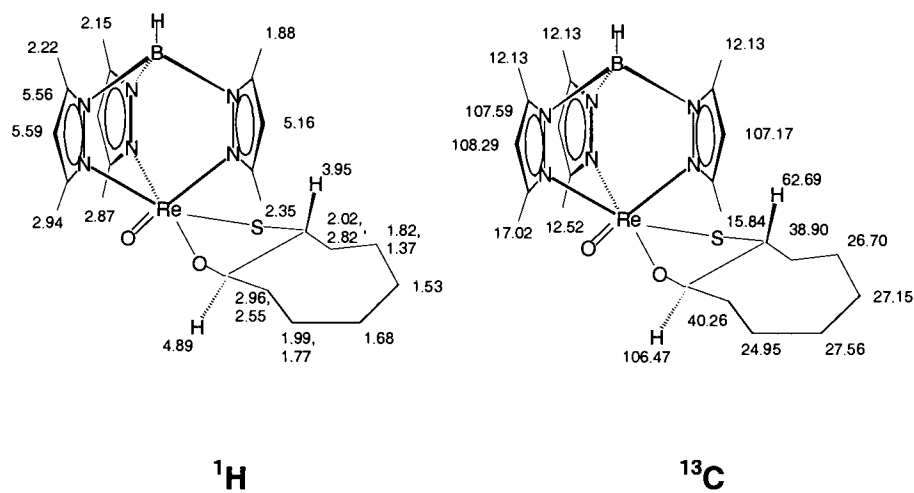
Figure 2.12: nOe of 1



A 1-D nOe (nuclear Overhauser enhancement) experiment illustrates this conclusively. Irradiation of the signal at 3.95 ppm gave a 4.98% nOe at 2.36 ppm while irradiation of the signal at 4.89 ppm signal gave 1.17% effect at the 2.87 ppm signal as shown in figure 2.12.

The proton and carbon assignments of *trans*-cyclooctanemonothiodiolate were done as shown in figure 2.13.

Figure 2.13: Proton and Carbon Assignments for 1



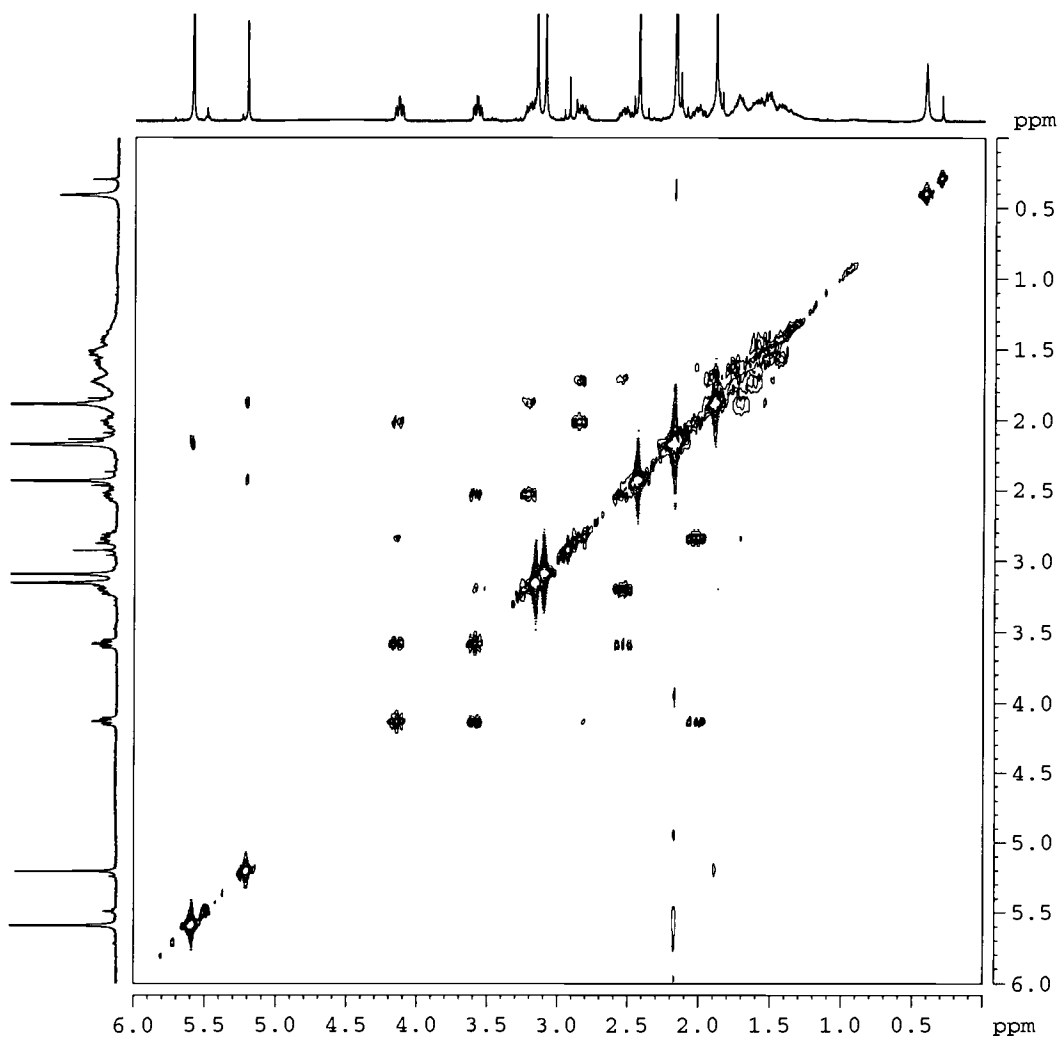
## 2.4.2 Synthesis and Characterization of Hydrido-*tris*-(3,5-dimethyl-1-pyrazoyl)borato(*trans*-cyclooctane-1,2-dithiodiolato)(oxo)rhenium(V) (2)

*trans*-Cyclooctene episulfide was allowed to react with  $\text{Tp}'\text{ReO}_3/\text{PPh}_3$  in dry  $\text{C}_6\text{D}_6$  under Ar at 75 °C to give a dark brown compound. After filtration, solvent was removed by in vacuo. The crude product was then purified by column chromatography. The dark blue product, **2**, was characterized by means of  $^1\text{H}$  NMR,  $^{13}\text{C}$  NMR, IR, and mass spectrometry. The integration ratio of 1:1:1 for vinylic protons and 3:3:3:3:3 for methyl protons from Tp' showed the  $\text{C}_1$  symmetry of this complex. An infrared band at  $940.96\text{ cm}^{-1}$  belonged to the  $\text{Re}=\text{O}$  stretch, and the mass spectrometry using FAB technique showed the  $\text{M}^+$  ion (Re 187) at 674.1 m/z.

COSY and HSQC spectra in Figure 2.14 allowed for the assignment of protons and carbons on Tp' and *trans*-cyclooctane rings.

Figure 2.14: COSY and HSQC Spectra of **2**

a) COSY



b) HSQC

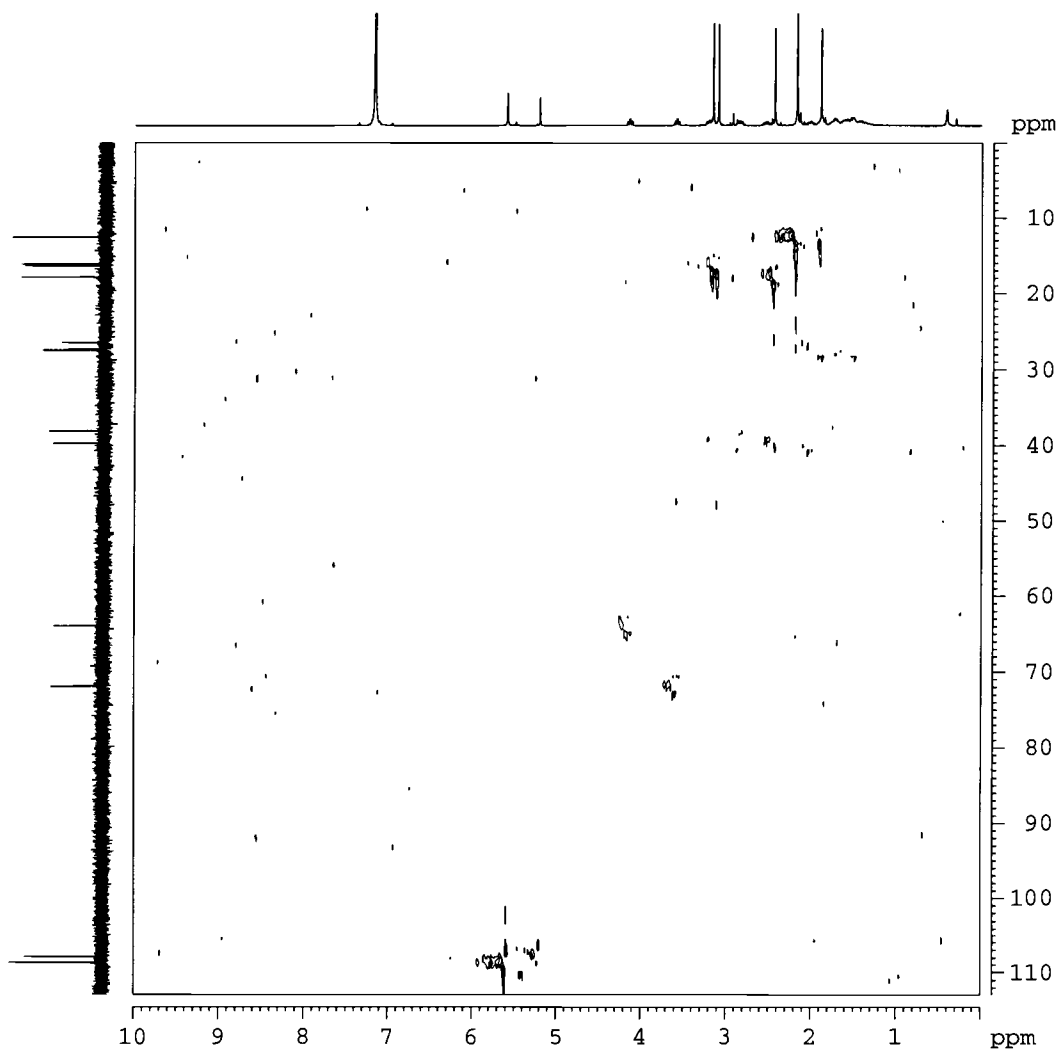


Table 2.4: NMR Results from 2D COSY and HSQC experiments

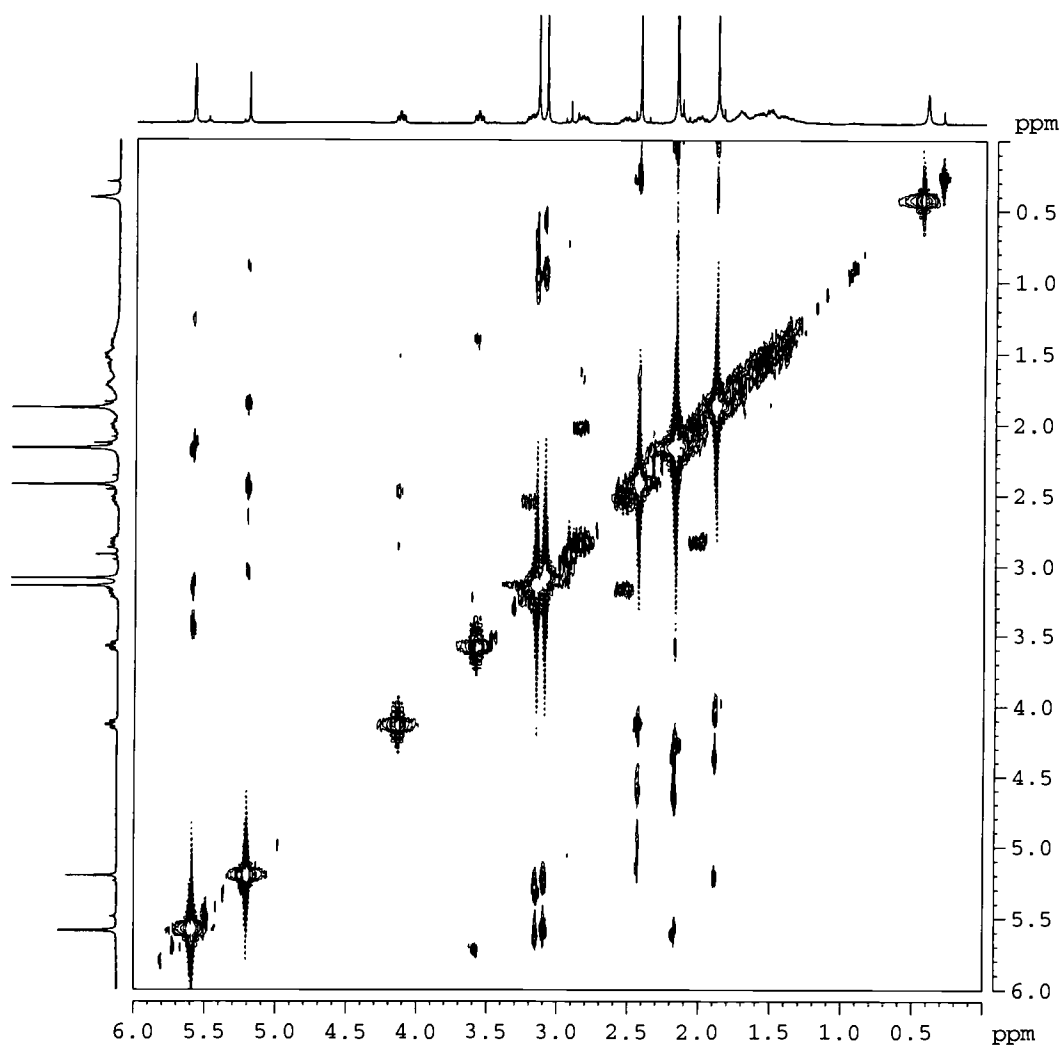
<sup>1</sup> H NMR shifts, ppm	Coupled protons	Coupled carbons
<b>Tp'</b>		
1.89(s, 3H)		12.17
2.17(s, 3H)		12.37
2.17(s, 3H)		12.37
2.43(s, 3H)		17.47
3.06(s, 3H)		16.10
3.16(s, 3H)		15.95
5.20(s, 1H)		107.84
5.58(s, 1H)		108.58
5.59(s, 1H)		108.60
<b>Cyclooctane ring</b>		
1.54(m, 2H)	1.74, *	27.17
1.63(m, 1H)	2.86, *	26.39
1.73(m, 2H)	1.92, *	26.96
1.74(m, 1H)	1.53, *	26.39
1.86(m, 1H)	2.52, 1.92	27.20
1.92(m, 1H)	1.73, *	27.20
2.01(m, 1H)	1.63, 2.86, 4.13	39.57
2.52(m, 1H)	3.20, 3.58, 1.86	38.02
2.86(m, 1H)	2.01, 1.74, 4.13	39.57
3.20(m, 1H)	3.58, 2.52, 1.86	38.02
3.58(ddd, J= 3.38, 9.70, 13.45, 1H)	4.13, 3.20, 2.52	71.77
4.13(ddd, J= 3.48, 9.61, 13.45, 1H)	3.58, 2.86, 2.01	63.88

\* Not clearly identified

NOESY and nOe experiments on the dithiodiolate **2** were done in order to give definitive assignments for the two diolate position hydrogens at 3.58 ppm and 4.14 ppm.

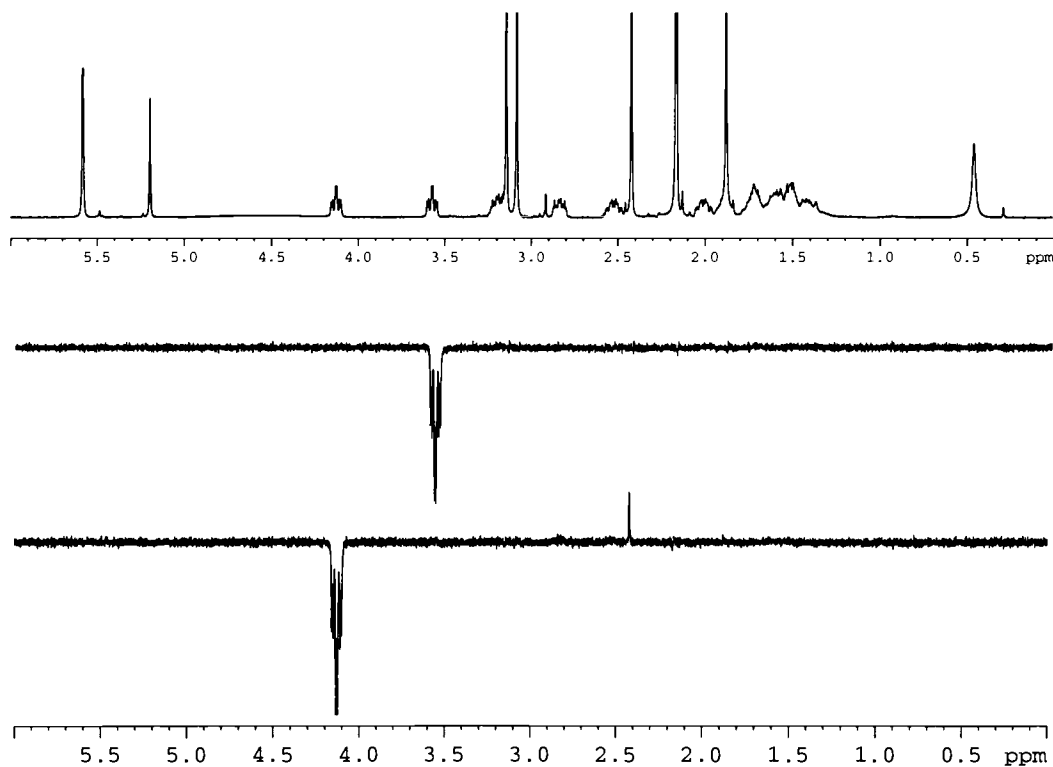
Figure 2.15: NOESY of **2**

a) NOESY



The cross peaks in the NOESY spectrum correlating the 4.13 ppm carbinolic signal and the 2.43 ppm methyl signal on the pyrazole ring allowed assignment of the carbinolic proton adjacent to that S-atom in the *syn* position vs. Tp' while the carbinolic proton adjacent to the other S-atom is in the *anti* position vs. Tp'. Strong correlations among vinylic protons and methyl groups confirmed the COSY experiment as shown in Figure 2.15.

Figure 2.16: nOe of **2**



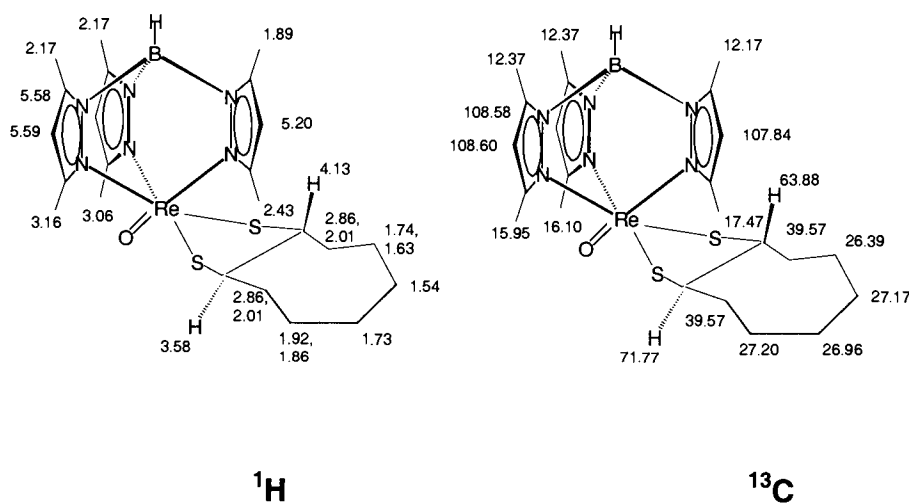
An nOe experiment was performed to confirm the position of carbinolic protons suggested by the NOESY spectrum. Irradiation of the



signal at 4.13 ppm gave a 5.68% nOe effect at the 2.43 ppm signal while irradiation of the signal at 3.58 ppm signal gave 0% nOe effect as shown in Figure 2.16.

The proton and carbon assignments of *trans*-cyclooctane dithiolate were made as shown in Figure 2.17.

Figure 2.17 : Proton and Carbon Assignments for 2



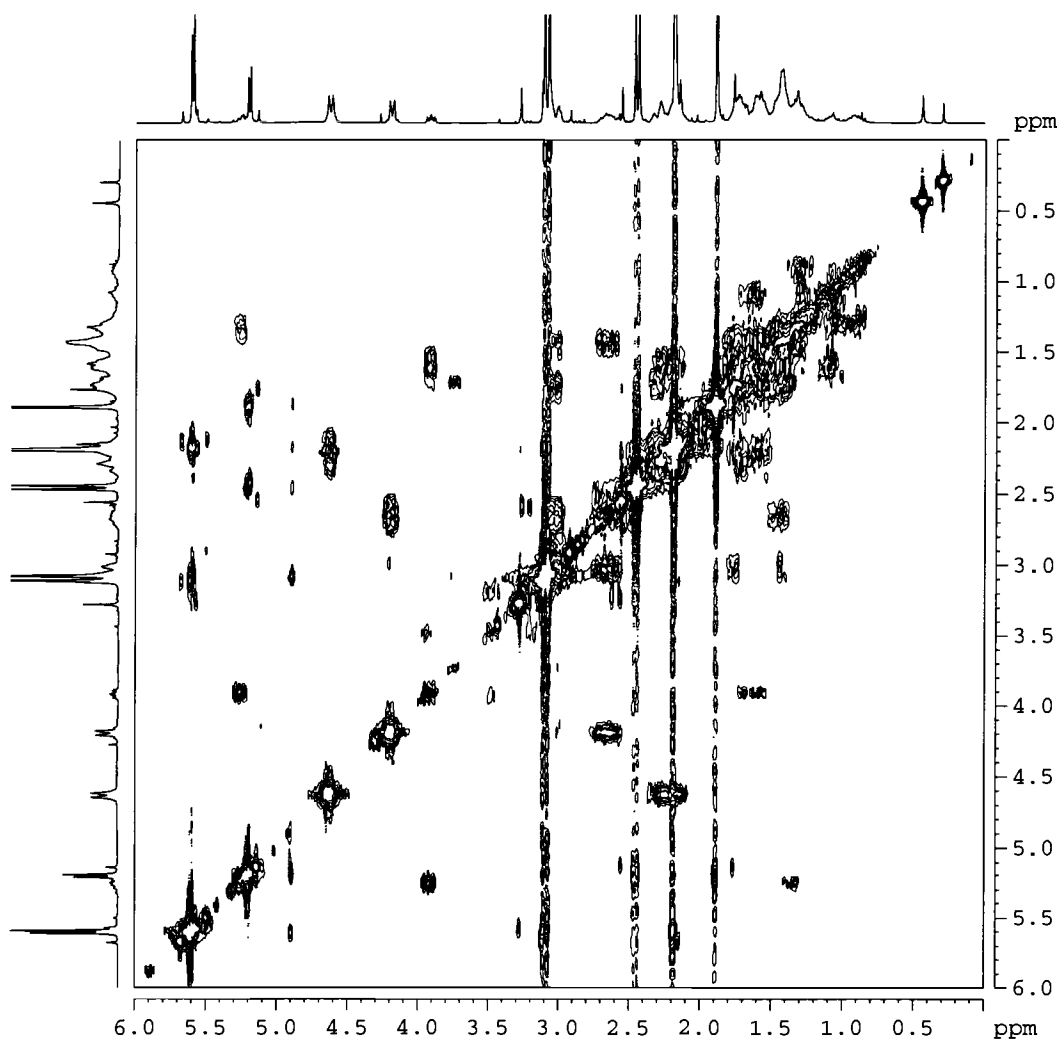
### 2.4.3 Synthesis and Characterization of Hydrido-*tris*-(3,5-dimethyl-1-pyrazoyl)borato(*cis*-cyclooctane-1,2-dithiodiolato)(oxo)rhenium(V) (**3**)

By the same manner as for **2**, *cis*-cyclooctene episulfide was allowed to react with  $\text{Tp}'\text{ReO}_3/\text{PPh}_3$  in dry  $\text{C}_6\text{D}_6$  at room temperature under Ar to give a dark brown compound. After filtration, solvent was removed in vacuo. The crude product was then purified by column chromatography. The dark brown product, **3** was characterized by means of  $^1\text{H}$  NMR,  $^{13}\text{C}$  NMR, IR, and mass spectrometry. An infrared band at  $941.18\text{ cm}^{-1}$  belonged to the  $\text{Re}=\text{O}$  stretch, and the mass spectrometry using FAB technique shown a  $\text{M}^+$  ion (Re 187) at  $674.6\text{ m/z}$ .

The  $^1\text{H}$  NMR spectrum showed *syn* and *anti* isomers in the product mixture at a 1:0.7 ratio. The product could not be purified by column chromatography ( $\text{CH}_2\text{Cl}_2/\text{hexane}$ ). The COSY and HSQC spectrum in Figure 2.18 allowed for the assignment of the mixture of isomers.

Figure 2.18: COSY and HSQC of mixture *syn*- and *anti*- isomer of **3**

a) COSY



From the correlation peaks in this COSY spectrum, the proton signals at 4.19, 3.03, 2.64, 1.71, and 1.60 ppm came from one isomer. The signals at 4.63, 2.29, 2.20, 1.60 and 1.43 ppm came from the other isomer.

## b) HSQC

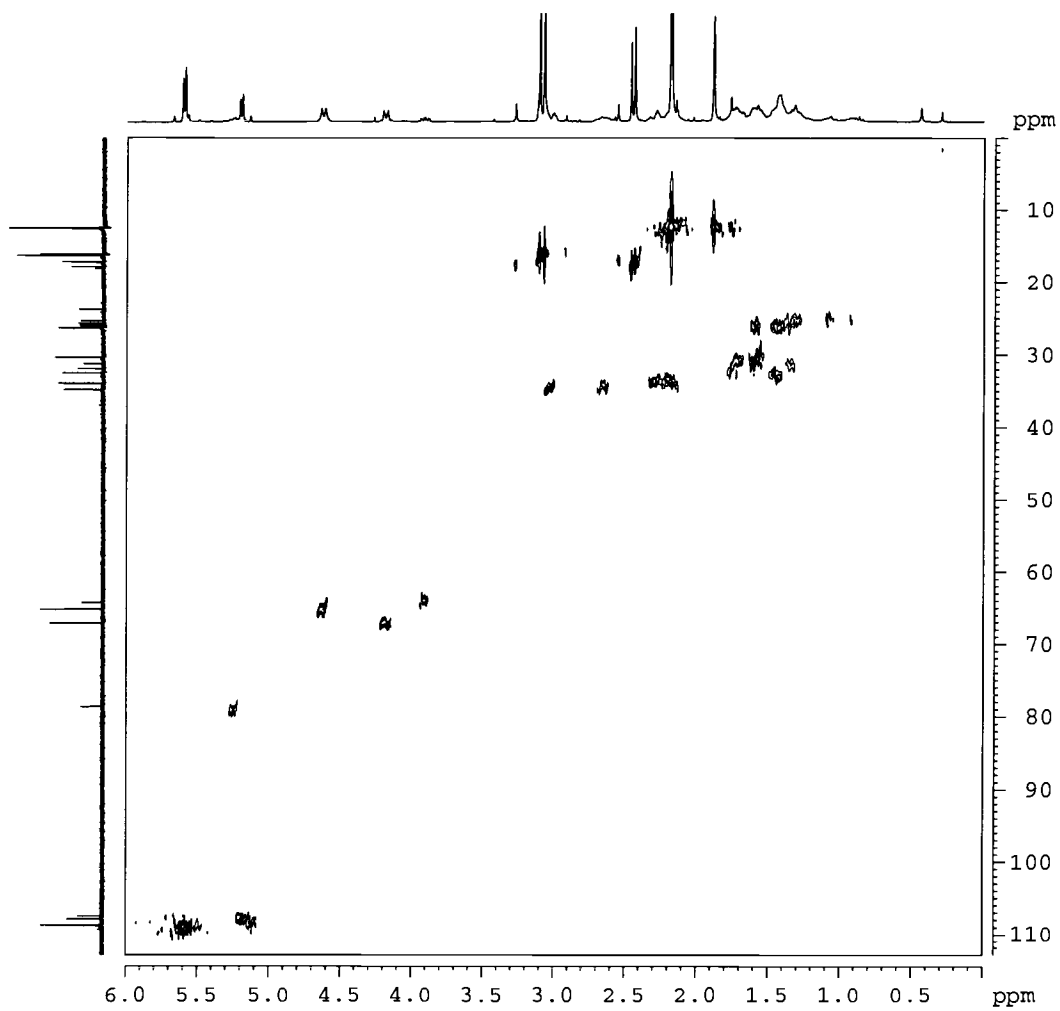


Table 2.5: NMR Results from 2D COSY and HSQC experiments of **3**a) *anti*- isomer

<sup>1</sup> H NMR shifts, ppm	Coupled protons	Coupled carbons
<b>Tp'</b>		
1.88(s, 3H)		12.62
2.18(s, 6H)		12.18
2.43(s, 3H)		17.07
3.07(s, 6H)		16.48
5.20(s, 1H)		107.62
5.59(s, 2H)		108.68
<b>Cyclooctane ring</b>		
1.43(m, 1H) x 2	1.60, 4.63	26.27
1.60(m, 1H) x 2	1.43, 4.63	26.27
2.20(m, 1H) x 2	2.29, 4.63	33.98
2.29(m, 1H) x 2	2.20, 4.63	33.98
4.63(m, 1H) x 2	1.43, 1.60, 2.20, 2.29	65.32

The integration ratio of 2:1 for vinylic protons and 2:2:1:1 for methyl protons from the Tp' ligand showed the C<sub>s</sub> symmetry of this complex.

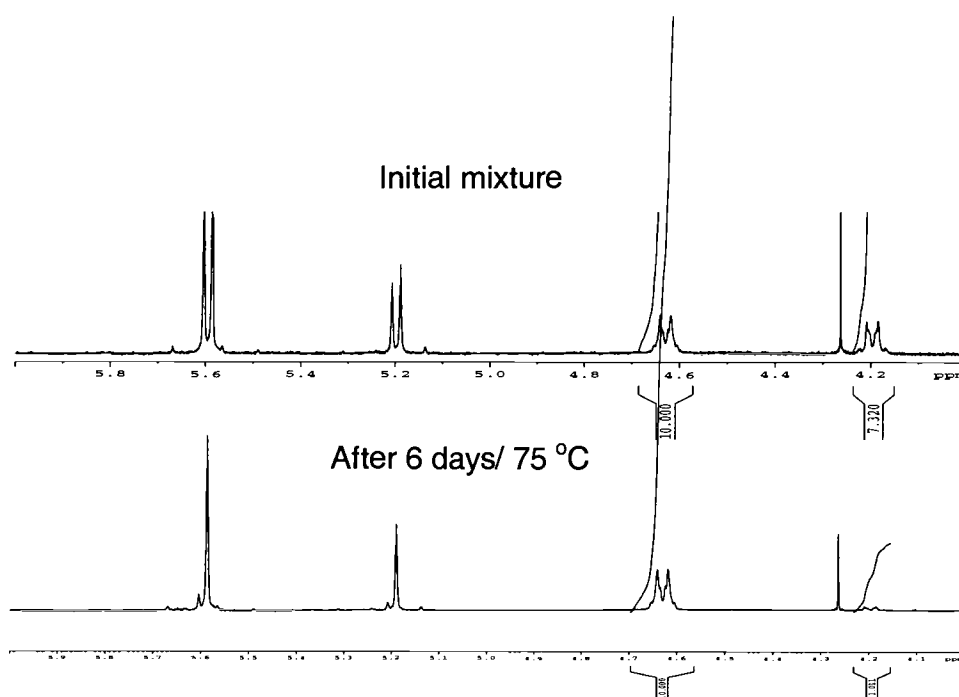
b) *syn*- isomer

<i>Syn</i> -Isomer		
<sup>1</sup> H NMR shifts, ppm	Coupled protons	Coupled carbons
<b>Tp'</b>		
1.89(s, 3H)		12.65
2.19(s, 6H)		12.19
2.46(s, 3H)		17.84
3.10(s, 6H)		16.48
5.21(s, 1H)		107.95
5.61(s, 2H)		108.80
<b>Cyclooctane ring</b>		
1.60(m, 1H) x 2	1.71, 4.19,	30.39
1.71(m, 1H) x 2	1.60, 4.63	30.39
2.64(m, 1H) x 2	3.03, 4.63	34.83
3.03(m, 1H) x 2	2.64, 4.63	34.83
4.19(m, 1H) x 2	1.60, 1.71, 2.64, 3.03	67.20

Isomerization of this isomeric mixture was observed at 75 °C in C<sub>6</sub>D<sub>6</sub>. After a sealed NMR sample was heated for 6 days, the ratio of carbinolic signals at 4.63 ppm and 4.19 was changed from 1:0.7 to 10:1 without any alkene formation (no cycloreversion to give an alkene, and also no change of total rhenium of this **3**, vs. anisole as an internal standard) as shown in Figure 2.19. The increasing amount of the major species vs. the minor was

attributed to the thermodynamic stability of the isomerized species. The thermally stable isomer was then assigned as the *anti* isomer by NOESY and 1-D nOe experiments.

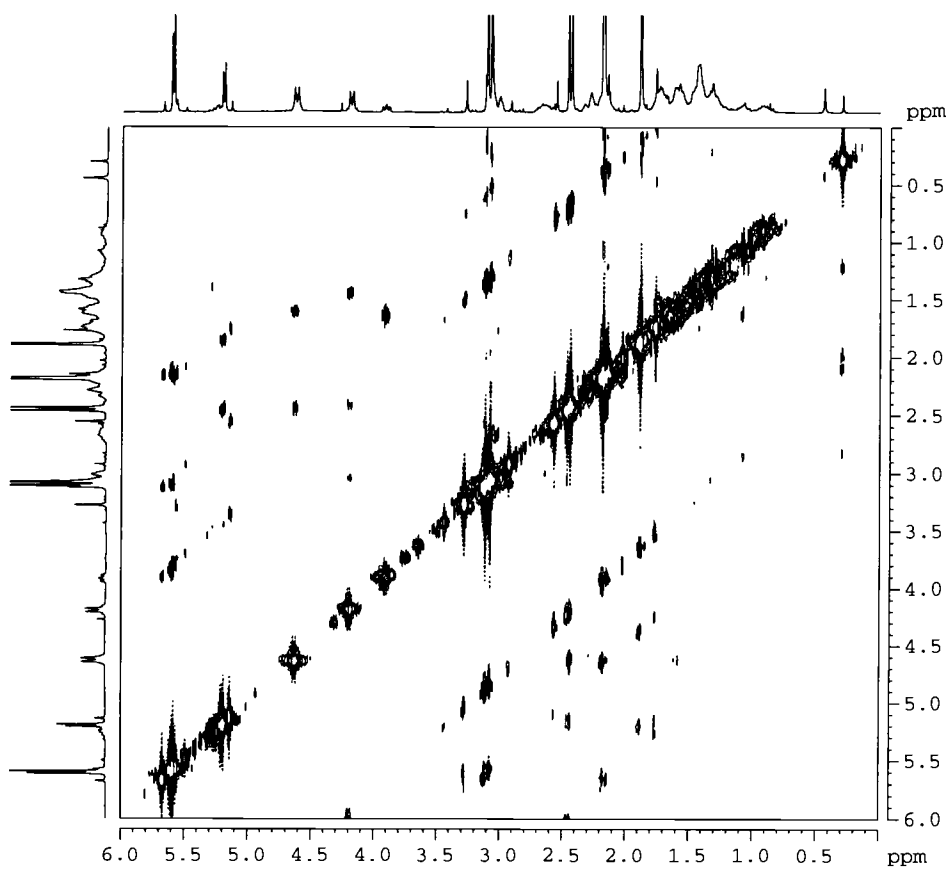
Figure 2.19: Different Thermal Stability of *syn*- and *anti*- isomers



The NOESY spectrum of this 10:1 mixture showed a strong correlation between signals at 4.63 and 2.43 ppm. This result confirms the provisional assignment based on the presumed thermodynamic preference for the *anti*- isomer.

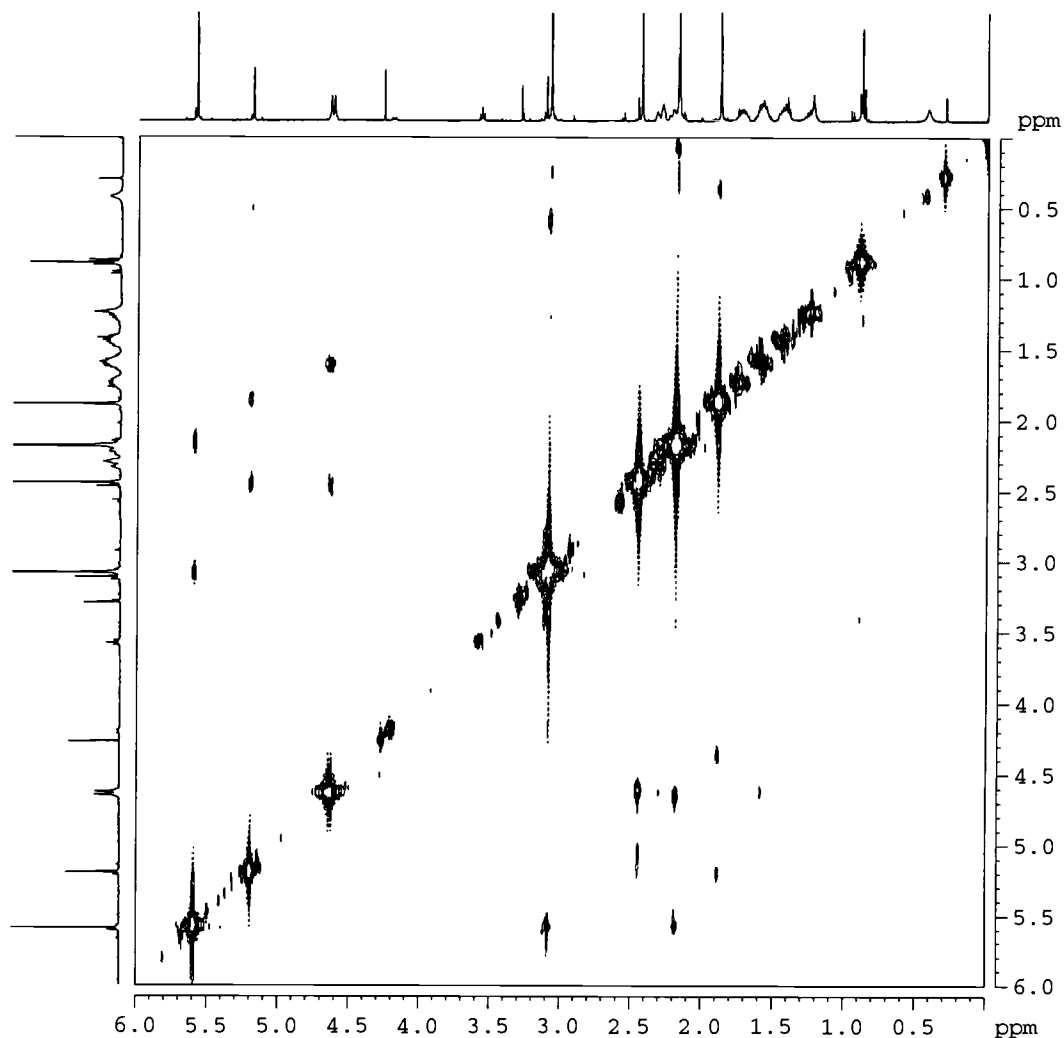
Figure 2.20: Comparing the NOESY from 10:7 and 10:1 mixture

a) 10:7





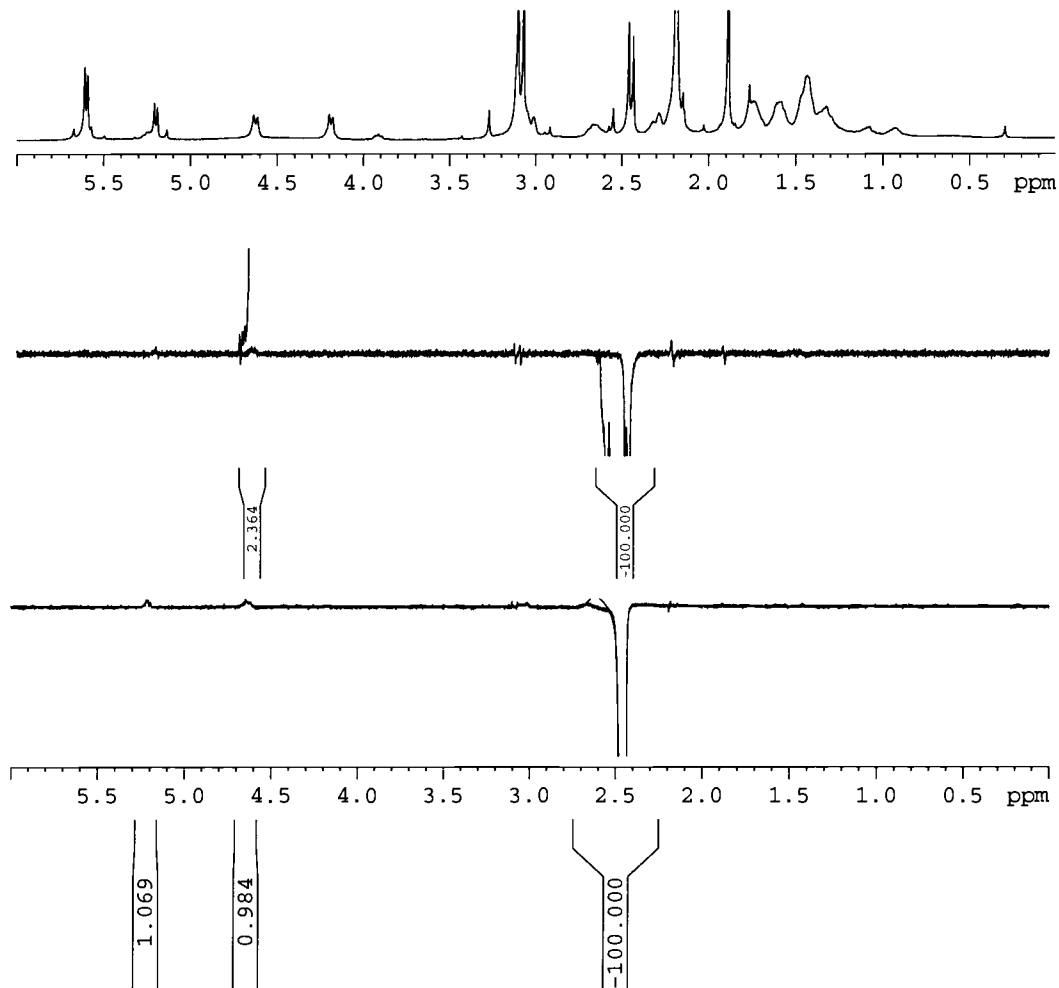
b) 10:1



A 1-D nOe experiment was performed to confirm the position of carbinolic protons suggested by NOESY. Irradiation of the signal at 2.43 ppm gave a 2.36% nOe effect at the 4.63 ppm signal while irradiation of the signal at 2.46 ppm signal gave 1.07% nOe effect at the 5.21 ppm and

0.98% nOe effect at the 4.63 ppm. The enhancement at 4.63 ppm was ascribed to the likely irradiation of the nearby peak at 2.36 ppm as shown in Figure 2.21. This result allowed conclusively establishing the stable isomer is the *anti*-isomer.

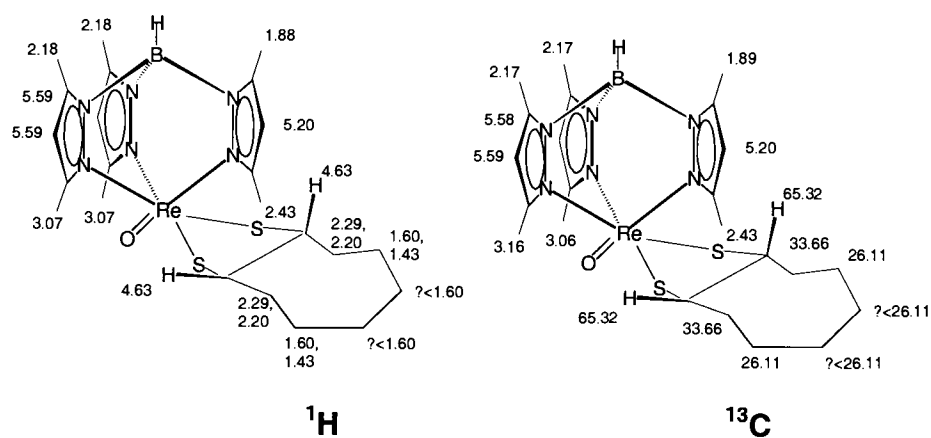
Figure 2.21: nOe of **3**



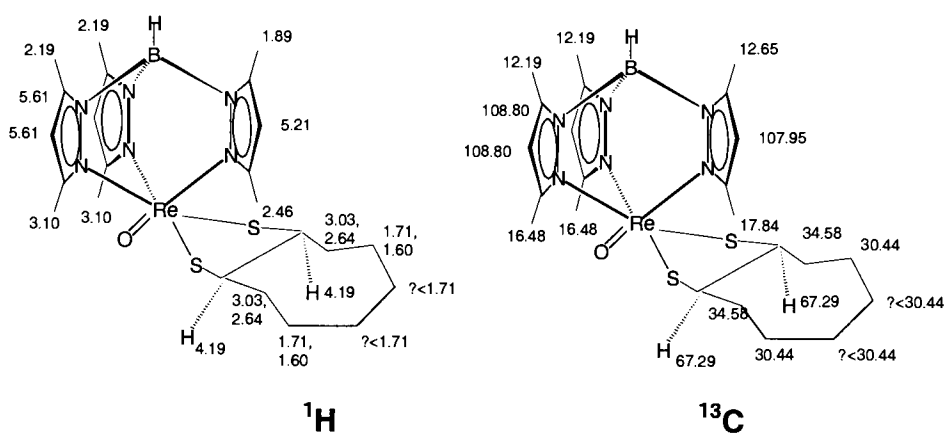
The proton and carbon assignments of *syn*- and *anti*-cyclooctane dithiodiolate were done as shown in Figure 2.22.

Figure 2.22: Proton and Carbon Assignments for *syn*-Cyclooctane dithiodiolate

a) *anti*-isomer



b) *syn*-isomer



#### 2.4.4 Selectivity and Desulfidation Product of Cyclooctene Episulfide

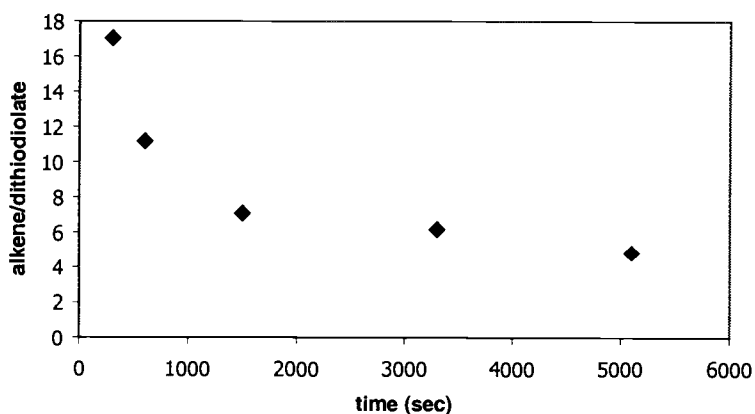
Cyclooctene episulfide was reacted with  $\text{Tp}'\text{ReO}_3/\text{PPh}_3$  under the same conditions as with cyclooctene oxide. In an NMR tube, desulfidation of *trans*-cyclooctene episulfide or *cis*-cyclooctene episulfide was followed in deuterated benzene at 75 °C by  $^1\text{H}$  and  $^{31}\text{P}$  NMR under pseudo-first order kinetic conditions: episulfide: $\text{PPh}_3$ : $\text{Tp}'\text{ReO}_3$  = 5:3:1,  $\text{Tp}'\text{ReO}_3$  9.03 mM in 0.50 mL  $\text{C}_6\text{D}_6$ . Tetramethylsilane was used as an internal integration standard. The sample tube was periodically removed and cooled to 25°C, and the  $^1\text{H}$  NMR and  $^{31}\text{P}$  spectra were collected. The products were characterized by NMR, MS(FAB) and compared with independently synthesized products. 1,2- *trans*-Cyclooctane dithiodiolate and 1,2- *cis*-cyclooctane dithiodiolate and the corresponding alkenes were established as major products from desulfidation of *trans*-cyclooctene episulfide and *cis*-cyclooctene episulfide, respectively, in an order, and also the ratio of alkene/dithiodiolate was measured as well. Both dithiodiolates are highly thermally stable to alkene loss; even heated at 75 °C for one week no alkene was observed.

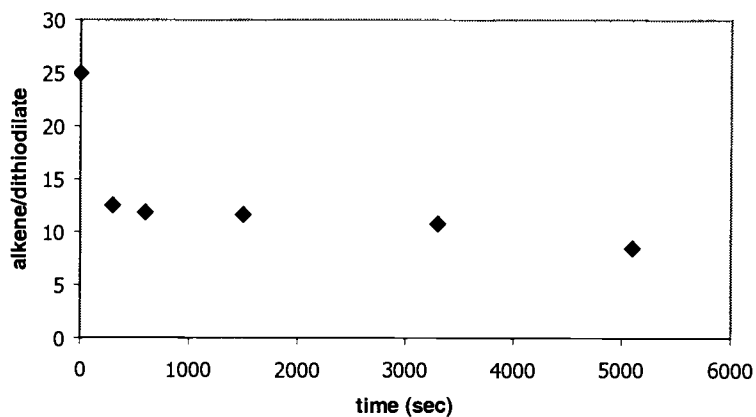
Dithiodiolate formation occurred very fast relatively to epoxide/diolate conversion. The ratio of alkene/dithiodiolate for *trans*-cyclooctene episulfide was 17.1:1 after the reaction proceeded for 5 minutes, and also a decrease in the alkene/dithiodiolate ratio was found over time as shown in Figure

2.23. Desulfidation of *cis*-cyclooctene episulfide gave an alkene/dithiodiolate ratio at 12.5, and a slower decrease in the alkene/dithiodiolate ratio was found over time relative to the *trans*-cyclooctene episulfide case as shown in Figure 2.8. Two possible conclusions can be drawn: (1) alkene underwent cycloaddition to  $\text{Tp}'\text{ReOS}_2$  to form dithiodiolate, or (2) dithiodiolate forms by ring expansion from  $\text{Tp}'\text{ReOS}$ .

Figure 2.23: Decrease in the Alkene /Dithiodiolate Ratio

a) *trans*-cyclooctene episulfide



b) *cis*-cyclooctene episulfide

From the  $^{31}\text{P}$  NMR, the ratio of  $\text{S}=\text{PPh}_3/\text{O}=\text{PPh}_3$  was obtained. (Table 2.6)

Table 2.6: Ratio of  $\text{S}=\text{PPh}_3/\text{O}=\text{PPh}_3$

a) *trans*-cyclooctene episulfide

Expt	t(sec)	[ $\text{S}=\text{PPh}_3$ ]mM	[ $\text{O}=\text{PPh}_3$ ]mM	[ $\text{PPh}_3$ ]mM	$\text{S}=\text{PPh}_3/\text{O}=\text{PPh}_3$
1	0	8.34	1.67	16.68	5.00
2	300	8.89	9.70	8.08	0.92
3	600	13.98	12.70	0.00	1.10
4	1500	13.34	13.34	0.00	1.00
5	3300	12.35	14.33	0.00	0.86
6	5100	12.47	14.21	0.00	0.88

b) *cis*-cyclooctene episulfide

Expt	t(sec)	[S=PPh <sub>3</sub> ]mM	[O=PPh <sub>3</sub> ]mM	[PPh <sub>3</sub> ]mM	S=PPh <sub>3</sub> /O=PPh <sub>3</sub>
1	0	10.24	1.91	12.91	5.37
2	300	18.04	4.23	0.00	4.26
3	600	17.56	4.17	0.00	4.21
4	1500	17.85	3.96	0.00	4.51
5	3300	17.78	3.53	0.00	5.04
6	5100	16.85	3.92	0.00	4.30

From Figure 2.23 and Table 2.6, desulfidation of *cis*-cyclooctene episulfide gave an alkene/dithiodiolate ratio of about 10:1 and S=PPh<sub>3</sub>/O=PPh<sub>3</sub> ratio of about 4:1 while *trans*-cyclooctene episulfide gave half alkene/dithiodiolate or 1:1 S=PPh<sub>3</sub>/O=PPh<sub>3</sub>, and also *cis*-cyclooctene episulfide consumed all PPh<sub>3</sub> after the reaction proceeded for 5 minutes at 75 °C. Consequently, direct S-atom transfer was favored by *cis*-cyclooctene episulfide by at least two times over *trans*-cyclooctene episulfide since both dithiodiolates are thermodynamically favored.

#### 2.4.5 Monothiodiolate vs. Dithiodiolate

Even though dithiodiolate formation was initially claimed via Tp'ReOS and Tp'ReO<sub>2</sub>S intermediates (ch 1.7, p. 19), monothiodiolate had never been observed, and for cyclooctene episulfide there was no

monothiodiolate formed either. Chemical properties of  $\text{Tp}'\text{ReO}_2\text{S}$  compared to  $\text{Tp}'\text{ReO}_3$  should be similar.

Earlier studies showed  $\text{Tp}'\text{ReO}_3$  undergoes cycloaddition to *trans*-cyclooctene to form 1,2-*trans*-diolate<sup>47</sup>, and also independently synthesized compounds *trans*-diolate, *trans*-monothiodiolate, *cis*- and *trans*-dithiodiolate as noted in 2.4.1-2.4.3 are stable for at least one week at 75 °C. One possibility was that  $\text{Tp}'\text{ReOS}_2$  might be very reactive toward with  $\text{PPh}_3$  to give  $\text{Tp}'\text{ReOS}$  followed by a final step to form dithiodiolate.

$\text{Tp}'\text{ReO}(\text{OH})(\text{OEt})$ , a phosphine free source of  $\text{Tp}'\text{ReO}_2$  (9.03 mM), was used to react with *cis*- or *trans*-cyclooctene episulfide (45.20 mM; TMS 0.23 mM as an internal standard in 0.5 mL  $\text{C}_6\text{D}_6$ ). *trans*-Monothiodiolate was observed in the reaction with *trans*- and *cis*-dithiodiolate as shown in Table 2.7. Formation of alkene and dithiodiolate supported the direct S-atom transfer.

Table 2.7  $\text{PPh}_3$ Free System

a ) *trans*-cyclooctene episulfide

Expt	t(sec)	[ <i>trans</i> -monothiodiolate]mM	[ <i>trans</i> -dithiodiolate]mM	[ <i>cis</i> -dithiodiolate]mM
1	0	0	0	0
2	300	0	0	0
3	86400	0.61	1.92	0.59



b) *cis*-cyclooctene episulfide

Expt	t(sec)	[ <i>cis</i> -monothiodiolate]mM	[ <i>cis</i> -dithiodiolate]mM	[ <i>cis</i> -cyclooctene]mM
1	0	2.5608*	0.8052	7.92
2	300	4.7784*	1.5312	8.1048

\* Structure not confirmed yet:  $^1\text{H NMR}$ : 5.23 (m, 1H), and 3.92 (m, 1H) ppm  
 Comparison with *trans*-cyclooctane dithiodiolate  $^1\text{H NMR}$ : 4.88 (m, 1H), and 3.95 (m, 1H) ppm

This result shows that the thermodynamically favored monothiodiolate will form under the right conditions, but the most possible reason why monothiodiolate had never been observed in the presence of  $\text{PPh}_3$  is due to kinetic control factors. Both systems (with and without  $\text{PPh}_3$ ) generate  $\text{Tp}'\text{ReO}_2$ . If monothiodiolate formed by ring expansion, then it would be expected to form under both conditions. However, if it forms by cycloaddition to  $\text{Tp}'\text{ReO}_2\text{S}$ , then suppressing accumulation of this intermediate would prevent monothiodiolate formation. Rapid reaction of  $\text{PPh}_3$  would form either  $\text{Tp}'\text{ReO}_2$  (S-atom transfer) and continued catalytic desulfidation, or  $\text{Tp}'\text{ReOS}$ . The latter can lead to dithiodiolate by either ring expansion (1 step) or by S-atom transfer and alkene cycloaddition (2 steps).

*cis*-Dithiodiolate formation in *trans*-cyclooctene episulfide system was attributed to isomerization of *trans*-cyclooctene. The control experiment

using  $\text{Tp}'\text{ReO}_3/\text{PPh}_3$  and *trans*-cyclooctene showed 10% of *trans*-cyclooctene converts to *cis*-cyclooctene within 19 hours at 75 °C. In contrast, *trans*-cyclooctene by itself showed no change, and also when only  $\text{Tp}'\text{ReO}_3$  was used with *trans*-cyclooctene, *trans*-diolate was the only product. This evidence suggested  $\text{Tp}'\text{ReO}_2$  (or  $\text{Tp}'\text{ReOS}$ ) can catalyzed the isomerization.

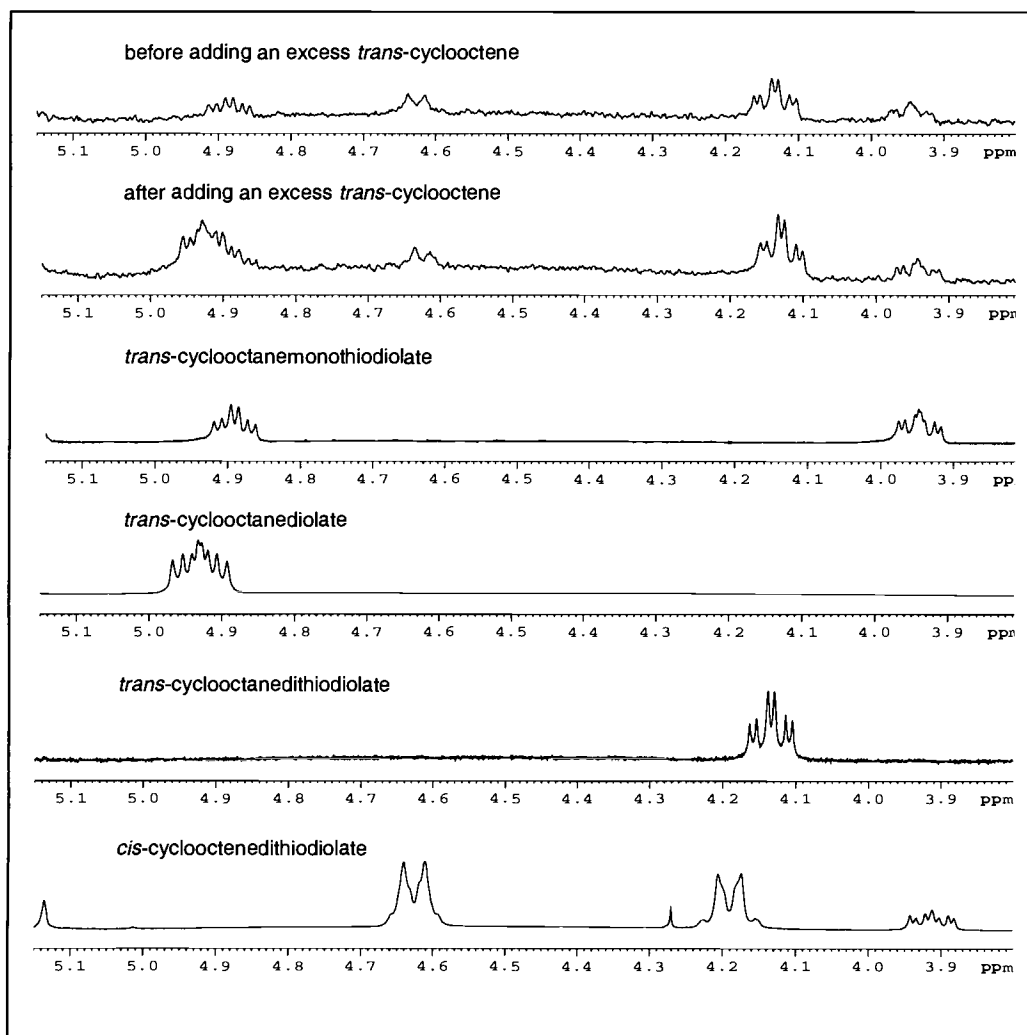
For *cis*-cyclooctene episulfide, there were 5 species formed during reaction; *cis*-cyclooctene was the major product forming by direct S-atom transfer since monothiolate and dithiodiolate are stable at 75 °C. *cis*-Dithiodiolate (*syn*, *anti*) was formed in a 1:4 ratio with alkene. *cis*-Monothiodiolate formation was assigned on the basis of comparison to *trans*-monothiodiolate's  $^1\text{H}$  NMR spectrum. The last one gave a multiplet NMR signal at 4.10 ppm in a 1: 2.5 with ratio alkene. The last two products also dominated in the reaction of  $\text{Tp}'\text{ReO}_3/\text{PPh}_3$  and *cis*-episulfide which may have contributed to rapid  $\text{PPh}_3$  consumption during the reaction. Even more, these unknown species would be involved in desulfidation.

For *trans*-cyclooctene desulfidation with  $\text{Tp}'\text{ReO}_3/\text{PPh}_3$ , there was no *cis*-dithiodiolate or *trans*-monothiodiolate to be observed but another unknown signal appeared:  $^1\text{H}$  NMR  $\delta$  4.38(m, 1H), 3.72(m, 1H) ppm in 1:3 ratio during the initial 30 minutes of reaction, and with *trans*-cyclooctane dithiodiolate in a 1:1.5 ratio with *trans*-dithiodiolate late in the reaction after

3 days at 75°C, and also the 10% isomerization of trans-cyclooctene to cis-cyclooctene was observed after 55 minutes of reaction .

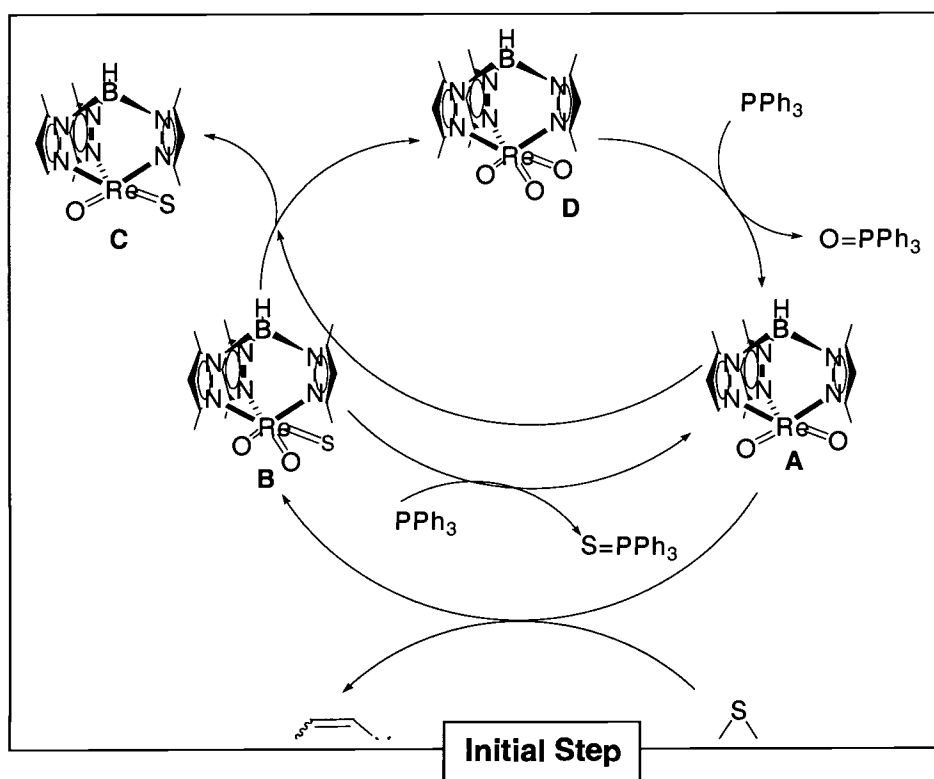
#### 2.4.6 Metal Oxo Donor and Acceptor

Formation of dithiodiolates under phosphine-free conditions, Table 2.7, showed the internal oxo transfer reaction<sup>18</sup> leading to metal-centered oxidation and reduction of reactants. In this reaction, a high-valent oxorhenium group is the atom donor, (Tp'ReO<sub>2</sub>S, Re(VII)) and a rhenium center with two oxo groups or one oxo and one sulfido the acceptors, (Tp'ReO<sub>2</sub> or Tp'ReOS, Re(V) ). Either O or S could be transferred, leading to a mixture of Tp'ReO<sub>3</sub>, Tp'ReO<sub>2</sub>S, Tp'ReOS<sub>2</sub> and Tp'ReS<sub>3</sub>. Tp'ReO<sub>3</sub> formation in reaction was tested by adding an excess amount, 2.5 mg, of *trans*-cyclooctene into reaction tube after sixth day. *trans*-Cyclooctene diolate was observed at 0.40 mM after heated 24 hours at 75±0.1 °C as shown in Figure 2.24. The initial concentration of Tp'ReO(OH)(OEt) was 9.03 mM, and *trans*-episulfide was 45.20 mM in 0.50 mL C<sub>6</sub>D<sub>6</sub>.

Figure 2.24: Diolate formation in  $\text{Tp}^*\text{ReO}(\text{OH})(\text{OEt})$  system

The new desulfidation catalytic cycle was proposed as shown in Fig 2.10 and 2.11.

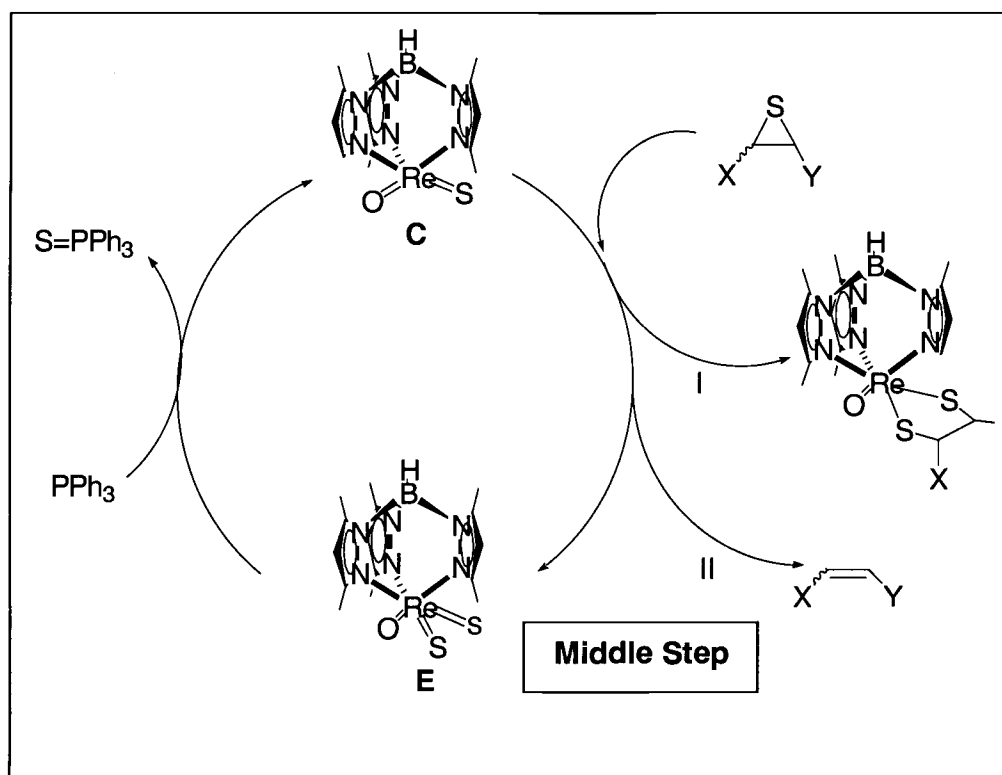
Figure 2.25: Desulfidation Catalytic Cycle, Initial Step



In the initial step, sulfur atom abstraction by the Tp'ReO<sub>2</sub>, **A**, gives Tp'ReO<sub>2</sub>S, **B**, which presumably is highly reactive with PPh<sub>3</sub>. It is rapidly reduced; without PPh<sub>3</sub> it can react with more Tp'ReO<sub>2</sub> to either do a degenerate S-atom transfer, or an O-atom transfer. Then Tp'ReO<sub>3</sub>, **D**, is reused in the catalytic cycle. Quantitatively, two moles of Tp'ReO<sub>3</sub> are

needed to give one mole of  $\text{Tp}'\text{ReOS}$ , **C**, for the next step leading to dithiodiolate.

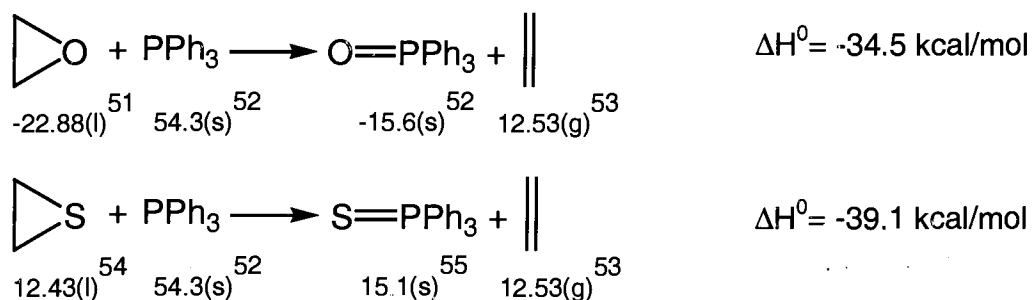
Figure 2.26: Desulfidation Catalytic Cycle, Middle Step



Obviously,  $\text{Tp}'\text{ReOS}$  or  $\text{Tp}'\text{ReO}_2$  can serve as S-atom carriers to  $\text{PPh}_3$ , leading to catalytic turnover via direct S-atom transfer while ring expansion or alkene cycloaddition processes will shut down the cycle by forming inert thiodiolates.

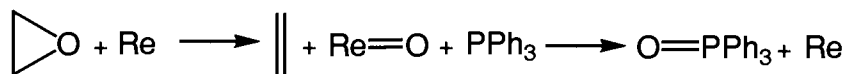
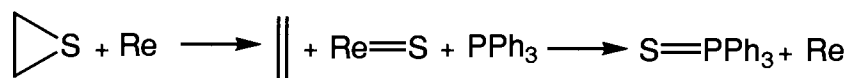
### 2.4.7 Epoxide vs. Episulfide Selectivity

Obviously, our results demonstrated for direct atom transfer that it is easier to abstract a sulfur atom from an episulfide mediated by rhenium species than it is to remove an oxygen atom from an epoxide, and also the enthalpy of reactions for the non-catalyzed reaction shows it is thermodynamically more favored to abstract a sulfur atom. The non-catalyzed reactions are given in kcal/mol unit as shown.



Since all PPh<sub>3</sub> was consumed rapidly in the catalyzed desulfidation for *cis*- and *trans*-episulfides, the rhenium complex effectively lowered the transition state barrier,  $\Delta G^\ddagger$ , of the desulfidation, more so than the deoxygenation.

Catalyzed reaction by rhenium species:



For *cis*- and *trans*-isomers, there will be more steric hindrance in *trans*-episulfide or epoxide complexes which is consistent with our result: the *trans*-isomer reacted more slowly in both cases. Although the *trans*-isomer has bond strain energy to drive the reaction, it needs to form the coordinated epoxide or episulfide complex first before reacting to give alkene or diolate.

Combining the kinetic data and thermodynamic data, *cis*-episulfide is the most reactive and *trans*-oxide is the least reactive as follow: *cis*-cyclooctene episulfide > *trans*-cyclooctene episulfide > *cis*-cyclooctene oxide > *trans*-cyclooctene oxide.



## Chapter 3. Experimental

### 3.1 General Methods

All reactions were performed using either standard bench top or inert atmosphere techniques<sup>56</sup> on a double-manifold Schlenk line or in a nitrogen-filled glove-box (Vacuum-Atmospheres Co. HE 493). All deuterated solvents were used as purchased from Cambridge Isotope Labs. Benzene, dichloromethane, and THF were dried, degassed and distilled under vacuum prior to use. Benzene was pre-dried with CaH<sub>2</sub> overnight then dried with Na/K alloy. Dichloromethane was distilled from CaH<sub>2</sub>. THF was distilled from Na/benzophenone. Chemical reagents were used as purchased from Aldrich or Acros (Fisher), unless otherwise noted. Triphenylphosphine was recrystallized from hexane. Silica gel (Scientific, Catalog Number: 162544, Particle Size: 32-63, Lot Number 322303201 and 322044201) was used for flash column chromatography. Molecular Sieves (4 Å, Fisher) were activated by heating at 150 °C overnight prior to use. Hydrido-*tris*-(3,5-dimethyl-1-pyrazolyl)borato(trioxo)rhenium(VII), Tp'ReO<sub>3</sub>, and Hydrido-*tris*-(3,5-dimethyl-1-pyrazolyl)borato(ethoxy)(hydroxyl)(oxo)-rhenium, Tp'ReO(OH)(OEt), were prepared according to the procedure described by Brown<sup>42</sup>.

GC-MS spectra were collected on an HP 5890 II GC/5971A MSD under 99.999% helium using an RTX-20 column, 0.25 mm diameter, 30 m long with a 5 m guard column, coated with a 1  $\mu\text{m}$  film of 20% diphenyl and 80% dimethyl polysiloxane.

Fast atom bombardment/mass spectroscopy (FAB/MS) were performed on a Kratos MS-50TC (Manchester, England, United Kingdom) double focusing instrument operated at unit resolution. The analyte of interest was mixed on the probe tip with a 3-nitrobenzyl alcohol (98%, Sigma-Aldrich) matrix. Xenon gas was used to generate the primary ionizing beam from an Ion-Tech gun operated at 7-8 kV. For high mass accuracy measurements with the FAB/MS, polyethylene glycol (PEG) was used a reference compound. The mixture consisted of PEG compounds in three masses: 600, 800, and 1000. The ratio of PEG's was 4:2:1, respectively.

Infrared spectra (KBR pellet) were run on a Nicolet Magna-IR560.

### **3.2 NMR Measurement**

All NMR spectra were collected on either a Brüker DP300 (operating at 300.13 MHz for  $^1\text{H}$  or 75.409 MHz for  $^{13}\text{C}$ , 121.50 MHz for  $^{31}\text{P}$ ) or a Brüker DPX400 (operating at 400.134 MHz for  $^1\text{H}$  or 100.614 MHz for  $^{13}\text{C}$ ). All chemical shifts were referenced to residual protons or carbons in

deuterated solvents and reported in ppm downfield from tetramethylsilane.  $T_1$  measurements were done by the inversion-recovery method<sup>57</sup>. Baseline correction was performed on all FIDs and Fourier transformed spectra. For quantitative NMR work, relaxation delays of 70 s ( $>5 T_1$ ,  $T_1 = 12.829$  s) per pulse for the sample using tetramethylsilane as an internal standard or 30 s ( $>5 T_1$ ) for the sample using anisole as an internal standard were collecting on the Brüker DPX400 at 16 scans.

### 3.3 Measurement of Kinetics

Reaction rates were followed by measuring  $^1\text{H}$  or  $^{31}\text{P}$  NMR integrations; a relaxation delay of 70 s ( $>5 T_1$ ) per pulse at 15 scans was used in collecting NMR spectra to ensure accurate integration. Tetramethylsilane or anisole was used as an internal integration standard. All epoxide and episulfide solutions were prepared by mixing epoxide or episulfide with  $\text{C}_6\text{D}_6$ ,  $\text{PPh}_3$  and pre-dried tetramethylsilane in  $\text{C}_6\text{D}_6$  solvent over  $\text{CaH}_2$ , decanting, then adding to solid  $\text{Tp}'\text{ReO}_3$  or  $\text{Tp}'\text{ReO}(\text{OH})(\text{OEt})$ .

A representative example is given for deoxygenation of *trans*-cyclooctene oxide. To make a stock solution of anisole/ $\text{C}_6\text{D}_6$ , anisole (5.0 mg, 46.24  $\mu\text{mol}$ ) was added to a 4 mL volumetric flask of  $\text{C}_6\text{D}_6$  then a 0.5 mL aliquot was dissolved with  $\text{C}_6\text{D}_6$  to make a stock solution totaling 3 mL of anisole in a 3 mL volumetric flask with *trans*-cyclooctene oxide

(21.40 mg, 0.17mmol, 56.60 mM) which was then pre-dried with  $\text{CaH}_2$  overnight at 10 °C. A 0.50 mL aliquot was then added to an NMR tube containing  $\text{Tp}^*\text{ReO}_3$  (2.4 mg, 0.0045 mmol) and triphenylphosphine (3.55 mg, 0.0135 mmol), then sealed under vacuum.

The tube was then submerged and heated to  $75.0 \pm 0.1^\circ\text{C}$  in a water/ethylene glycol bath. The sample tube was periodically removed and cooled to  $25^\circ\text{C}$  and the  $^1\text{H}$  NMR spectrum was collected. Other kinetic measurements used analogous procedures.

### 3.4 Synthetic Procedures

#### 3.4.1 *trans*-Cyclooctene Oxide

*trans*-Cyclooctene was prepared according to Cope's procedure<sup>58</sup>. By adopting Sharpless's epoxidation procedure<sup>59</sup>, *trans*-cyclooctene oxide was obtained in high yield. To a solution of *trans*-cyclooctene (1.15 g, 9.13 mmol) in 1.60 mL THF was added *bis*-(trimethylsilyl) peroxide, BTSP, (3.30 g, 18.5 mmol). The reaction vial was placed into an ice/water bath under an argon atmosphere. Portions of a solution of  $\text{Re}_2\text{O}_7$  (0.567g, 0.117 mmol, 1.3 mol-% based on *trans*-cyclooctene) in 0.94 mL THF were added very slowly over 30 minutes. After stirring an addition of 40 minutes at  $2^\circ\text{C}$ , the solution turned a light yellow color. The mixture was allowed to warm to room

temperature overnight and stirred. Water (3 drops) and manganese dioxide (ca. 5.5 mg) were added in order to decompose the remaining peroxide as noted by the disappearance of the yellow color. The filtered clear solution was dried over  $\text{Na}_2\text{SO}_4$ . The mixture was again filtered, and the volatiles removed under reduced pressure. The product was purified by flash column chromatography on silica gel. Dichloromethane was used to elute the colorless *trans*-cyclooctene oxide. Yield: 1.0036 g (7.97 mmol, 75.5%).  $^1\text{H}$  NMR ( $\text{C}_6\text{D}_6$ ):  $\delta$  0.80 (m, 2H), 0.96 (m, 2H), 1.23 (m, 2H), 1.68 (m, 2H), 1.80 (m, 2H), 2.12 (m, 2H), 2.52 (m, 2H).  $^{13}\text{C}$  NMR ( $\text{C}_6\text{D}_6$ ):  $\delta$  28.83, 28.88, 33.10, 59.02. GC-MS (EI): 126 [ $\text{M}^+$ ].

### 3.4.2 *trans*-Cyclooctene Episulfide

This was prepared according to Adam<sup>60</sup>. Into a 250 mL thick walled glass bomb equipped with a Teflon valve were placed  $\text{MoO}(\text{S}_2\text{CNEt}_2)_2$  (ca. 0.7797 g, 2.23 mmol), sulfur (1.7375 g, 54.2 mmol), and *trans*-cyclooctene (3.4102 g, 27.1 mmol) in 50 mL of acetone. The solution was then freeze-pump-thaw degassed. The vessel was stirred at 74 °C for 24 hours. The mixture was filtered, and the volatiles removed under reduced pressure. The product was purified by flash column chromatography on silica gel. A 3:1 mixture of dichloromethane and petroleum ether was used to elute the product. Removal of solvent left *trans*-cyclooctene episulfide. Yield: 2.8796

g (20.3 mmol, 74.9%).  $^1\text{H}$  NMR ( $\text{C}_6\text{D}_6$ ):  $\delta$  0.87 (m, 2H), 0.94 (m, 2H), 1.35 (m, 2H), 1.67 (m, 2H), 2.31 (m, 2H), 2.45 (m, 2H).  $^{13}\text{C}$  NMR ( $\text{C}_6\text{D}_6$ ):  $\delta$  28.53, 32.08, 37.32, 43.06 GC-MS (EI): 142 [ $\text{M}^+$ ].

### 3.4.3 *cis*-Cyclooctene Episulfide

This was prepared according to Takido<sup>61</sup>. Into a 500 mL round bottom flask was placed *cis*-cyclooctene oxide (25.00 g, 176 mmol) in 200 mL of dichloromethane. A solution of dimethylthioformamide (39.23 g, 440 mmol) and trifluoroacetic acid (2.53 g, 22 mmol) was added. The reaction flask was stirred at 71 °C for 6 hours under a nitrogen atmosphere. The volatiles were removed under reduced pressure. The residual mixture was extracted with 300 mL of petroleum ether and then washed with water (300 mL) to remove the remaining dimethylthioformamide and trifluoroacetic acid. The organic layer was dried over  $\text{Na}_2\text{SO}_4$ . Removal of solvent left *cis*-cyclooctene episulfide. Yield: 16.50 g (116.2 mmol, 66.0%).  $^1\text{H}$  NMR ( $\text{C}_6\text{D}_6$ ):  $\delta$  1.35 (m, 10H), 2.20 (m, 2H), 2.67 (m, 2H).  $^{13}\text{C}$  NMR ( $\text{C}_6\text{D}_6$ ):  $\delta$  26.65, 29.69, 30.02, 40.93. GC-MS (EI): 142 [ $\text{M}^+$ ].

#### 3.4.4 *trans*-Mercaptocyclooctanol

This was prepared according to Whitham<sup>62</sup>. Into a 100 mL round bottom flask were added sulfur (9.60 g, 300 mmol), and sodium borohydride (3.80 g, 100 mmol). The reaction flask was then placed in an ice/water bath and 80 mL of dry tetrahydrofuran added rapidly. The reaction flask was then placed under a nitrogen atmosphere while a large amount of hydrogen was generated. After evolution of hydrogen had ceased (10 minutes), *cis*-cyclooctene oxide (6.30g, 50 mmol) was added. Then the mixture was heated under reflux at 66 °C for 42 hours. To work up the reaction, aqueous sodium hydroxide (10% w/v 100ml) was added into the reaction flask followed by extraction with chloroform. After removal of solvent, this gave a glassy solid of crude bis-(2-hydroxycyclooctyl) disulfide (4.60g, 14.4 mmol) which was added into a 50 mL reaction flask containing 25 mL of dry ether. Excess LiAlH<sub>4</sub> (0.1 M, 30.0 mL, 30.0 mmol) was then added dropwise to reduce bis-(2-hydroxycyclo-octyl) disulfide. The mixture was heated under reflux for 3 hours and cooled to 10 °C for 16 hours. Water (7.20 g) was added dropwise into the reaction flask to decompose the remaining LiAlH<sub>4</sub>, and ether was used to extract *trans*-mercaptocyclooctanol. The volatiles were removed under reduced pressure to leave *trans*-mercaptocyclooctanol. Yield: 2.80 g (17.5 mmol, 35.0%). <sup>1</sup>H NMR (C<sub>6</sub>D<sub>6</sub>): δ 1.45 (m, 2H), 1.66 (m, 2H), 1.81 (m, 2H), 2.751 (m, 1H), 3.56 (m, 1H). <sup>13</sup>C

NMR ( $C_6D_6$ ):  $\delta$  24.91, 25.73, 33.53, 33.64, 48.22, 77.70 GC-MS (EI): 160 [M<sup>+</sup>].

#### **3.4.5 Hydrido-*tris*-(3,5-dimethyl-1-pyrazolyl)borato(*trans*-cyclooctane-1,2-diolato)(oxo)rhenium(V)**

This was prepared from *trans*-cyclooctanediol according to Ness<sup>63</sup>.

#### **3.4.6 Hydrido-*tris*-(3,5-dimethyl-1-pyrazolyl)borato(*cis*-cyclooctane-1,2-diolato)(oxo)rhenium(V)**

This was prepared from *cis*-cyclooctanediol according to Gable<sup>35</sup>.

#### **3.4.7 Hydrido-*tris*-(3,5-dimethyl-1-pyrazolyl)borato(*trans*-cyclooctane-1,2-monothiodiolato)(oxo)rhenium(V)**

This was prepared according to Gable<sup>64</sup>. Into a 250 mL thick-walled glass bomb equipped with a Teflon valve were placed  $Tp'ReO_3$  (0.1441 g, 0.27 mmol), triphenylphosphine (0.0822 g, 0.31 mmol), *p*-toluenesulfonic acid monohydrate (0.0507 mg, 0.27 mmol), ground molecular sieves (1.0 g), and *trans*-2-mercaptocyclooctanol (0.043 g, 0.27 mmol) in 5.0 mL of dry THF. The solution was then freeze-pump-thaw degassed. The vessel was stirred



at room temperature for 24 hours. The blue-green solution was filtered, and the volatiles removed under reduced pressure. The product was purified by flash column chromatography on silica gel. A 1:1 mixture of dichloromethane and hexane was used to elute the blue-green product. Removal of solvent left a light blue solid. Yield: 0.0109 g (0.0166 mmol, 6.1%). The stereochemistry of this compound was determined by the NOESY and nOe experiments discussed in Chapter 2.  $^1\text{H}$  NMR ( $\text{C}_6\text{D}_6$ ):  $\delta$  1.38 (m, 1H), 1.53 (m, 2H), 1.68 (m, 2H), 1.77 (m, 1H), 1.82 (m, 1H), 1.88 (s, 3H), 1.99 (m, 1H), 2.02 (m, 1H), 2.22 (s, 3H), 2.35 (s, 3H), 2.55 (m, 1H), 2.82 (m, 1H), 3.95 (ddd,  $J= 4.85, 9.15, 13.90$ , 1H), 4.89 (ddd,  $J= 4.76, 10.70, 13.90$ , 1H), 5.16 (s, 3H), 5.56 (s, 1H), 5.56 (s, 1H).  $^{13}\text{C}$  NMR ( $\text{C}_6\text{D}_6$ ):  $\delta$  12.13, 12.13, 12.13, 12.52, 15.84, 17.02, 24.95, 26.70, 27.15, 27.56, 38.90, 40.26, 62.69, 106.47, 107.17, 107.95, 108.29. IR (KBr): 2921, 2852, 2538 ( $\nu_{\text{BH}}$ ), 1545, 1452, 1416, 1383, 1206, 1066, 1044, 950 ( $\nu_{\text{ReO}}$ ), 920, 816, 657  $\text{cm}^{-1}$ . MS (FAB): ( $^{187}\text{Re}$ ) 658.6 [ $\text{M}^+$ ].

#### **3.4.8 Hydrido-*tris*-(3,5-dimethyl-1-pyrazolyl)borato(*trans*-cyclooctane-1,2-dithiodiolato)(oxo)rhenium(V)**

Into a 250 mL thick-walled glass bomb equipped with a Teflon valve were placed  $\text{Tp}'\text{ReO}_3$  (0.5752 g, 1.08 mmol), triphenylphosphine (0.9935 g, 3.79 mmol), *trans*-cyclooctene episulfide (0.5006 g, 3.52 mmol) in 4 mL of dry

$C_6D_6$ . The solution was then freeze-pump-thaw degassed. The vessel was stirred at  $75^\circ C$  for 24 hours. The dark brown solution was filtered, and the volatiles removed under reduced pressure. The product was purified by flash column chromatography on silica gel. A 1:1 mixture of dichloromethane and hexane was used to elute the dark brown product. Removal of solvent left a dark brown solid. Yield: 0.1748 g (0.259 mmol, 23.59%). The stereochemistry of this compound was determined by the NOESY and nOe experiments discussed in Chapter 2.  $^1H$  NMR ( $C_6D_6$ ):  $\delta$  1.54 (m, 2H), 1.63 (m, 1H), 1.73 (m, 2H), 1.74 (m, 1H), 1.86 (m, 1H), 1.89 (s, 3H), 1.92 (m, 1H), 2.01 (m, 1H), 2.17 (s, 3H), 2.17 (s, 3H), 2.43 (s, 3H), 2.52 (m, 1H), 2.86 (m, 1H), 3.06 (s, 3H), 3.20 (m, 1H), 3.58 (ddd,  $J = 3.38, 9.70, 13.45$ , 1H), 4.13 (ddd,  $J = 3.48, 9.61, 13.45$ , 1H), 5.20 (s, 1H), 5.58 (s, 1H), 5.59 (s, 1H).  $^{13}C$  NMR ( $C_6D_6$ ):  $\delta$  12.17, 12.37, 12.37, 15.95, 16.10, 17.47, 26.39, 26.96, 27.17, 27.20, 38.02, 39.57, 63.88, 71.77, 107.84, 108.58, 108.60. IR (KBr): 2923, 2549 ( $\nu_{BH}$ ), 1545, 1452, 1417, 1384, 1213, 1067, 1041, 941 ( $\nu_{ReO}$ ), 669, 649  $cm^{-1}$ . MS (FAB): ( $^{187}Re$ ) 674.1 [ $M^+$ ]. Also a 1:1 mixture of dichloromethane and acetone was used to elute the yellow-green product, an unknown. Removal of solvent left a yellow-green solid 18.1 mg. Spectroscopy data of this unknown compound is in appendix II.

### 3.4.9 Hydrido-*tris*-(3,5-dimethyl-1-pyrazolyl)borato(*cis*-cyclooctane-1,2-dithiodiolato)(oxo)rhenium(V)

Into a 250 mL thick-walled glass bomb equipped with a Teflon valve were placed  $\text{Tp}'\text{ReO}_3$  (0.136 g, 0.256 mmol), triphenylphosphine (0.236 g, 0.90 mmol), *cis*-cyclooctene episulfide (0.128 g, 0.901 mmol) in 3 mL of dry  $\text{C}_6\text{D}_6$ . The solution was then freeze-pump-thaw degassed. The vessel was stirred at room temperature for 24 hours. The dark brown solution was filtered, and the volatiles removed under reduced pressure. The product was purified by flash column chromatography on silica gel. A 1:1 mixture of dichloromethane and hexane was used to elute the dark brown product. Removal of solvent left a dark brown solid. Yield: 0.0123 g (0.018 mmol, 7.03%). By NMR analysis, it was confirmed products are 10:7 ratio of *anti* and *syn* isomers. The stereochemistry of this compound was determined by the NOESY and nOe experiments discussed in Chapter 2.

IR and MS of Mixture:

IR (KBr): 2924, 2850, 2548, 2360 ( $\nu_{\text{BH}}$ ), 1525, 1452, 1416, 1367, 1213, 1066, 1041, 941 ( $\nu_{\text{ReO}}$ ), 861, 818, 778, 648  $\text{cm}^{-1}$ . MS (FAB): ( $^{187}\text{Re}$ ) 674.6  $[\text{M}^+]$ .

Spectroscopic data for *anti*-isomer:

$^1\text{H}$  NMR ( $\text{C}_6\text{D}_6$ ):  $\delta$  1.43 (m, 1H), 1.60 (m, 1H), 1.88 (s, 3H), 2.18 (s, 6H), 2.20 (m, 1H), 2.29 (m, 1H), 2.43 (s, 3H), 3.07 (s, 6H), 4.63 (m, 1H), 5.20 (m, 1H), 5.59 (s, 2H)  $^{13}\text{C}$  NMR ( $\text{C}_6\text{D}_6$ ):  $\delta$  12.18, 12.62, 16.48, 17.07, 26.27, 33.98, 65.32, 107.62, 108.68.

Spectroscopic data for *syn*-isomer:

$^1\text{H}$  NMR ( $\text{C}_6\text{D}_6$ ):  $\delta$  1.60 (m, 1H), 1.71 (m, 1H), 1.89 (s, 3H), 2.19 (s, 6H), 2.46 (m, 3H), 2.64 (m, 1H), 3.03 (m, 1H), 3.10 (s, 6H), 4.19 (m, 1H), 5.21 (m, 1H), 5.61 (s, 2H)  $^{13}\text{C}$  NMR ( $\text{C}_6\text{D}_6$ ):  $\delta$  12.19, 12.65, 16.48, 17.84, 30.39, 34.83, 67.20, 107.95, 108.80.

### **3.5 Procedure for Recrystallization of Hydrido-*tris*-(3,5-dimethyl-1-pyrazolyl) borato(*trans*-cyclooctane-1,2-dithiodiolato)(oxo)rhenium(V)**

Crystals of hydrido-*tris*-(3,5-dimethyl-1-pyrazolyl)borato(*trans*-cyclooctane-1,2-dithiodiolato)(oxo)rhenium(V) were grown by re-crystallization from  $\text{CH}_3\text{CN}/\text{H}_2\text{O}$ . A saturated solution of the *trans*-cyclooctanedithiodiolate complex was prepared by adding dark brown solid to 5 mL acetonitrile until no more solid dissolved. The vial was sealed and left overnight. Then the

solution was filtered, and the filtrate was placed into the new 5 mL vial. This solution was then placed into a saturated atmosphere of water vapor at 10°C. The crystals of *trans*-cyclooctanedithiodiolate were obtained by filtration after 4 weeks.

## Chapter 4. Conclusion and Future Work

Catalyst development for O-atom and S-atom transfer is important in academic and industrial chemistry. Our research has developed rhenium oxo complexes to use in deoxygenation or desulfidation. Both applications are very powerful approaches to saving environmental resources by converting low value materials to more valuable substances since the reactivity and selectivity have been studied. Since our rhenium complex is similar to molybdenum complexes, understanding desulfidation mediated by the rhenium species can lead to developing new catalysts to substitute for molybdenum sulfide derivatives for HDS.

We succeeded in measuring deoxygenation rate constants for *trans*-cyclooctene oxide. The ring expansion rate constant is  $(1.24 \pm 0.03) \times 10^{-5} \text{ s}^{-1}$  and direct atom transfer is  $(6.02 \pm 0.02) \times 10^{-6} \text{ s}^{-1}$ . *cis*-Cyclooctene showed a higher preference to give alkene (24.5:1) than *trans*-cyclooctene. The observed rate constant for direct atom transfer is  $5.07 \times 10^{-5} \text{ s}^{-1}$  and the ring expansion rate constant is  $2.07 \times 10^{-6} \text{ s}^{-1}$ .

The desulfidation catalytic model was extended in this work. We observed  $\text{Tp}'\text{ReO}_3$  in the  $\text{PPh}_3$  free system which used  $\text{Tp}'\text{ReO}(\text{OH})(\text{OEt})$  as  $\text{Tp}'\text{ReO}_2$  source, and also direct atom transfer was also confirmed by forming dithiodiolate and alkene in this experiment.

### Bibliography

1. *Homogeneous Catalysis*; Parshall, G. W., Wiley : New York 1980.
2. (a) Cuenoud, B.; Szostak, J. W. *Nature* **1995**, 375(6532), 611-4. (b) Opazo, C. H. X.; Cherny, R. A.; Moir, R. D.; Masters, C.L.; Tanzi, R. E.; Inestrosa, N. C.; Bush, A.I.; *J. Biol. Chem.* **2002**, 277(43), 4.0302-8.
3. *Cytochrome P-450: Structure, Mechanism, and Biochemistry*; Ortiz de Montellano, P. R., Ed.; Plenum: New York, 1985.
4. (a) Chianelli, R. R.; Pecordo, T.A. *J. Catal* **1981**, 67, 430-445. (b) Bianchini, C.; Meli, A. *Acc. Chem. Res.* **1998**, 31, 109-116.
5. (a) Evans, D. A.; Bender, S. C.; Morris, J. *J. Am. Chem. Soc.* **1998**, 110, 2506. (b) Hanson, Rm.; Sharpless, K. B. *J. Org. Chem.* **1986**, 51, 1992.
6. *Advance Organic Chemistry*, 4<sup>th</sup> Ed., Part B; Carey , F. A., Sunberg R. J.; Plenum: New York, 2001, 501.
7. Dittman , W.; Kirchhof, W.; Stumpf, W.; *Ann. Chem. (Liebigs)*. **1965**, 481, 30.
8. Jacobsen, E. N. In *Catalytic Asymmetric Synthesis*, Ojima, I., Ed.; VCH Publishers: New York, 1993 and references cited therein.
9. Lee, D.G.; Chen, T. *J. Am. Chem. Soc.* **1989**, 111, 1534.
10. Kolb, H.C.; Anderson, P.G.; Sharpless, K.B. *J. Am. Chem. Soc.* **1994**, 116, 1278.
11. N. A. Milas, *J. Am. Chem. Soc.* **1937**, 58, 1302.
12. *Fundamental Reaserch in Organometallic Chemistry*, Tsutsui, M., Ishii, Y., Yaozeng, H.; Science Press, 1980.
13. Hanson, R. M.; Sharpless, K. B. *J. Org. Chem.* **1986**, 51, 1922.
14. Zhang, W.; Loebach, J. L.; Wilson, S. R.; Wilson, S. R.; Jacobson, E. N. *J. Am. Chem. Soc.* **1990**, 112, 2801.

15. Adam, W.; Bargon, R. M.; Schenk, W. A.; *J. Am. Chem. Soc.* **2003**, *125*, 3871-3876.
16. *Transition Metal Sulfur Chemistry*; Stiefel, E. I., Matsumoto, K., Ed.; ACS Symp. Ser. 1996 No. 653,
17. Riaz, U.; Curnow, O.; Curtis, M.D. *J. Am. Chem. Soc.* **1991**, *113*, 1416.
18. Holm, R. H. *Chem. Rev.* **1987**, *87*, 1401-1449.
19. Sharpless, K. B.; Teranishi, A. Y.; Backvall, J. -E. *J. Am. Chem. Soc.* **1977**, *99*, 3120.
20. Brown, S. N.; Mayer, J. M. *J. Am. Chem. Soc.* **1996**, *118*, 12119.
21. (a) Cook, G. K.; Andrews, M. A. *J. Am. Chem. Soc.* **1996**, *118*, 9448. (b) Andrews, M. A.; Klaeren, S. A.; Gould, G. L. In *Carbohydrates as Organic Raw Materials II*, Descotes, G., Ed; VCH: New York, 1993.
22. (a) McCoy, M. *Chem. Eng. News* **1999**, 17-25 (b) Upson, L. L.; Schnaith, M. W. *Oil Gas J.* **1977**, 47-51
23. Chianelli, R. R.; Pecoraro, T. A.; Halbert, T. R.; Pan, W. H.; Stiefel, E.I. *J. Catal.* **1984**, *84*, 226-230
24. Sweeny, Z. K.; Polse, J. L.; Anderson, R. A.; Bergman, R.G. *J. Am. Chem. Soc.* **1998**, *120*, 7285-7834.
25. Rakowski DuBois, M.; Jagirdar, B.; Noll, B.; Dietz, S. *ACS Symp. Ser.* **1996**, No. 653, 259-281.
26. Bianchini, C.; Mealli, C.; Meli, A.; Sabat, M. *Inorg. Chem.* **1986**, *25*, 4617-4618.
27. Coucouvanis, D. *Adv. Inorg. Chem.* **1998**, *45*, 1-73.
28. Goodman, J.T.; Rauchfuss, T.B. *Angew. Chem., Int. Ed. Engl.* **1997**, *36*, 2083-2084.
29. Herrman, W. A.; Marz, D.; Herdtwick, E.; Schafer, A.; Wagner, W.; Kneupe, H. *J. Angew. Chem., Int. Ed. Engl.* **1987**, *26*, 462-464.
30. Cook, G. K.; Andrews, M. A. *J. Am. Chem. Soc.* **1996**, *118*, 9448.



31. Herrmann, W. A.; Serrano, R.; Küsthardt, U.; Ziegler, M. L.; Guggolz, E.; Zahn, T. *Angew. Chem., Int. Ed. Engl.* **1984**, *23*, 515.
32. Gable, K. P.; Juliette, J. J. J.; Gartman, M.A. *Organometallics* **1995**, *14*, 3138.
33. Gable, K. P.; Zhuravlev, F. A.; Yokochi, A. F. T. *Chem. Commun.* **1998**, 799-900.
34. Herrmann, W. A., et al, *Inorg. Chem.*, **1992**, *31*, 4431-4432.
35. (a) Trofimenko, S. *J. Am. Chem. Soc.* **1967**, *89*, 3170-3177. (b) Mayer, J. M.; Northcutt, T. O.; Brugman, J.; Bennett, B. K.; Lovell, S. *Organometallics*, **2000**, *19*, 2781-2790.
36. Gable, K. P.; Abubaker, A.; Zientara, K.; Wainwright, A. M. *Organometallics* **1999**, *18*, 173-179.
37. Gable, K. P.; Chuawong, P.; Yokochi, A. F. T. *Organometallics* **2002**, *21*, 929-933.
38. Murray, H. H.; Wei, L. W.; Sherman, S. E.; Greney, M. A.; Eriksen, K. A.; Carstensen, B.; Halbert, T.R.; Stiefel, E.I. *Inorg. Chem.* **1995**, *34*, 841-853.
39. Goodman, J.T.; Rauchfuss, T. B. *J. Am. Chem. Soc.* **1999**, *121*, 5017-5022.
40. Rappe, A. K.; Goddard, W.A.; *J. Am. Chem. Soc.* **1982**, *104*, 3287-3294.
41. Gable, K. P.; Brown, E. C.; *Organometallics*, **2000**, *19*, 944-946.
42. Brown, E. C., Ph.D. Dissertation, Oregon state University, Corvallis, OR 2002 Chapter 2.
43. Gable, K. P.; Brown, E. C.; *J. Am. Chem. Soc.*; 2003, *125*, Web Edition published 8/13/03.
44. Gable, K. P.; Brown, E. C.; *Organometallics*, **2003**, *22*, 3096-3101.

45. Rakowski-DuBois, M.; Pawicki, S. H.; Noll, B. C.; Kanney, J. A. *Inorg. Chem.* **2003**, *42*, 1556-1563.
46. Parkin, G. *Prog. Inorg. Chem.* **1998**, *47*, 1-166.
47. Chuawong, P., M.S. Thesis, Oregon State University, Corvallis, OR, 20001 Chapter 2.
48. Gable, K.P. Unpublished Work.
49. (a) *Organic Syntheses by oxidation with Metal compounds*; Mijs, W.J.; deJonghe C. R. H. I. Plenum: New York, 1986. (b) *Metal Catalyzed Oxidation of Organic Compounds*; Sheldon, R. A.; Kochi, J. K. Academic: New York, 1981 (c) *Encyclopedia of Reagents for Organic Synthesis*; Paquette, L. A., Ed.; Wiley: New York, 1995; Vol. 3 pp 1649, 2078.
50. Sharpless, K. B.; Umbreit, M. A.; Nieh, M. T.; Flood, T. C. *J. Am. Chem. Soc.* **1972**, *94*, 6538.
51. *Thermochemistry of Organic and Organometallic Compounds*; Cox, J.D.; Pilcher, G.; Academic Press, New York, 1970, 1-636.
52. Bedford, A. F.; Mortimer, C. T. *J. Chem. Soc.* **1960**, 1622-5.
53. *NIST-JANAF Thermochemical Tables*, 4<sup>th</sup> Ed, J. Phys. Chem. Ref. Data, Monograph 9; Chase, M.W., Jr.; 1998, 1-1951.
54. Sunner, S. *Acta Chem. Scand.*, **1963**, *17*, 728-730.
55. Kirklín, Duane R.; Chickos, James S.; Liebman, Joel F. *Chemical Structural Chemistry*, **1996**, *7*(5/6), 355-361.
56. *Manipulation of Air-sensitive Compounds*; Shriver, D. F., Drezdson, M. A.; Wiley: New York, 1986.
57. *150 and More Basic NMR Experiments*; Braun, S. Kalinowski, H, -O; Wiley-VCH: New York, 1987.
58. Cope, A.C.; Bach, R.D. *Org. Syn.* **1969**, *49*, 39-44.
59. Sharpless, K. B.; Yudin, A. K. *J. Am. Chem. Soc.* **1997**, *119*, 11536-11537.
60. Adam, W.; Bargon, R. M. *Chem. Commun.* **2001**, 1910-1911.

61. Takido, T.; Kobayashi, Y.; Itabashi, K. *Synthesis* **1989**, *9*, 779-8.
62. Whitham, G. H.; Jones, M.; Temple, P.; Thomas, E.J.; *J. Chem. Soc., Perkin Trans. I* **1974**, 433.
63. Ness, S. L., M.S. Thesis, Oregon State University, Corvallis, OR, 1999, Chapter 3.
64. Gable, K. P. *Organometallics* **1994**, *13*, 2486-2489

**Appendix**

kk191db 1 1H NMR C6D6

Current Data Parameters  
NAME kk191db  
EXPNO 1  
PROCNO 1  
DU /m  
USER ake

F2 - Acquisition Parameters  
Date\_ 20021123  
Time 0.18  
INSTRUM dpx400  
PROBHD 5 mm BBO Z-G  
PULPROG zg30  
TD 32768  
SOLVENT C6D6  
NS 16  
DS 2  
SWH 5995.204 Hz  
FIDRES 0.182959 Hz

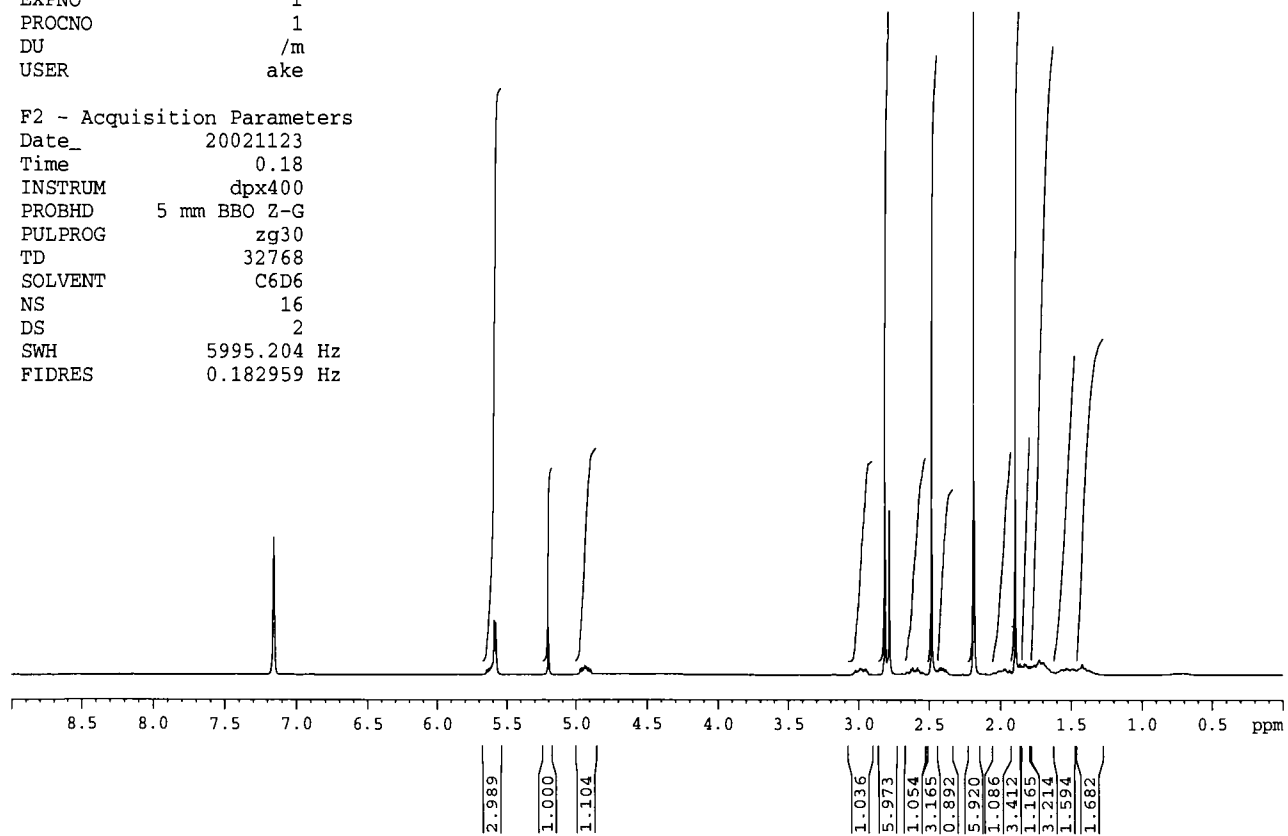


Figure A1.1: <sup>1</sup>H NMR and <sup>13</sup>C of 1,2-*trans*-Cyclooctanediolate

Appendix I. NMR Spectra in C<sub>6</sub>D<sub>6</sub>

kk191db Exp 3 Stdcarb Tp;Re000trans-cycloocene C6D6

Current Data Parameters  
 NAME kk191db  
 EXPNO 3  
 PROCNO 1  
 DU /m  
 USER ake

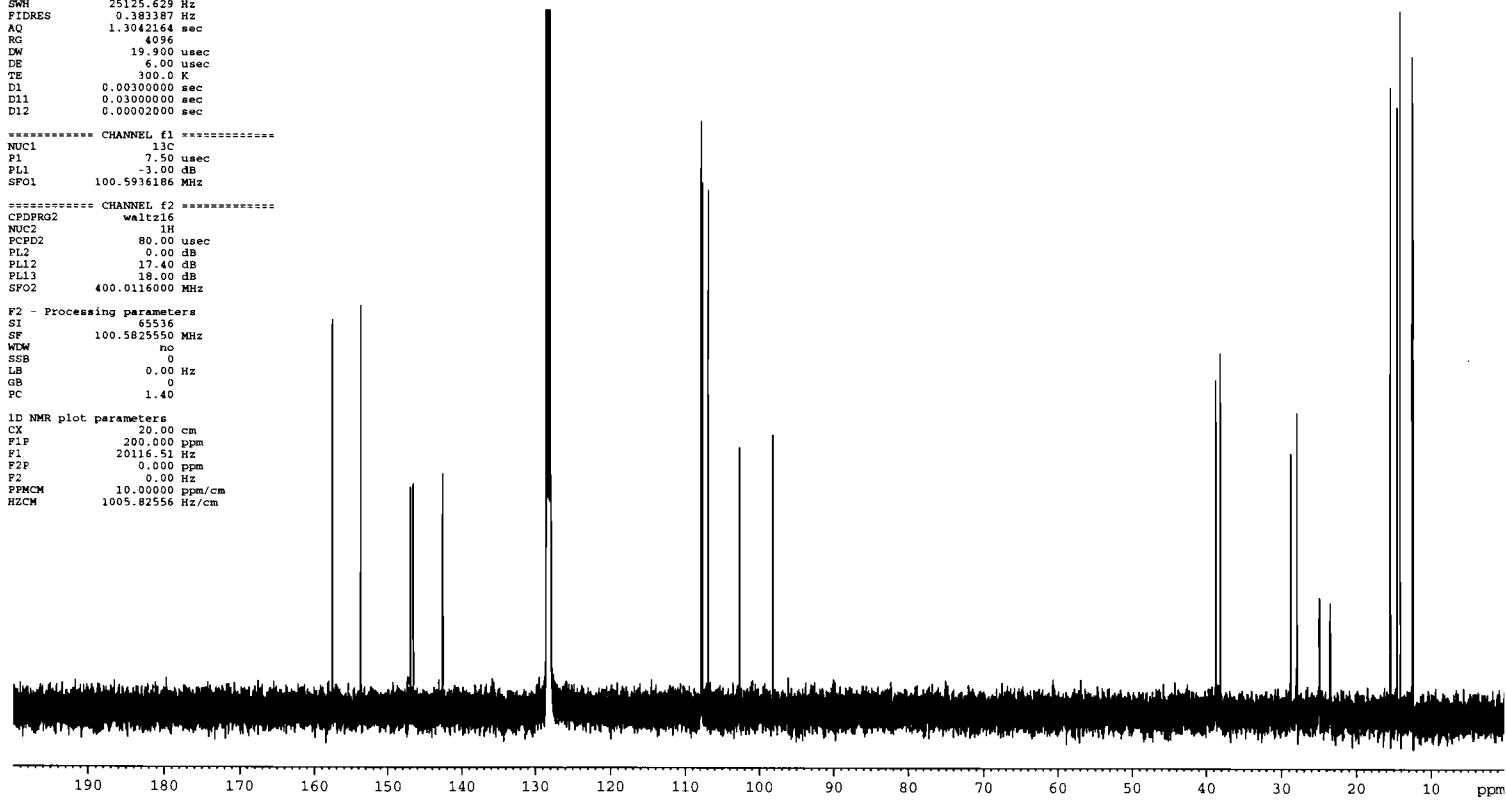
F2 - Acquisition Parameters  
 Date\_ 20021212  
 Time 20.24  
 INSTRUM dpx400  
 PROBHD 5 mm BBO Z-G  
 PULPROG zgpg30  
 TD 65536  
 SOLVENT C6D6  
 NS 1258  
 DS 4  
 SWH 25125.629 Hz  
 FIDRES 0.381387 Hz  
 AQ 1.3042164 sec  
 RG 4096  
 DW 19.900 usec  
 DE 6.00 usec  
 TE 300.0 K  
 D1 0.00300000 sec  
 D11 0.03000000 sec  
 D12 0.00002000 sec

===== CHANNEL f1 =====  
 NUC1 13C  
 P1 7.50 usec  
 PL1 -3.00 dB  
 SFO1 100.5916186 MHz

===== CHANNEL f2 =====  
 CPDPRG2 waltz16  
 NUC2 1H  
 PCPD2 80.00 usec  
 PL2 0.00 dB  
 PL12 17.40 dB  
 PL13 18.00 dB  
 SFO2 400.0116000 MHz

F2 - Processing parameters  
 SI 65536  
 SF 100.5825550 MHz  
 WMW no  
 SSB 0  
 LB 0.00 Hz  
 GB 0  
 PC 1.40

1D NMR plot parameters  
 CX 20.00 cm  
 F1P 200.000 ppm  
 F1 20116.51 Hz  
 F2P 0.000 ppm  
 F2 0.00 Hz  
 PPMCM 10.00000 ppm/cm  
 HZCM 1005.82556 Hz/cm



Current Data Parameters  
NAME kk192  
EXFNO 1  
PROCNO 1  
DU /m  
USER ake

kk192 1 stdprot C6D6 Dec 20, 02

F2 - Acquisition Parameters  
Date\_ 20021122  
Time 20.34  
INSTRUM qn400  
PROBHD 5 mm BBO Z-G  
PULPROG zg30  
TD 32768  
SOLVENT C6D6  
NS 16  
DS 2  
SWH 5995.204 Hz  
FIDRES 0.182959 Hz  
AQ 2.7329011 sec  
RG 256  
DW 83.400 usec  
DE 6.00 usec  
TE 300.0 K  
D1 30.0000000 sec

\*\*\*\*\* CHANNEL f1 \*\*\*\*\*  
NUC1 1H  
P1 11.30 usec  
PL1 0.00 dB  
SFO1 400.0126001 MHz

F2 - Processing parameters  
SI 65536  
SF 400.0100493 MHz  
WDW no  
SSB 0  
LB 0.00 Hz  
GB 0  
PC 1.00

1D NMR plot parameters  
CX 42.91 cm  
F1P 5.672 ppm  
F1 2268.92 Hz  
F2P 1.381 ppm  
F2 552.57 Hz  
PRCM 0.10000 ppm/cm  
HZCM 40.00100 Hz/cm

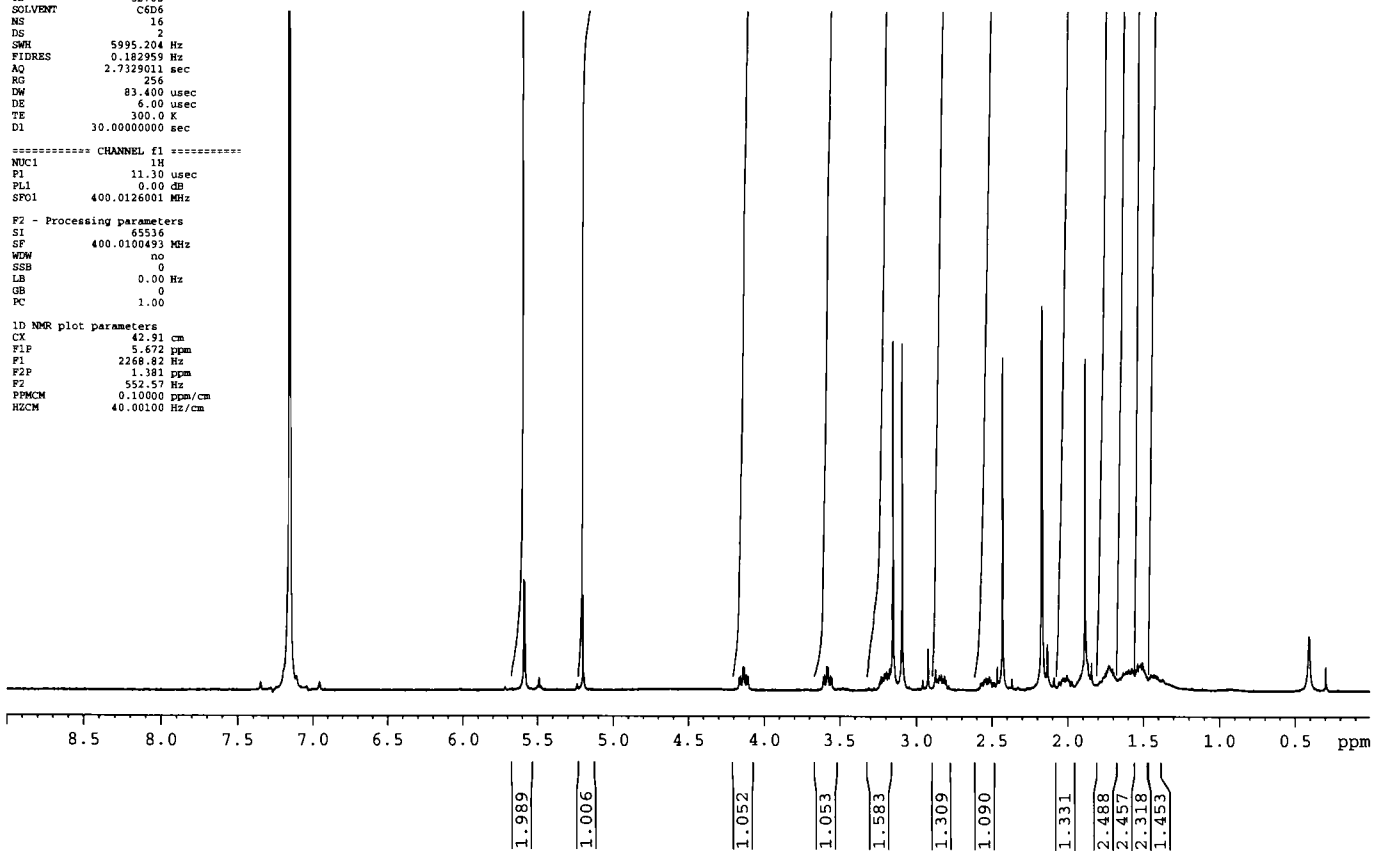


Figure A1.2:  $^1\text{H}$  NMR and  $^{13}\text{C}$  of 1,2-*trans*-Cyclooctanedithiolate

kk192 3 stdcarb Tp'ReOSstrans-cyclooctene C6D6 Dec 12, 02

Current Data Parameters  
NAME kk192  
EXPNO 3  
PROCNO 1  
IN /m  
USER ake

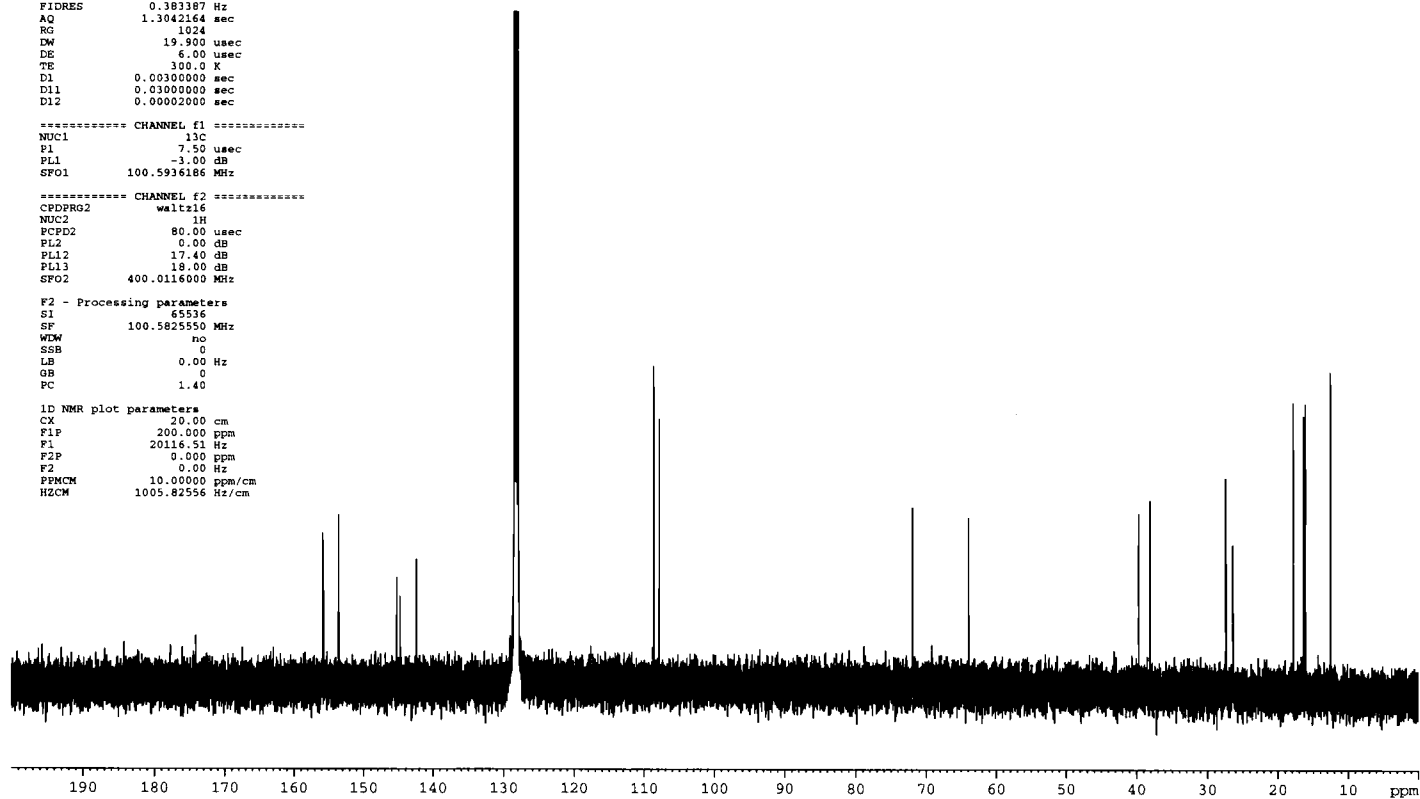
F2 - Acquisition Parameters  
Date\_ 20021212  
Time 21.53  
INSTRUM apx400  
PROBHD 5 mm BBO 7-G  
PULPROG zgpg30  
TD 65536  
SOLVENT CDCl3  
NS 1922  
DS 4  
SWH 25125.629 Hz  
FIDRES 0.383387 Hz  
AQ 1.3042164 sec  
RG 1024  
DW 19.900 usec  
DE 6.00 usec  
TE 300.0 K  
D1 0.0300000 sec  
D11 0.0300000 sec  
D12 0.0002000 sec

\*\*\*\*\* CHANNEL f1 \*\*\*\*\*  
NUC1 13C  
P1 7.50 usec  
PL1 -3.00 dB  
SFO1 100.5936186 MHz

\*\*\*\*\* CHANNEL f2 \*\*\*\*\*  
CPDPRG2 waltz16  
NUC2 1H  
PCPD2 80.00 usec  
PL2 0.00 dB  
PL12 17.40 dB  
PL13 18.00 dB  
SFO2 400.0116000 MHz

F2 - Processing parameters  
S1 65536  
SF 100.5825550 MHz  
WDW no  
SSB 0  
LB 0.00 Hz  
GB 0  
PC 1.40

1D NMR plot parameters  
CX 20.00 cm  
F1P 200.000 ppm  
F1 20116.51 Hz  
F2P 0.000 ppm  
F2 0.00 Hz  
PFMCM 10.00000 ppm/cm  
HZCM 1005.82556 Hz/cm





kk207 cis-cycloocteneOO Tp'ReO C6D6 Jan 15, 02

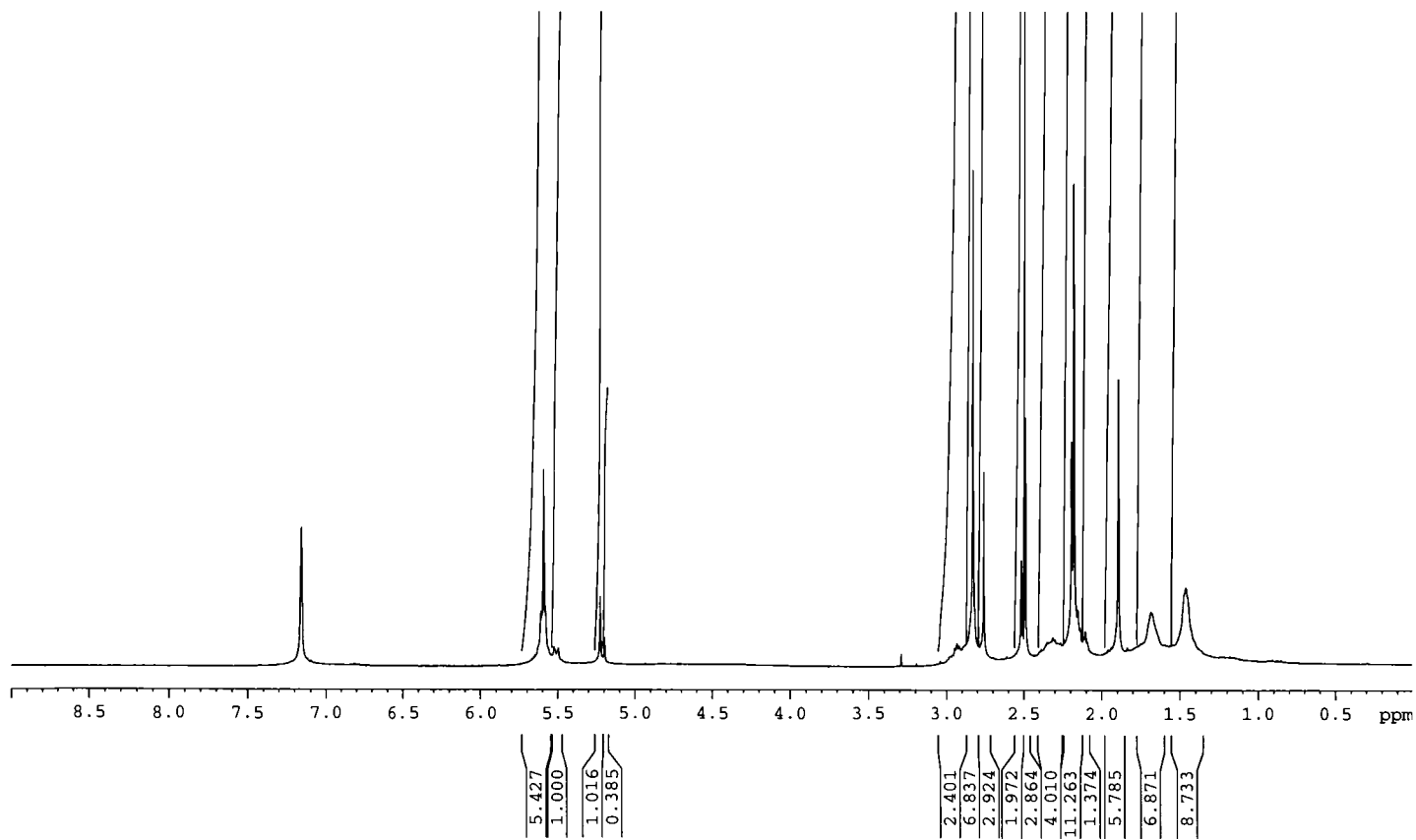


Figure A1.3: <sup>1</sup>H NMR of 1,2-cis-Cyclooctanediolate

kk204 Tp'Recis-cyclooctene episulfide C6D6, Dec 17, 02

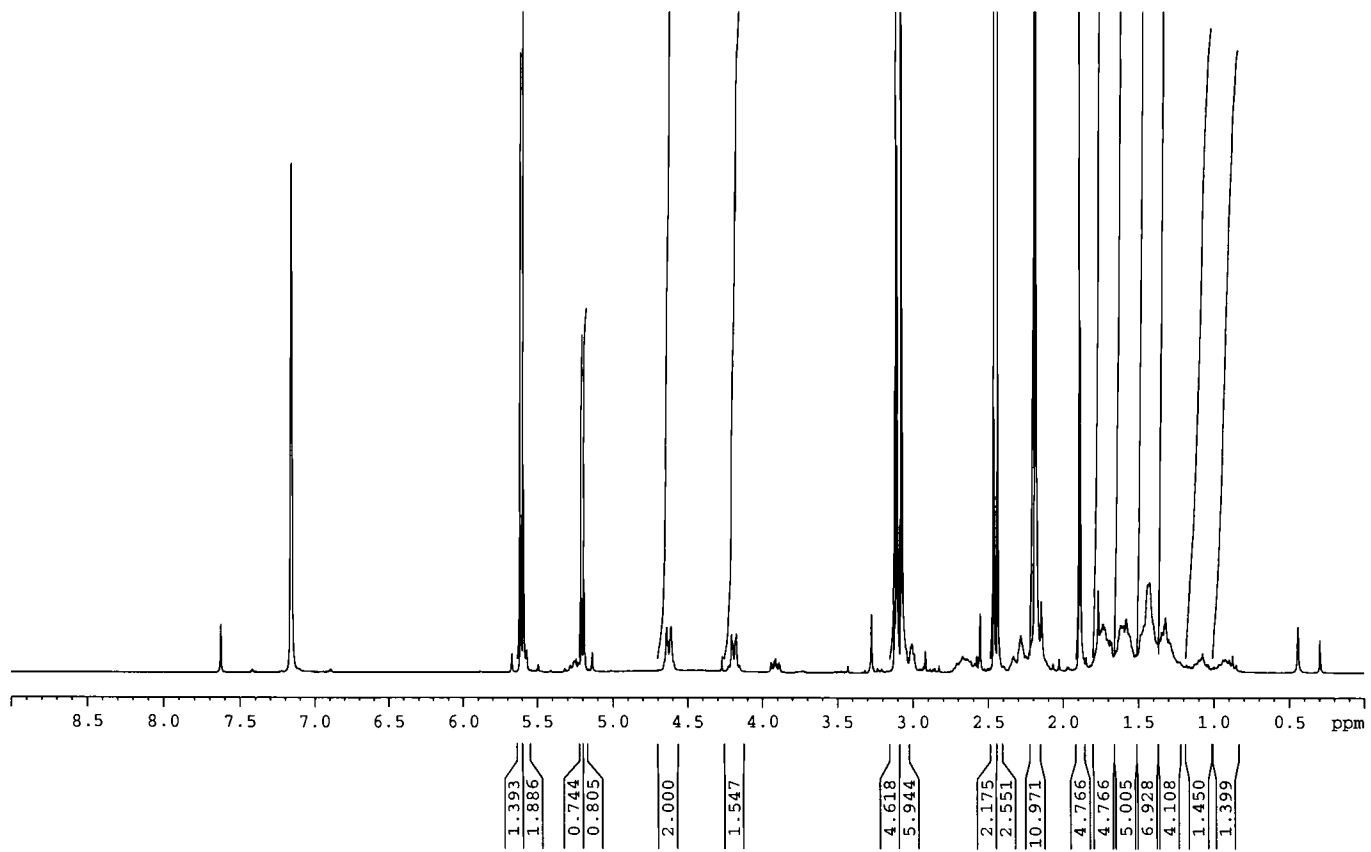


Figure A1.4:  $^1\text{H}$  NMR and  $^{13}\text{C}$  of 1,2-*cis*-Cyclooctanedithiolate

kk204 3 dept135 C6D6 Dec 17, 02

Current Data Parameters  
NAME kk204  
EXPNO 3  
PROCNO 1  
DU /m  
USER ake

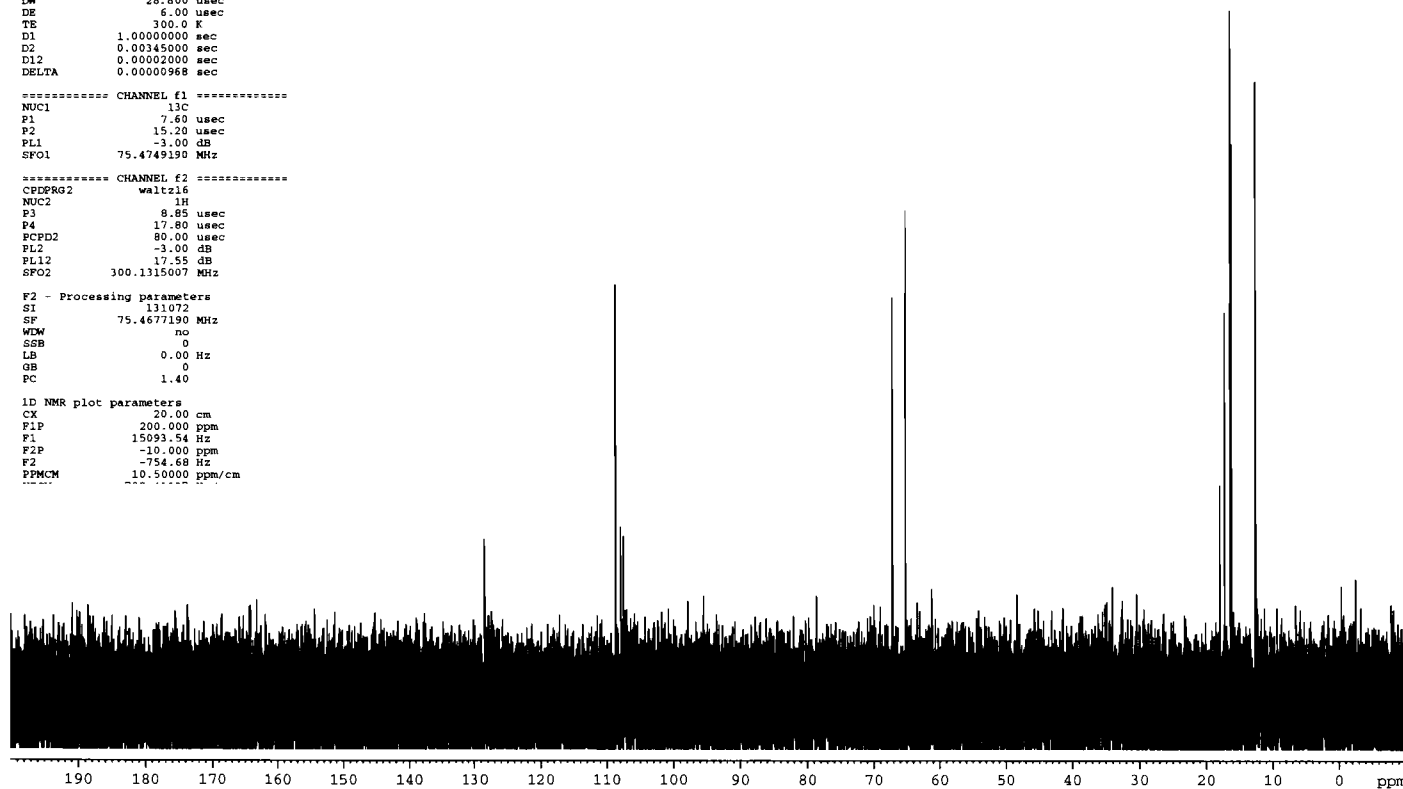
F2 - Acquisition Parameters  
Date\_ 20021217  
Time 23.10  
INSTRUM dpx300  
PROBHD 5 mm QNP 1H  
PULPROG dept135  
TD 65536  
SOLVENT  
NS 263  
DS 2  
SWH 17361.111 Hz  
FIDRES 0.264910 Hz  
AQ 1.8874868 sec  
RG 9195.2  
DM 28.800 usec  
DE 6.00 usec  
TE 300.0 K  
D1 1.00000000 sec  
D2 0.00345000 sec  
D12 0.00002000 sec  
DELTA 0.00000968 sec

\*\*\*\*\* CHANNEL f1 \*\*\*\*\*  
NUC1 13C  
P1 7.60 usec  
PL1 15.20 usec  
PL1 -3.00 dB  
SFO1 75.4749190 MHz

\*\*\*\*\* CHANNEL f2 \*\*\*\*\*  
CDEPRG2 waltz16  
NUC2 1H  
P3 8.85 usec  
P4 17.80 usec  
PCPD2 80.00 usec  
PL2 -3.00 dB  
PL12 17.55 dB  
SFO2 300.1315007 MHz

F2 - Processing parameters  
SI 131072  
SF 75.4677190 MHz  
WEW no  
SBB 0  
LB 0.00 Hz  
GB 0  
PC 1.40

1D NMR plot parameters  
CX 20.00 cm  
FIP 200.000 ppm  
F1 15093.54 Hz  
F2P -10.000 ppm  
F2 -754.68 Hz  
PFMCM 10.50000 ppm/cm



kk197b C6D6 Nov 21, 02

```
Current Data Parameters
NAME          kk197b
EXPNO         1
PROCNO        1
DU             /m
USER          ake

F2 - Acquisition Parameters
Date_         20021220
Time          12.34
INSTRUM       gpc400
PROBHD        5 mm BBO Z-G
PULPROG       zg30
TD            32768
SOLVENT       C6D6
NS            16
DS            2
SWH           5995.264 Hz
FIDRES        0.182959 Hz
AQ            2.7329011 sec
RG            128
DW            83.400 usec
DE            6.00 usec
TE            300.0 K
D1            30.0000000 sec

***** CHANNEL f1 *****
NUC1          1H
P1            11.30 usec
PL1           0.00 dB
SFO1         400.0126001 MHz

F2 - Processing parameters
SI            65536
SF            400.0100000 MHz
WDW           no
SSB           0
LB            0.00 Hz
GB            0
PC            1.00

1D NMR plot parameters
CX            70.72 cm
F1P           7.529 ppm
F1            3011.72 Hz
F2P           0.457 ppm
F2            182.81 Hz
FPMCM        0.11000 ppm/cm
HZCM         40.00100 Hz/cm
```

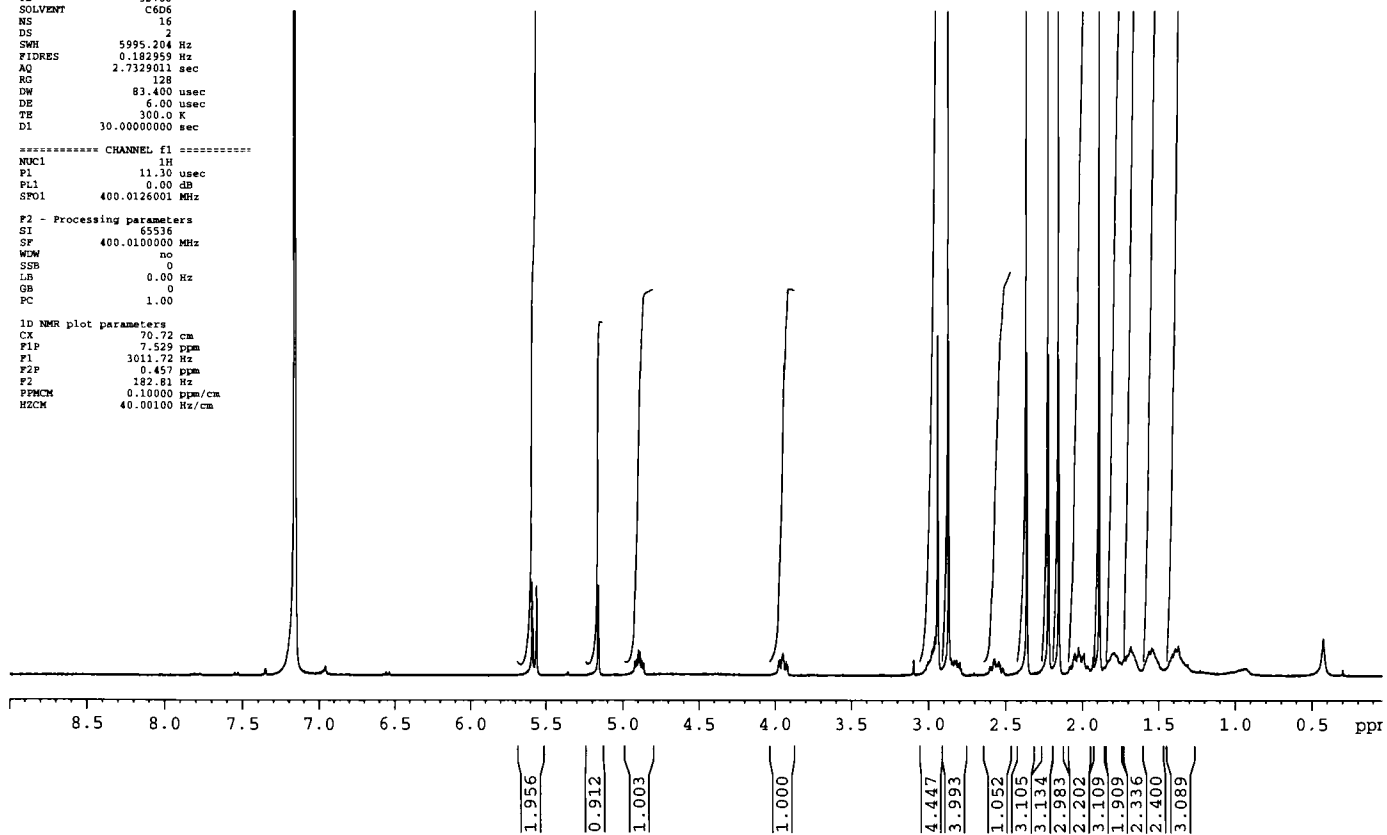


Figure A1.5:  $^1\text{H}$  NMR and  $^{13}\text{C}$  of 1,2-trans-Cyclooctanemonothiodiolate

kk197b 3 C-13 C6D6 Dec 20, 02

Current Data Parameters  
NAME kk197b  
EXPNO 3  
PROCNO 1  
DU /m  
USER ake

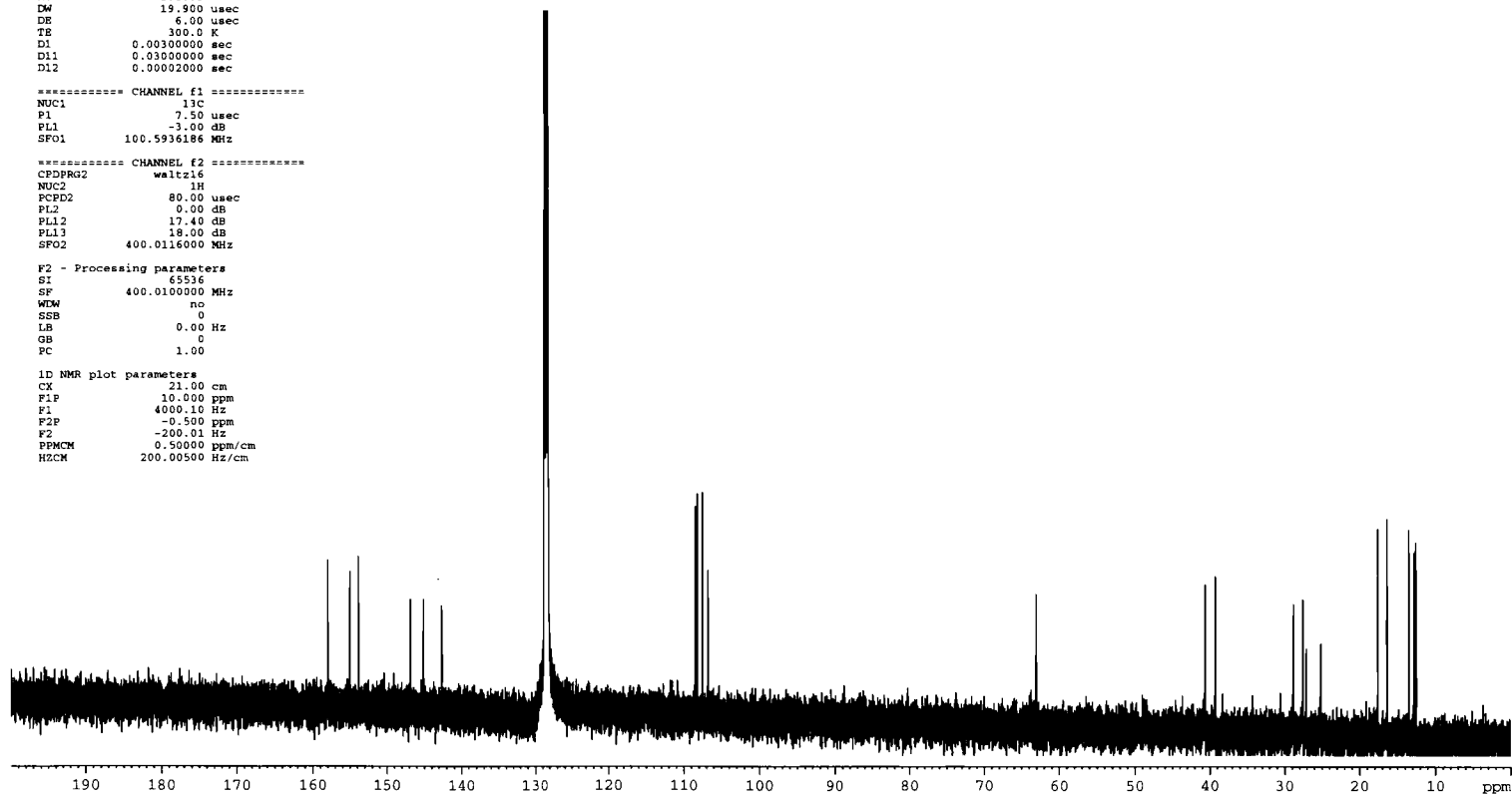
F2 - Acquisition Parameters  
Date\_ 20021219  
Time 20.46  
INSTRUM dpx400  
PROBHD 5 mm BBO Z-g  
PULPROG zgpg30  
TD 65536  
SOLVENT C6D6  
NS 3500  
DS 4  
SWH 25125.629 Hz  
FIDRES 0.383387 Hz  
AQ 1.3042164 sec  
RG 2580.3  
DW 19.900 usec  
DE 6.00 usec  
TE 300.0 K  
D1 0.00300000 sec  
D11 0.03000000 sec  
D12 0.00020000 sec

\*\*\*\*\* CHANNEL f1 \*\*\*\*\*  
NUC1 13C  
P1 7.50 usec  
PL1 -3.00 dB  
SFO1 100.5936186 MHz

\*\*\*\*\* CHANNEL f2 \*\*\*\*\*  
CPDPRG2 waltz16  
NUC2 1H  
PCPD2 80.00 usec  
PL2 0.00 dB  
PL12 17.40 dB  
PL13 18.00 dB  
SFO2 400.0116000 MHz

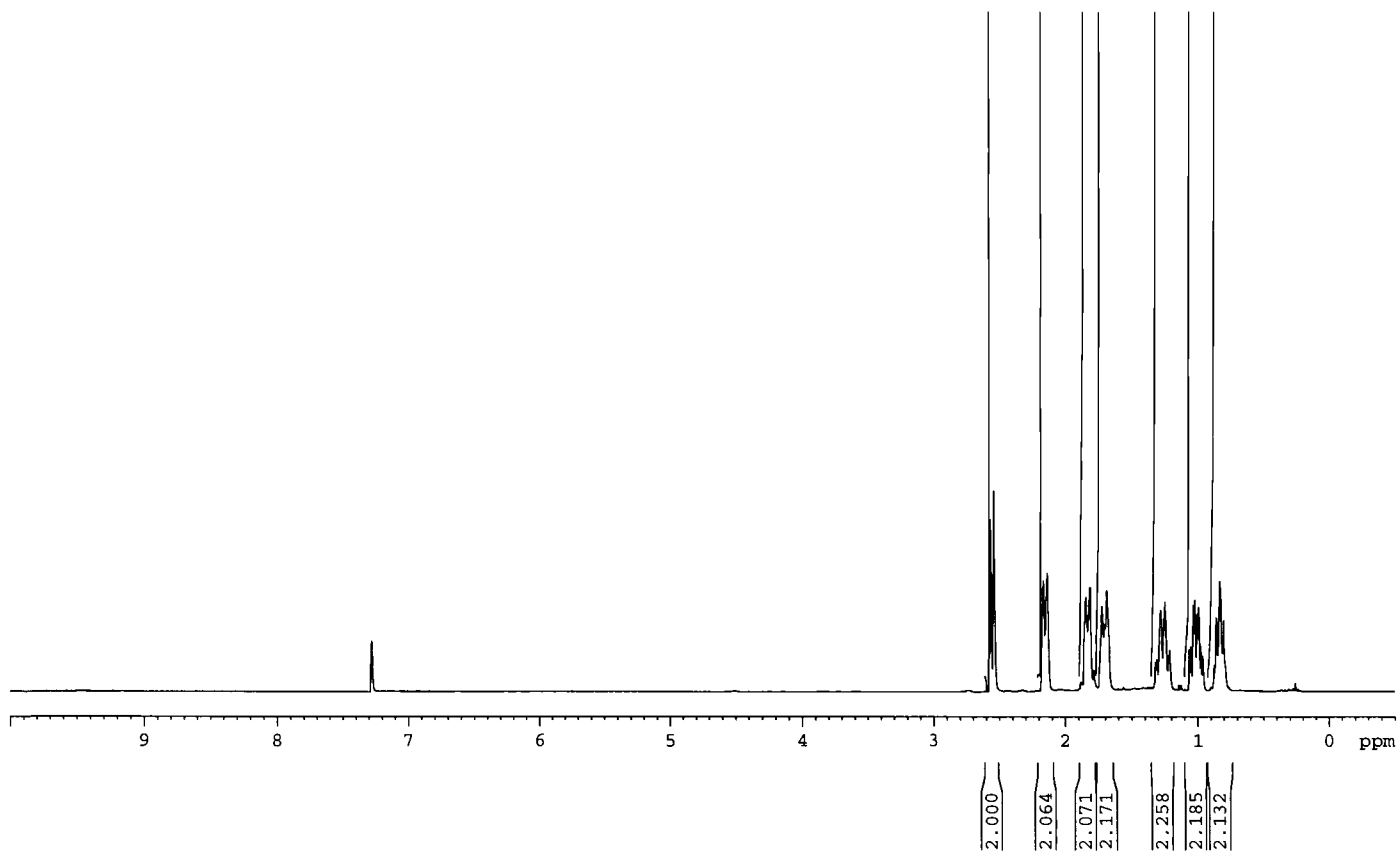
F2 - Processing parameters  
SI 65536  
SF 400.0100000 MHz  
WDW no  
SSB 0  
LB 0.00 Hz  
GB 0  
PC 1.00

1D NMR plot parameters  
CX 21.00 cm  
F1P 10.000 ppm  
F1 4000.10 Hz  
F2P -0.500 ppm  
F2 -200.01 Hz  
PPMCM 0.50000 ppm/cm  
HZCM 200.00500 Hz/cm



kk299 4 trans-cyclooctene oxide C6D6, July 27, 03

Figure A1.6: <sup>1</sup>H NMR of *trans*-Cyclooctene Oxide



kk299 6 trans-cyclooctene episulfide C6D6 July 29, 03

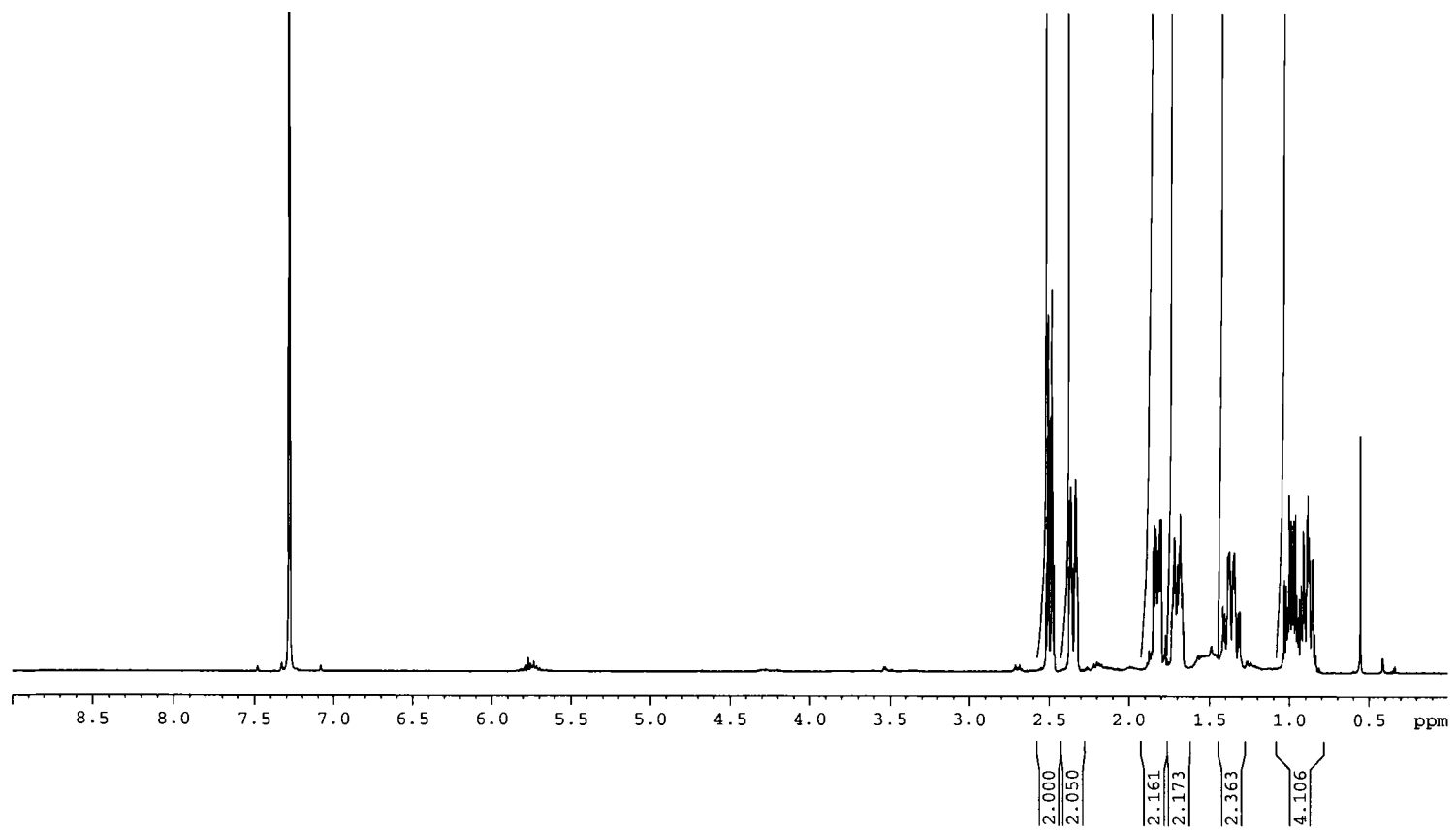


Figure A1.7:  $^1\text{H}$  NMR of *trans*-Cyclooctene Episulfide

kk299 3 cis-cyclooctene oxide C6D6, July 27, 03

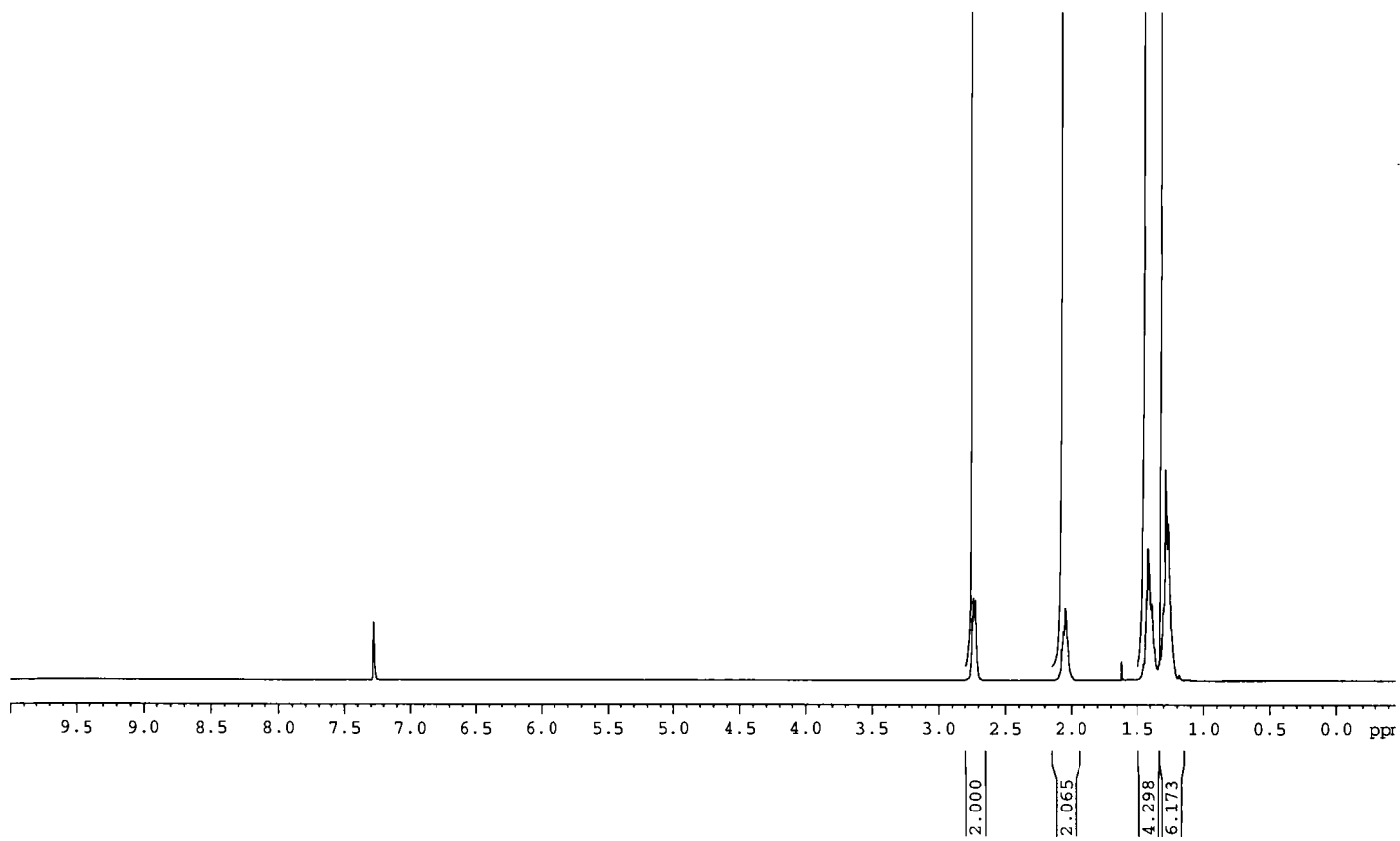


Figure A1.8:  $^1\text{H}$  NMR of *cis*-Cyclooctene Oxide



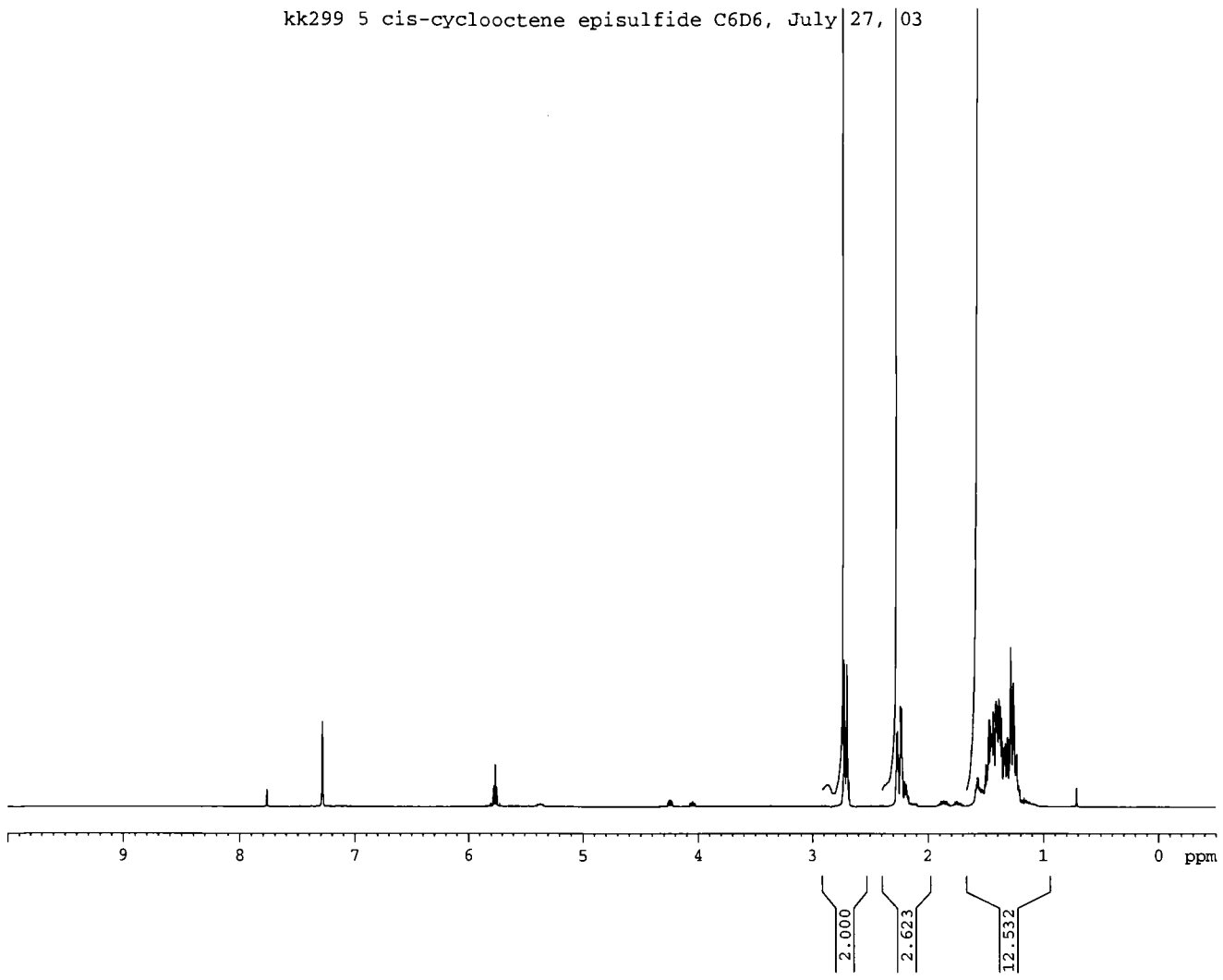
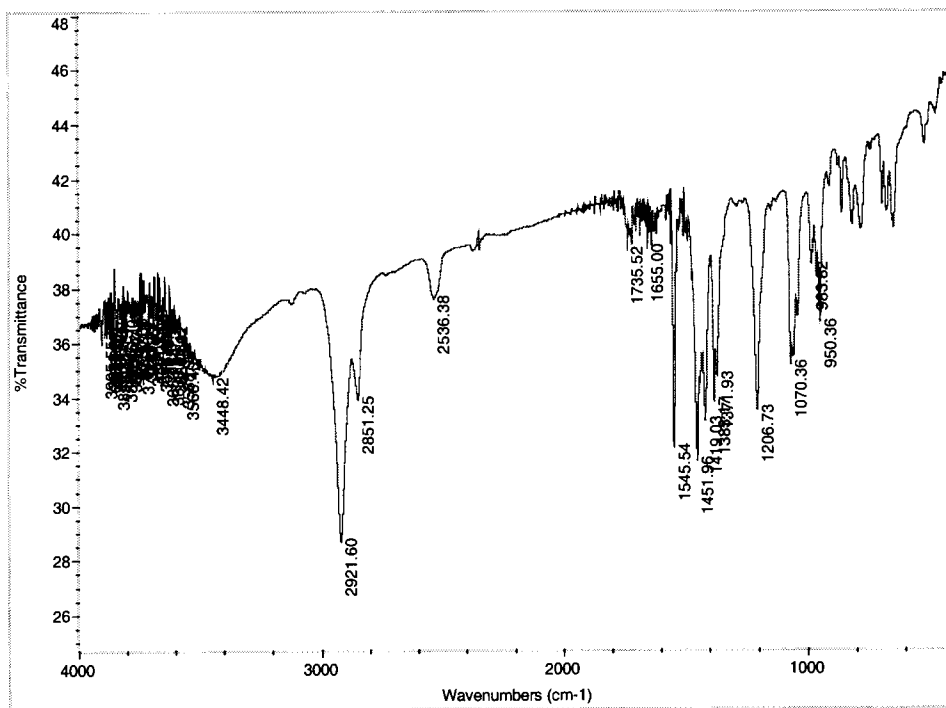


Figure A1.9: <sup>1</sup>H NMR of *trans*-Cyclooctene Episulfide

## Appendix II. Spectra of Yellow-Green Compound

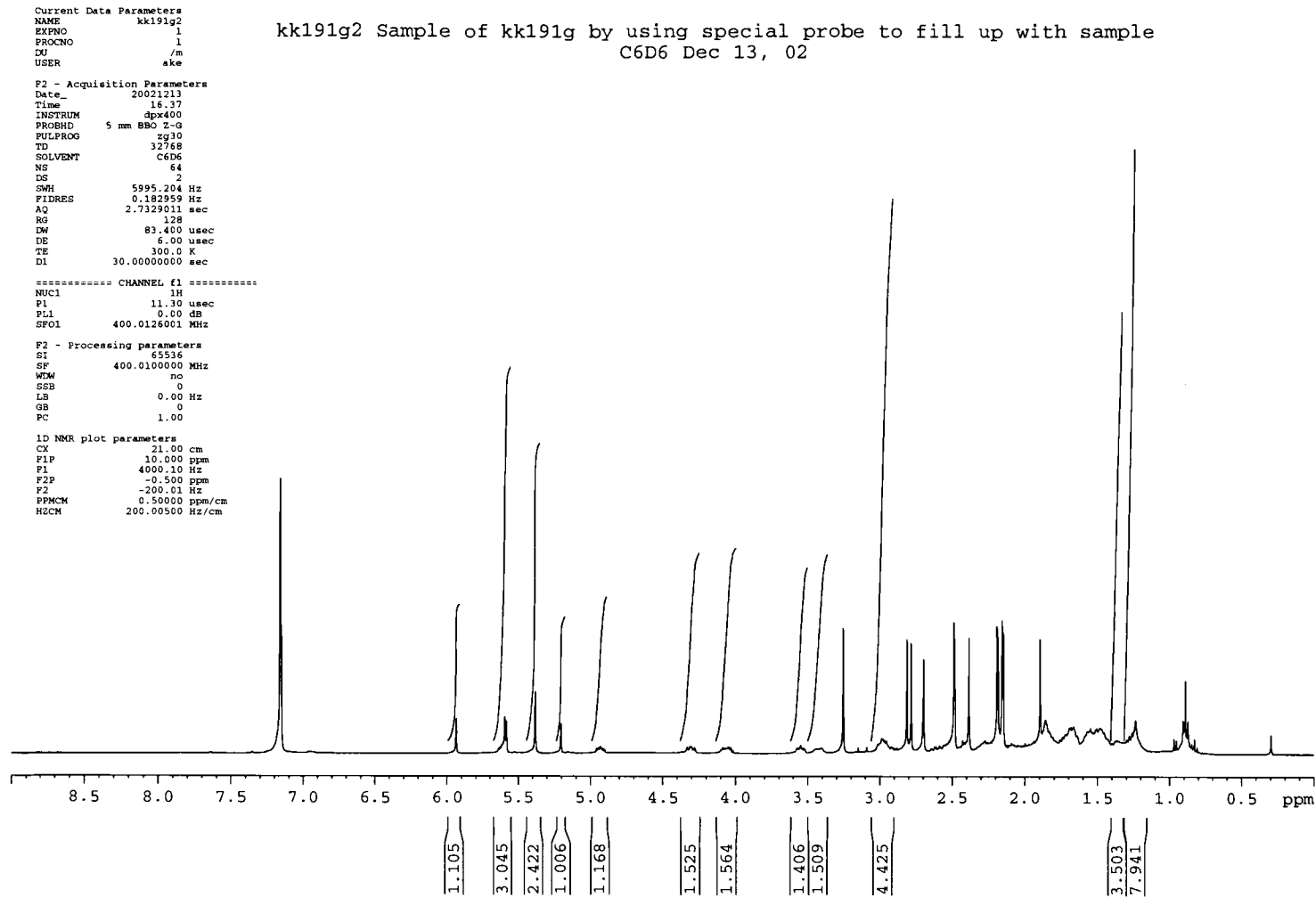
Figure A2.1: IR



IR (KBr): 2921, 2851, 2536.36, 1735, 1655, 1545, 1451, 1419, 1207, 1070, 950, 904  $\text{cm}^{-1}$ .

MS (FAB): 816.1, 707.8, 673.9, 655.9, 641.9, 531.8, 499.8 391.2, 371.2, 307, 219.1, 154, 107  $m/z$ .

Figure A2.2: <sup>1</sup>H NMR and <sup>13</sup>C



Current Data Parameters  
NAME kk191g2  
EXPNO 2  
PROCNO 1  
DU /m  
USER ake

kk191g2 2 C-13 Green compound C6D6, Dec 14, 02

F2 - Acquisition Parameters  
Date\_ 20021214  
Time 14.29  
INSTRUM dpx400  
PROBHD 5 mm BBO Z-G  
PULPROG zgpg30  
TD 65536  
SOLVENT C6D6  
NS 2055  
DS 4  
SWH 25125.629 Hz  
FIDRES 0.383387 Hz  
AQ 1.3042164 sec  
RG 1024  
DW 19.900 usec  
DE 6.00 usec  
TE 300.0 K  
D1 4.00000000 sec  
D11 0.03000000 sec  
D12 0.00002000 sec

===== CHANNEL f1 =====  
NUC1 13C  
P1 7.50 usec  
PL1 -3.00 dB  
SFO1 100.5936186 MHz

===== CHANNEL f2 =====  
CPDPRG2 waltz16  
NUC2 1H  
PCPD2 80.00 usec  
PL2 0.00 dB  
PL12 17.40 dB  
PL13 18.00 dB  
SFO2 400.0116000 MHz

F2 - Processing parameters  
SI 65536  
SF 100.5825550 MHz  
WDW no  
SSB 0  
LB 0.00 Hz  
GB 0  
PC 1.40

1D NMR plot parameters  
CX 20.00 cm  
F1P 200.000 ppm  
F1 20116.51 Hz  
F2P 0.000 ppm  
F2 0.00 Hz  
PPMCM 10.00000 ppm/cm  
HZCM 1005.82556 Hz/cm

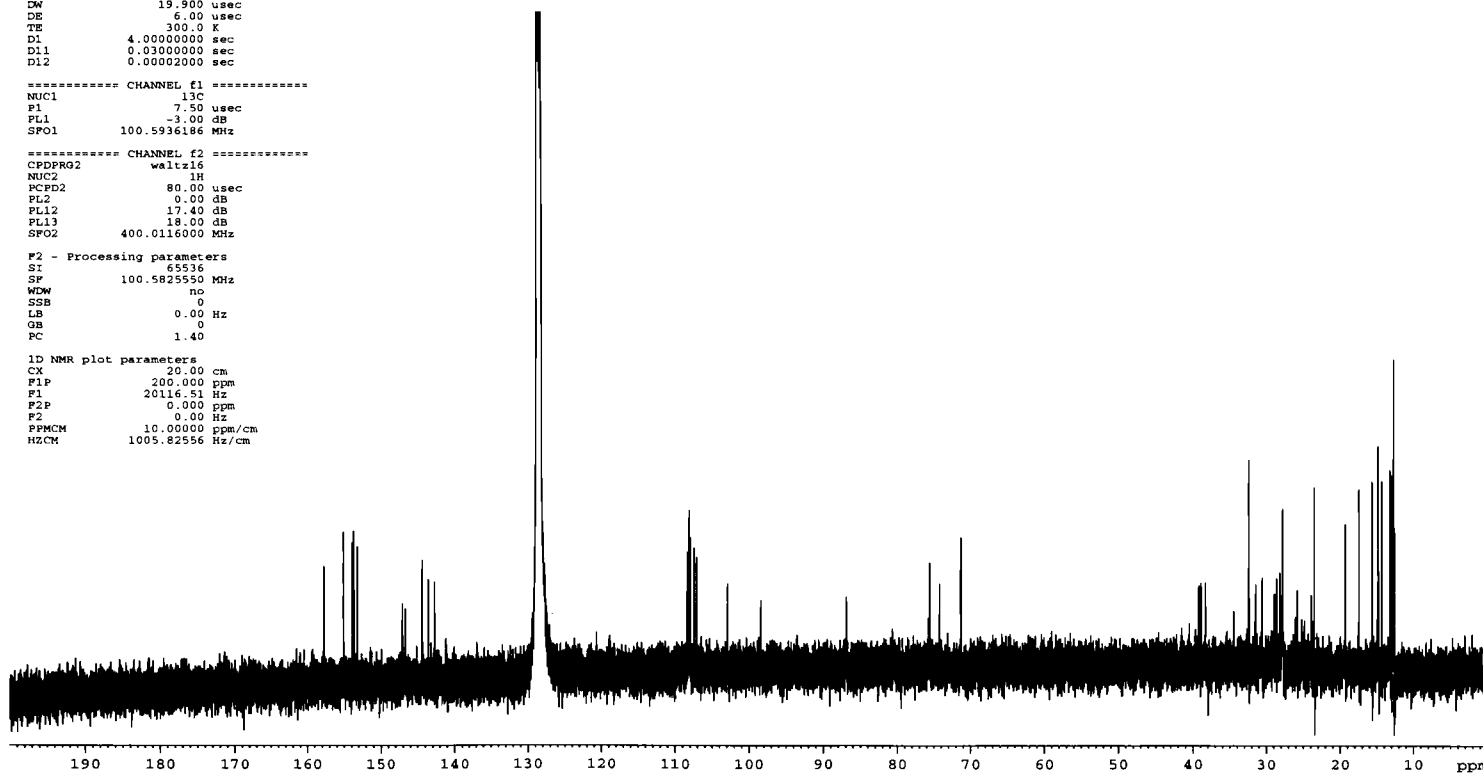


Figure A2.3: COSY

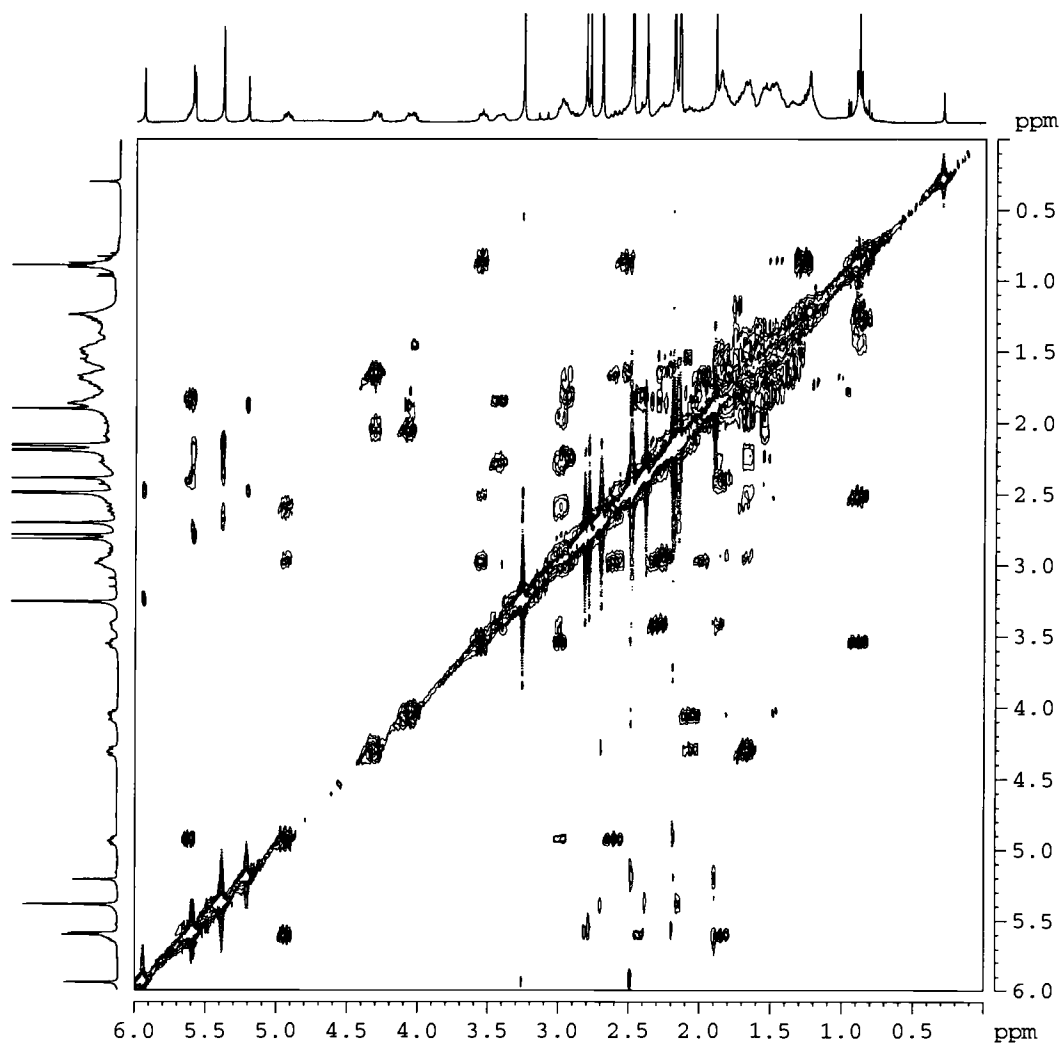


Figure A2.4: HSQC

